FORCES ON LABORATORY MODEL

DREDGE CUTTERHEAD

A Thesis

by

DUSTIN RAY YOUNG

Submitted to the Office of Graduate Studies of
Texas A&M University
in partial fulfillment of the requirements for the degree of

MASTER OF SCIENCE

December 2009

Major Subject: Ocean Engineering

FORCES ON LABORATORY MODEL

DREDGE CUTTERHEAD

A Thesis

by

DUSTIN RAY YOUNG

Submitted to the Office of Graduate Studies of
Texas A&M University
in partial fulfillment of the requirements for the degree of

MASTER OF SCIENCE

Approved by:

Chair of Committee,	Robert E. Randall
Committee Members,	Moo-Hyun Kim
	Achim Stoessel
Interim Head of Department,	John Niedzwecki

December 2009

Major Subject: Ocean Engineering

ABSTRACT

Forces on Laboratory Model Dredge Cutterhead. (December 2009)
Dustin Ray Young, B.S., Texas A&M University
Chair of Advisory Committee: Dr. Robert Randall

Dredge cutting forces produced by the movement of the cutterhead through the sediment have been measured with the laboratory dredge carriage located at the Haynes Coastal Engineering Laboratory. The sediment bed that was used for the dredging test was considered to be relatively smooth and the sediment used was sand with a d_{50}=0.27 mm. Forces on the dredge carriage were measured using five 13.3 kN (3000 lb) one directional load cells placed on the dredge ladder in various places so the transmitted cutting forces could be obtained. The objectives for this study are to determine the vertical, horizontal, and axial forces that are produced by the cutterhead while testing. So, to find these cutter forces, a static analysis was performed on the carriage by applying static loads to the cutterhead in the vertical, horizontal, and axial directions, and for each load that was applied, readings were recorded for all five of the load cells. Then, static equilibrium equations were developed for the dredge carriage ladder to determine loads in the five load cells. Also, equilibrium equations can be applied to a dredging test to find the cutterhead forces by taking the measured data from the five load cells and applying the known forces to the equations, and the cutterhead forces can be determined. These static equilibrium equations have been confirmed by using a program called SolidWorks, which is modeling software that can be used to do static finite element analysis of structural systems to determine stresses, displacement, and pin and bolt forces. Data that were gathered from the experimental procedure and the theoretical calculations show that the force on the dredge cutterhead can be determined.

However, the results from the static equilibrium calculations and the results from the SolidWorks program were compared to the experiment procedure results, and from the comparison the procedure results show irregularities when a force of approximately

0.889 kN (200 lb) or above is applied to the cutterhead in a north, south, west, or east orientation. The SolidWorks program was used to determine the results for displacements of the dredge carriage ladder system, which showed that large displacements were occurring at the location of the cutterhead, and when the cutterhead displaces it means that the carriage ladder is also moving, which causes false readings in the five load cells. From this analysis it was determined that a sixth force transducer was needed to produce more resistance on the ladder; and the cell #1 location needed to be redesigned to make the ladder system as rigid as possible and able to produce good testing results. The SolidWorks program was used to determine the best location where the sixth force transducer would give the best results, and this location was determined to be on the lower south-west corner oriented in the direction east to west. The static equilibrium equations were rewritten to include the new redesigned cell #1 location and the new location of the sixth load cell. From the new system of equations, forces on the cutterhead can be determined for future dredging studies conducted with the dredge carriage.

Finally, the forces on the laboratory cuttersuction dredge model cutterhead were scaled up to the prototype 61 cm (24 in) cuttersuction dredge. These scaled up cutting forces on the dredge cutterhead can be utilized in the design of the swing winches, swing cable size, ladder supports, and ladder.

ACKNOWLEDGEMENTS

The forces induced on a model cutterhead research was performed at the Reta and Bill Haynes Laboratory, and the dredge carriage design was funded by the Barrett G. Hindes Foundation. Without this facility and funding this research would not have been completed. The conceptual design of the dredge carriage was completed by Glover in 2002 and Glover and Randall in 2004; the final design of the carriage was completed by Digital Automation and Control Systems, Inc. (DACS) Oilfield Electric Marine (OEM); and the completed dredge carriage was installed in the laboratory in April 2005. Thanks to the development of this facility and the development of the dredge carriage, this research was possible.

NOMENCLATURE

		Units
$\bar{A}$	= Average axial cutterhead force	lb
α	= Blade angle with horizontal	rad
β	= Average angle of shear zone with horizontal	rad
b	= Width of cutting blade	in
b_c	= Cutting force per unit layer thickness	lb/ft
b_n	= Normal force per unit layer thickness	lb/ft
c_1, c_2	= Cutting force coefficients (non-cavitating)	-
D, z	= water depth	ft
d_1, d_2	= Cutting force coefficients (cavitating)	-
d_{50}	= Mean grain diameter	mm
D_c	= Depth of Cut	in
D_{cutter}	= Diameter of cutterhead	in
d_{c1Ax}	= Distance between cell1 to center of mass of cutter in x direction	in
d_{c1Az}	= Distance between cell1 to center of mass of cutter in z direction	in
d_{c1gax}	= Distance between cell1 to center of mass of articulating arm and cutter in x direction	in
d_{c1AzR}	= Distance between redesigned cell1 to center of mass of cutter in z direction	in
ε	= Phase shift	rad
ϕ_c	= Cavitation transition angle	rad
F_a	= Axial cutting force	lb
F_h	= Horizontal cutting force ($F_{\#nc}$ represents non-cavitating)	lb
F_v	= Vertical cutting force ($F_{\#ca}$ represents cavitating)	lb
F_v	= Cutting force perpendicular to swing direction and perpendicular to axis of excavating element	lb
F_{c1x}	= Shear force along x-axis	lb

		Units
F_{c1y}	= Shear force along y-axis	lb
F_{cx}	= cutting force along x-axis	lb
F_{cy}	= Cutting force along x-axis	lb
F_{cz}	= Cutting force along z-axis	lb
F_{c1}	= Force in load cell #1	lb
F_{c2}	= Force in load cell #2	lb
F_{c3}	= Force in load cell #3	lb
F_{c4}	= Force in load cell #4	lb
F_{c5}	= Force in load cell #5	lb
F_{c6}	= Force in load cell #6	lb
$F_{cutting}$	= Cutterhead forces	lb
Fr	= Froude Number	-
γ	= Specific weight of water	lb/ft^3
g	= Gravitational constant	ft/s^2
Γ	= Torque	ft-lb (in-lb)
Γ_{cutter}	= Cutterhead torque	ft-lb (in-lb)
h_i	= Initial thickness of layer cut	in
$\bar{H}$	= Average horizontal cutterhead force	lb
ι	= Angle of blades with axis cutterhead	rad
φ	= Angular position of cutterhead blade	rad
φ_{IN}	= Angular position of cutterhead blade through entire cut	rad
φ_o	= Angular position of cutterhead blade at start of cut	rad
κ	= Cutterhead profile angle	rad
k_m	= Average permeability	ft/s
k_{max}	= Maximum permeability	ft/s
l	= Length of cutterhead along axis	in
λ_c	= Hydrostatic pressure factor	-
m	= Ratio of cutterhead tangential velocity to swing speed	-

		Units
n	= porosity	%
n_i	= Initial porosity	%
n_{max}	= Maximum porosity	%
n_{cr}^{w}	= Wet critical porosity	%
N	= Normal force of sand on cutting blade	lb
$\bar{N}$	= Average normal cutterhead force	lb
N_{cutter}	= Cutterhead rotational speed (rpm)	rpm
Ω	= Angle covered by blade of excavating element	rad
Ω_o	= Total angle covered (cutterhead)	rad
P	= Power	hp
p	= Cutterhead blade pitch	-
$p_{cavitation}$	= Cavitation pore pressure	psi
R	= Resultant force of N and S	lb
r	= Cutterhead radius	in
Re	= Reynolds Number	-
ρ_{water}	= Water density	lb/ft^3
S	= Shear force of cutting blade due to sand	lb
$\bar{T}$	= Average tangential cutterhead force	lb
$\bar{V}$	= Average vertical cutterhead force	lb
V_c, v	= Cutting velocity	in/s
V_{swing}	= Cutterhead swing velocity	in/s (ft/min)
W_{aa}	= Weight of articulating ladder and cutterhead	lb
W_{lad}	= Weight of dredge carriage ladder	lb
θ	= Dredging angle	degrees
θ_o	= Angle between cutting force and x-axis at start of cut	rad
θ_{IN}	= Angle between cutting force and x-axis through entire Cut	rad
ξ	= Top angle covered by blade of excavating element	rad

TABLE OF CONTENTS

LIST OF FIGURES

FIGURE Page

LIST OF TABLES

CHAPTER I
INTRODUCTION

Dredging

Dredging in the world today is a very important aspect on the world's economy because without dredging shipping channels, wetlands, ports and harbors etc. would be in great distress due to sediment buildup in these areas. To keep pace with the great demand for dredging, improvements in dredging technology and the manufacturing of new dredges have to be satisfied. A lot of time and money have gone into the research and development in different dredging areas, so that new and more productive dredges can be built to satisfy this great demand in dredging.

Studies have been done in a number of areas of the aspect of dredging and one specific area is cuttersuction dredges. Cuttersuction dredges are used in all aspects of dredging and an example of a cuttersuction dredge can be seen in Figure 1 which is one of the largest dredges to date. Figure 1 shows the locations of the cutterhead, swing pulleys, dredge pump, ladder, and the dredge control tower.

The main components on a cuttersuction dredge are the cutterhead and the suction pump. The cutterhead is basically a digging device that is lowered into the sediment bed to loosen or cut into the sediment where it can be pumped by the dredge pump and placed in a desired placement area or where it can be used for various projects such as building wetlands and beach nourishment etc. There are two main types of cuttersuction dredges in production, one is the fixed spud configuration and the other is the spud carriage configuration and these are shown in Figure 2 and Figure 3.

This thesis follows the style and format of the Journal of Dredging Engineering.

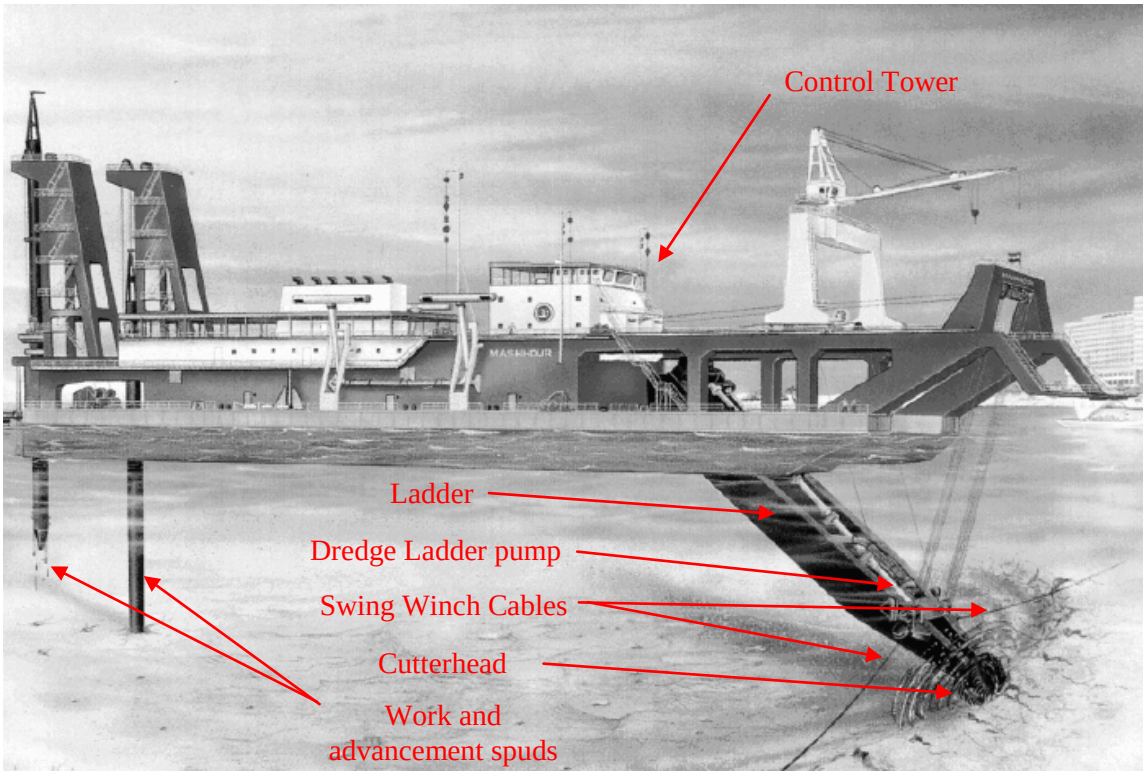

Figure 1. Prototype cuttersuction dredge (Vlasblom 2005)

The fixed spud configuration uses an advancement spud shown in Figure 2 to advance forward through the sediment. The digging operation consist of swinging approximately 45 degrees to the starboard and then swinging back approximately 35 degrees and then dropping your advancement spud and raise your work spud and then continue in the port direction approximately 20 degrees and drop the work spud and raise the advancement spud and this operation is repeated until the dredging operation is done (Herbich 2000).

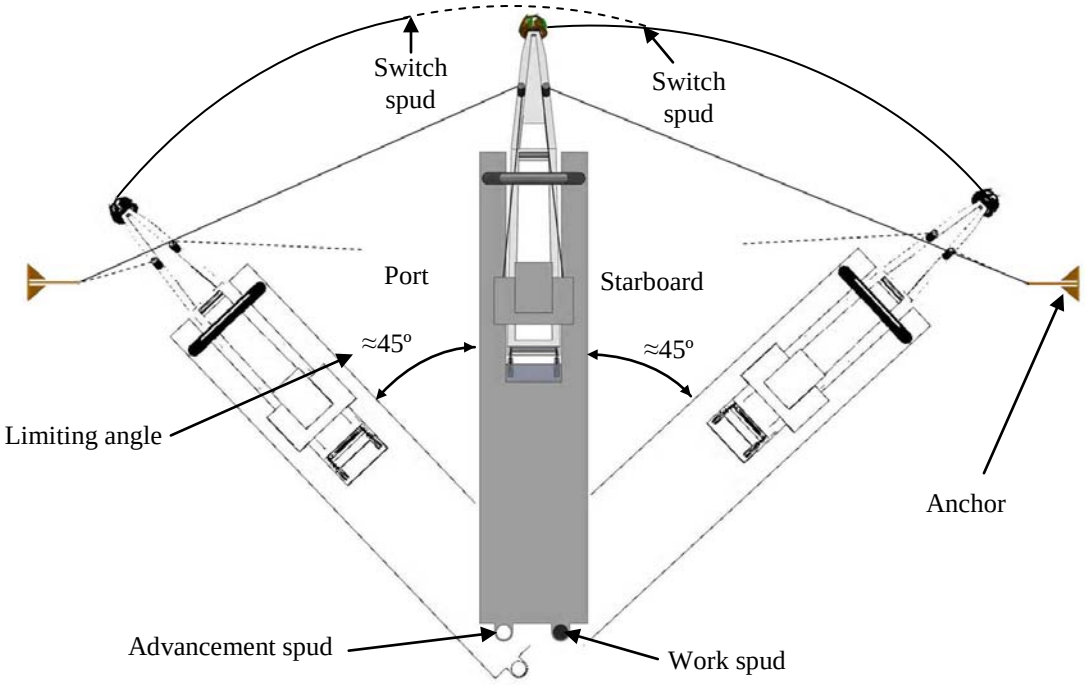

Figure 2. Example of fixed spud cuttersuction dredge

The second main type of cuttersuction dredge is the spud carriage configuration which is shown in Figure 3. This configuration is a little different than the fixed spud configuration because it has a spud carriage reset and not an advancement spud. Also, the production for the fixed spud cuttersuction dredge is around 50 percent and the spud carriage cuttersuction dredge is 75 percent and this is due to the way the two different configurations advance (Herbich 2000). The spud carriage cutting procedure consists of swinging approximately 45 degrees starboard and then advance and start swinging to the port and this process is repeated until the spud carriage has to be reset by dropping the reset spud and then the process can be repeated as many times as needed to finish the dredging project (Herbich 2000).

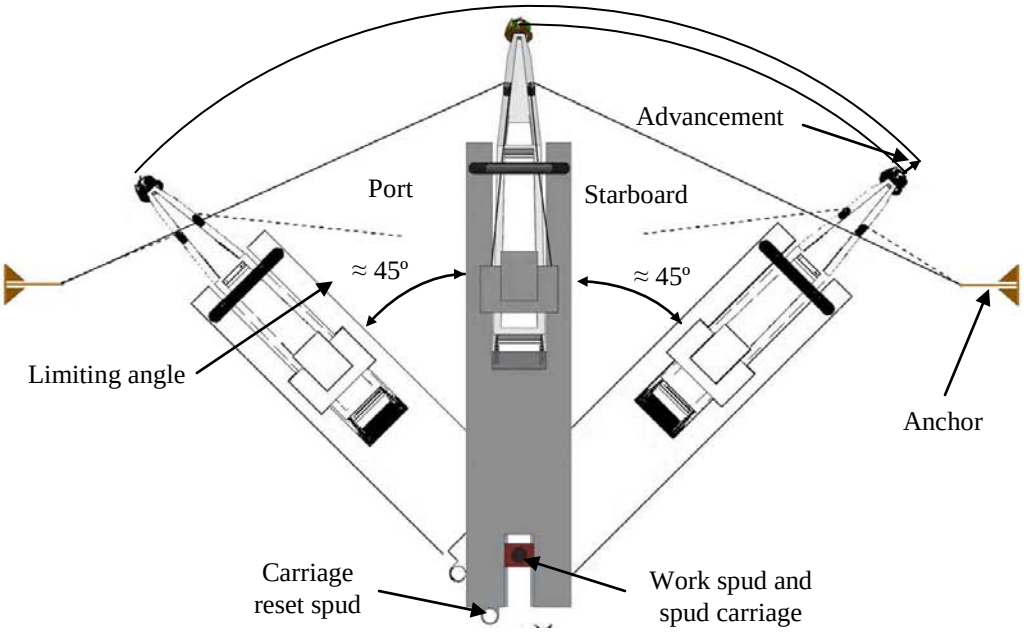

Figure 3. Example of spud carriage cuttersuction dredge

Purpose of Study

The purpose of this research of cutting forces on a laboratory cuttersuction dredge model was to produce cutting force results using force transducers on the dredge carriage ladder to determine these cutting forces. Theoretical results of forces on a model dredge cutterhead were calculated and by doing that, the results can be compared with the results from the experimental procedure and can be determined if the results are accurate. The experimental results were obtained in the summer of 2008. These results show how the cutterhead reacts to the variables of depth of cut, cutter rpm, angle of cut, swing speed, and the advancement of the cutter. From this research the dredging industry can be benefited because if cutting forces are better understood then the dredging ladder design and its supports can be optimized. Also, the design of the swing winches and cables used on the dredge can be optimized because the forces on the cutterhead are better understood. So, this research will better define the forces on the cutterhead and compare theoretical results with experimental results.

So, by knowing the forces on the cutterhead using this concept of using the dredge carriage at the Haynes Coastal Engineering Laboratory many studies can be done in the future. This research was also performed to develop a system of equations that can be used to take the readings from the force transducers and determine the forces at the cutterhead. Also, this study was conducted to determine if the forces transducers are producing accurate readings.

CHAPTER II
PREVIOUS CUTTERSUCTION DREDGE CUTTING FORCE STUDIES

To be able to understand how cutting forces on a cuttersuction dredge cutterhead are determined, it is necessary to determine how the procedure has been done in the past and how the past studies will benefit this research. These studies need to be examined very carefully to make sure that good results are determined by the new cutting force research. So, the first step in determining cuttersuction dredge cutterhead forces is to review the information that has been previously gathered in this area of research.

The previous research review on cuttersuction dredge cutting forces has found information that pertains to this thesis. However, for most of the information found, it is based on theoretical calculations, but none of the studies that have been researched are similar to the concept used at the Haynes Coastal Engineering Laboratory. Also, most of the studies are dealing with prototype cutterheads and not model cutterheads. The first study that was observed was an example that takes into account the variables of cutting forces, line pull, and anchor holding force. Cutting force, line pull, and anchor holding force are all a function of the type of sediment being dredged, depth of cut, cutter RPM, and swing speed.

The line pull is considered a main part of the dredging operation because the line pull of the ladder must be greater than the cutting force plus however much force it takes to move the dredge itself (Turner 1996). This is true because if the cutting force is greater than the line pull then there is no swing velocity. So this is an example of how important cutting forces are in the dredging industry. The anchor force of the pull line also has to be greater than the cutting force because if the cutting force is greater, then the anchor will slip which causes production losses. It is said that the line pull force is approximated to be 1.5 to 1.6 times greater than the cutting force to overcome water, wind, wave, and current resistance (Turner 1996). When looking at Figure 2 and Figure 3 it can be seen that a fixed spud and spud carriage cuttersuction dredges are limited to

how far it can swing before it will run into the swing anchor cable. The limiting angle before the dredge starts to cut the swing anchor cable is less than or approximately 45 degrees and the line pull needs to be much greater at this angle because the component force is less due to this angle (Turner 1996). This is another important example of knowing the cutting forces. Also, the anchor is said to be designed to hold 1.6 to 2.0 times the cutting force to keep the anchor from slipping (Turner 1996). This procedure takes into account the assumptions of the cutting force and factors the load up on the line pull or anchor system as described above, but this procedure doesn't go into detail on how the cutting forces were calculated.

In a number of cases cutter horsepower is used to determine how much power is necessary to excavate material from a sediment bed, but a better estimate is calculated if torque or cutting force is used to determine how much power is necessary (Turner 1996). To calculate the torque or cutting force, Equations 2.1 and 2.2 are used. In Equation 2.1, HP is the horsepower delivered to the cutter drive and RPM is the revolutions per minute of the cutterhead. In Equation 2.2 the cutter radius is the mean radius of the cutter head and cutting force is the force per inch of the length of the cutterhead (Turner 1996). So from Equations 2.1 and 2.2 the cutting force can be estimated if the cutter horsepower and cutter RPM is known. This calculation is an estimate of the cutting force because the only variables associated in Equations 2.1 and 2.2 are cutter radius, torque, and cutter RPM and the variables of depth of cut, swing speed etc. are not taken into account, but as for the current research will give a more precise estimate of cutting forces because these variables are accounted for.

$$\mathrm{HP} = \frac{\text{torque} \times \mathrm{RPM}}{5250} \tag{2.1}$$

$$\text{Torque} = \text{cutting force} \times \text{cutter radius} \tag{2.2}$$

The next cutting force calculation takes into account a totally different concept, which consist of taking one blade of the cutterhead and applying frictional effects of saturated sand to find out the cutting forces on each blade of the cutterhead. This is a much more in depth calculation and is fully explained in Miedema (1987 and 1989), and this review only gives an overview of the calculation of cutting forces on one blade in saturated sand. Shown in Figure 4, the F_S (force in swing direction), and F_v (force on cutter in vertical direction) can be seen with the variation in swing velocity direction (V_s). The direction of V_s determines whether the dredge cutter is overcutting or undercutting. These forces were defined by Miedema (1989) which described the reaction force on each cutting blade. The basic model that was used in the two-dimensional calculation can be seen in Figure 4, which involves the example of one cutting blade being pushed through the sediment. This movement through the sediment produces a shear plane that develops from the tip of the cutting blade to the top of the cutting layer and this shear plane develops at a shear angle β. The cutting blade has a set angle (α) and height (h_b) and has a constant cutting velocity (v_c). Using this two dimensional method the horizontal and vertical cutting force Equations 2.3 and 2.4 were developed by Miedema (1989).

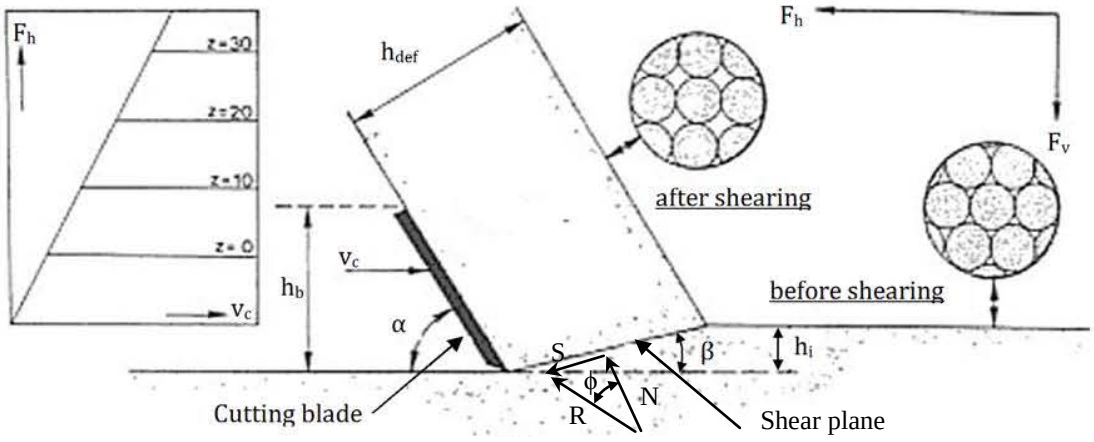

Figure 4. Two-dimensional cutting process (Miedema 1989)

$$F_{hnc} = c_1 \cdot \rho_w \cdot g \cdot v_c \cdot h_i^2 \cdot b \cdot e/k_m \quad (2.3)$$

$$F_{vnc} = c_2 \cdot \rho_w \cdot g \cdot v_c \cdot h_i^2 \cdot b \cdot e/k_m \quad (2.4)$$

$$e = \frac{n_{max} - n_i}{1 - n_{max}} \quad (2.4a)$$

$$k_m \approx 0.5 \cdot k_i + 0.5 \cdot k_{max} \quad (2.4b)$$

Equations 2.3 and 2.4 were determined for the non cavitation case which means that the absolute pore pressure has not reached water vapor pressure, and further calculations were done to determine the cutting forces on one blade for the cavitation case (Miedema 1987). The cavitation of the blade has a strong influence on the cutting forces. The area of cavitation and non-cavitation is shown in Figure 5 (lower) for the undercutting case. Equations 2.5 and 2.6 were developed for the horizontal and vertical cutting forces when cavitation is present in the cutting process. In Equations 2.3, 2.4, 2.5, and 2.6 the coefficient c_1, c_2, d_1, and d_2 are all dependent on ϕ (angle of internal friction of sand shown in Figure 4), δ (soil interface friction angle), α (blade angle), and h_b/h_i (blade height-shell thickness ratio) (Miedema 1989).

$$F_{hca} = d_1 \cdot \rho_w \cdot g \cdot (z + 10) \cdot h_i \cdot b \quad (2.5)$$

$$F_{vca} = d_2 \cdot \rho_w \cdot g \cdot (z + 10) \cdot h_i \cdot b \quad (2.6)$$

So, to be able to use the horizontal and vertical cutting force equations for the non-cavitation and cavitation case for a typical cutting process of a cuttersuction dredge, a different concept had to be implemented to be able to find the axial, swing, vertical cutting forces developed on the cutterhead. This process takes into account three dimensions and this is when the axial force comes into effect. In Figure 5, the coordinate system that is used is shown, and in the figure all of the variables that have an

effect on the axial, swing, and vertical cutting force calculations are shown. Also, the effects of undercutting and overcutting are demonstrated in the figure.

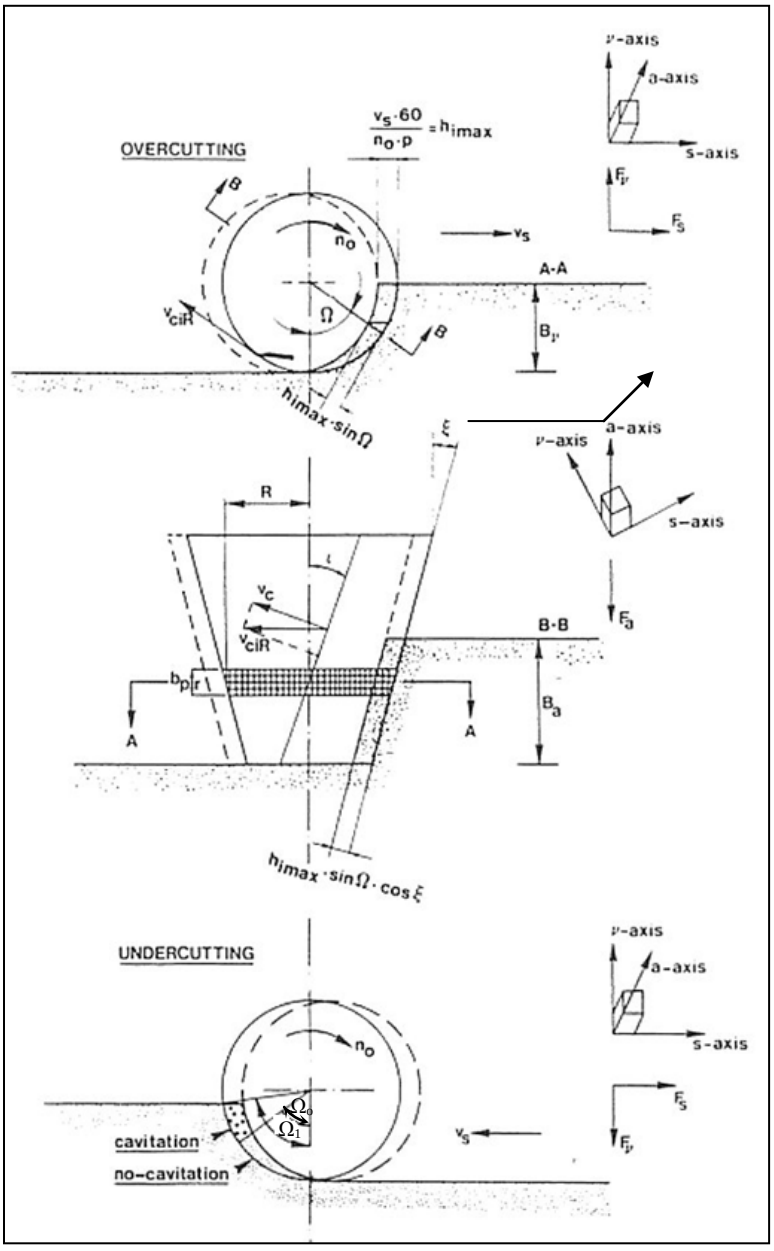

Figure 5: Description of forces on cutter when overcutting (Top) and undercutting (Bottom) (Miedema 1989)

So, by using Figure 5 and Equations 2.3, 2.4, 2.5, and 2.6 the axial, swing, and vertical cutting forces were developed by Miedema (1987) and are illustrated by Equations 2.7, 2.8, and 2.9. From Equations 2.7, 2.8, and 2.9 it can be concluded that the axial force (F_a), the swing force (F_s), and the vertical force (F_v) can be determined, however in these equations there are a lot more assumptions and calculations and are described in detail in Miedema (1987) and (1989). However, these equations are somewhat simplified and some conclusions can be drawn on how to calculate cutting forces in the axial, swing, and vertical directions. In looking at Equations 2.8 and 2.9 it can be seen that a plus sign indicates overcutting and undercutting is indicated by the minus sign (Miedema 1989). In Equations 2.7, 2.8, and 2.9, the cutting forces are a function of the horizontal cutting force (F_h), vertical cutting force (F_v), angle of blades with axis cutterhead (ι), angle covered by blade of cutterhead (Ω), and top angle conical cutterhead (ξ). However, to get a total force on the cutterhead the cutting forces F_a, F_s, and F_v have to be integrated over one blade to get a total force for one blade on the cutterhead. This integration is done by using Equation 2.10 which takes into account each integration of the three cutting forces. So, this equation can be used to determine the total force on the cutter, where Ω_o is the angle that the blade covers, p is the number of blades on the cutter, and F_{ct} , F_c can be replaced with F_{at}, F_a and F_{st}, F_c and F_{vt}, F_v (Miedema 1989). However, it is said that the integration used in Equation 2.10 is very difficult to solve and it was said that the calculation would take over 15 pages, so for this review the integration was not attempted but it can be reviewed in Miedema's dissertation.

$$F_a = F_h * \sin\iota * \cos\xi - F_v * \sin\xi \tag{2.7}$$

$$F_s = F_h \cos\iota * \cos\Omega \pm (F_h \sin\iota * \sin\xi + F_v \cos\xi) * \sin\Omega \tag{2.8}$$

$$F_v = F_h \cos\iota * \sin\Omega \pm (-F_h \sin\iota * \sin\xi + F_v \cos\xi) * \cos\Omega \tag{2.9}$$

$$F_{ct} = \frac{p}{2\pi}\int_0^{\Omega_0} F_c \, d\Omega \qquad (2.10)$$

It has been seen that cutting forces on a dredge cutterhead can be very complicated and very drawn out. There have been some very complex and very simple methods applied in determining the cutting forces as seen above. However, cutting procedures have been researched for a number of years and there is one program that was implemented between 1970 and 1978 in the area of cutting of sand under water (Van Os 1987). This study used a cutting blade that was pushed though the sediment and from this process cutting forces were determined based on the shape of the cutting blade (Van Os 1987). This is an example of how basic cutting forces were determined and from these basic forces the cutting procedure improved the understanding of the process of excavating sediment under the water. This study improved the understanding of how the cutting process works and from this understanding more productive dredges could be designed and built.

It is said that to have excavation equipment that is good quality and productive it is important that theoretical models are used so that cutting forces and power estimates of dredges can be estimated effectively (Van Os 1987). So a theoretical model was needed to improve the understanding further of the cutting process of a dredge. For this model the same principles were applied as Miedema's procedure in determining cutting forces on one single cutting blade. The process used in this theoretical calculation is shown in Figure 6 which demonstrates all forces in cutting a set sediment layer thickness (h=cutting depth, h_m=the blade height , v=the cutting velocity, α=the blade angle). From this distribution of force, Equation 4 and 5 where developed by Van Os and Van Leussen (1987), which represent the horizontal and vertical component forces acting on the cutterhead blade, but this calculation only takes into account the two-dimensional problem and that means that no axial force can be calculated.

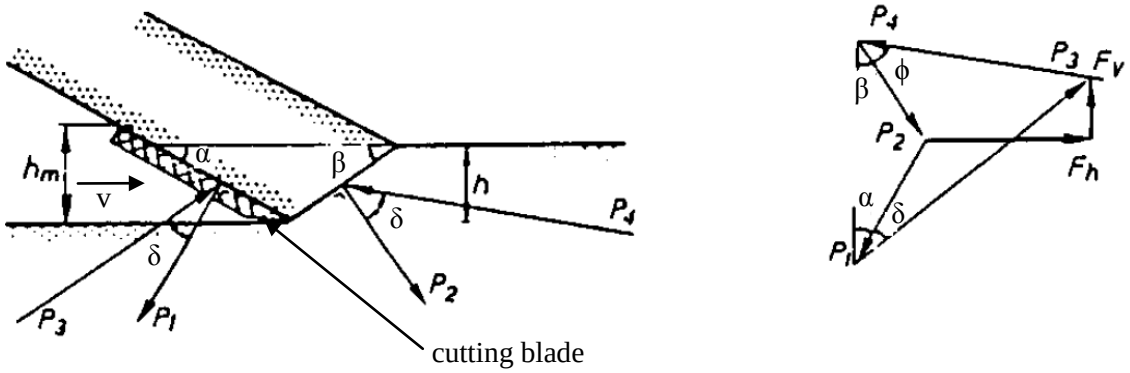

Figure 6: Force equilibrium of cutting process (Van Os 1987)

In the Equations 2.11 and 2.12 f_1 and f_2 are functions of α, β, δ, and ϕ and are shown by Equations 2.13 and 2.14. If no cavitation is present then Equation 15 is used and if cavitation is present then Equation 2.16 is used to substitute into Equations 2.11 and 2.12. Again a number of assumptions and experimental values have to be implemented into these equations to get the total cutting forces on the dredge cutterhead and more detailed calculations and assumptions to these equations can be found in Van Os and Van Leussen (1987).

$$F_h = \gamma bhH[p_1 f_1 + p_1 f_2] \tag{2.11}$$

$$F_v = \gamma bhH[p_1 f_1 \cot g(\alpha + \delta) - p_2 f_2 \mathrm{cotg}(\beta + \phi)] \tag{2.12}$$

$$f_1 = \frac{\sin(\alpha+\delta)\cdot\sin\phi}{\sin(\alpha+\beta+\delta+\phi)} \tag{2.13}$$

$$f_2 = \frac{\sin(\alpha+\phi)\cdot\sin\delta}{\sin(\alpha+\beta+\delta+\phi)} \tag{2.14}$$

$$H = h \cdot \frac{v}{k'} \cdot \frac{n_{cr}^{w} - n_1}{1 - n_{cr}^{w}} \tag{2.15}$$

$$H = D + 10 \tag{2.16}$$

So, looking at the current overview it can be seen that cutting forces that are induced on the cutterhead of a dredge can be researched in great detail. However the current research at Texas A&M University only took into account the forces produced by the dredge carriage cutterhead and from those forces equations were found to satisfy the calculated theoretical values, and these values are compared with the experimental values gathered in the summer of 2008 in the proceeding chapters.

The final cutting force study that was found consists of the same principles as the above studies, but this study is slightly more straightforward. So, this theoretical calculation of forces on a cutterhead starts out with a free body diagram of one cutting tooth which is demonstrated in Figure 7. This shows each individual force that is acting on the cutting tooth with respect to the center of the cutterhead. So, to determine the tangential force on the cutterhead the pole-coordinate of tooth for y_c (φ_0), the angle between cutting force and X-axis for y_c (θ_0), pole coordinate of the result force (φ_{IN}), and the angle between cutting force and X-axis for the result force (θ_{IN}) have to be determined. The equations for φ_0, θ_0, φ_{IN}, and θ_{IN} were developed by Vlasblom (1998) and are shown below in Equations 2.17, 2.18, 2.19, and 2.20. In these equations the value (m) is the ratio of swing speed over cutter speed.

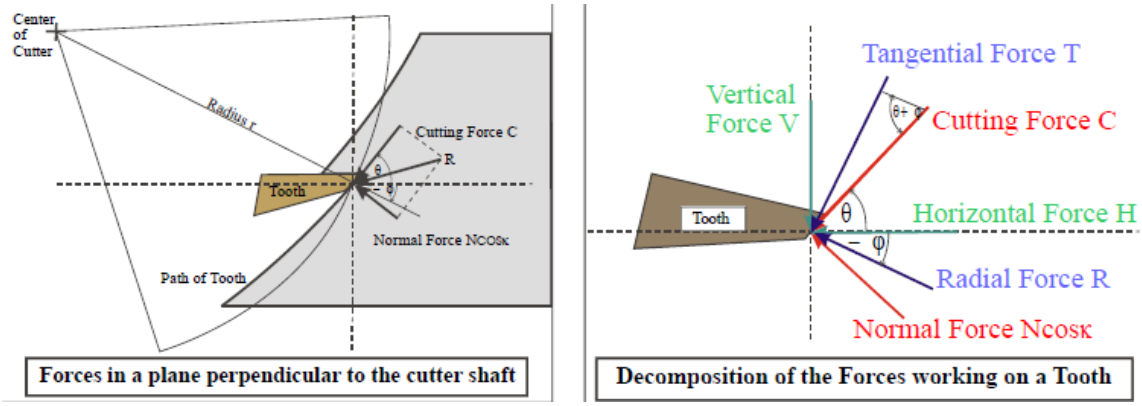

Figure 7. Forces acting on one cutting tooth (Vlasblom 2005)

$$\varphi_0 = \arcsin\left(\frac{D_c}{r} - 1\right) \tag{2.17}$$

$$\theta_0 = \arctan\left[\frac{\cos\varphi_0}{m - \sin\theta_0}\right] \tag{2.18}$$

$$\theta_{IN} = \frac{\theta_0 \cos\theta_0 - \sin\theta_0}{\cos\theta_0 - 1} \tag{2.19}$$

$$\varphi_{IN} = \theta_{IN} - \arccos(m \cdot \sin\theta_{IN}) \tag{2.20}$$

Now by using Equations 2.17, 2.18, 2.19, and 2.20 the mean tangential force on a cutterhead ($\bar{T}$) was developed by Vlasblom (1998) and is shown in Equation 2.21. In this equation the b_c/b_n is considered the ratio of cutting force to normal force which is assumed to be approximately 8 for a cutting blade that is sharp and this number could be as low as 0.5 depending on the wear of the cutting tooth (Miedema 1987). However, with this information Equation 2.21 cannot be determined because the mean normal force ($\bar{N}$) is unknown, but Equations 2.22 and 2.23 can be used to calculate the mean tangential force and from that calculation the mean normal force can be determined by back calculating Equation 2.21 (Glover 2002).

$$\overline{T} = \overline{N}\left[\frac{b_c}{b_n}\sin(\theta_{IN} - \varphi_{IN}) - \cos\kappa\cos(\theta_{IN} - \varphi_{IN})\right] \quad (2.21)$$

$$\frac{P_{cutter}}{N_{cutter}}63025 = \Gamma_{cutter} \quad \text{(in-lb)} \quad (2.22)$$

$$\frac{\Gamma_{cutter}}{D_{cutter}\ /2} = \overline{T} \quad (2.23)$$

Now that the mean tangential and mean normal forces can be calculated the mean horizontal, vertical, and axial forces can be determined by using Equations 2.24, 2.25, and 2.26 which were developed by Vlasblom (1998). In the axial force calculation equation the value κ is the profile angle of the cutterhead.

$$\overline{H} = \overline{N}\left[\frac{b_c}{b_n}\cos\theta_{IN} - \cos\kappa\cos\theta_{IN}\right] \quad (2.24)$$

$$\overline{V} = \overline{N}\left[\frac{b_c}{b_n}\sin\theta_{IN} - \cos\kappa\cos\theta_{IN}\right] \quad (2.25)$$

$$\overline{A} = \overline{N}\sin\kappa \quad (2.26)$$

Also, in Vlasblom (2005) there are some simplified calculations of the horizontal, vertical, and axial cutting forces. Shown in Figure 8 is a free body diagram of an entire cuttersuction dredge which demonstrates all of the forces acting on the dredge. If the vertical, horizontal, and axial forces on the cutterhead are to be assumed constant and which this assumption which can be made only if the specifics of the soil conditions are desirable, then Equation 2.27 can be used to estimate the forces on the cutterhead (Vlasblom 2005).

$$\frac{F_h R_{cutter}}{M_{cutter}} = c_h,\ \frac{F_v R_{cutter}}{M_{cutter}} = c_v,\ \frac{F_a R_{cutter}}{M_{cutter}} = c_a \quad (2.27)$$

The R and M in Equation 2.27 is the cutter radius and cutter torque, and the values for c_h, c_v, and c_a are said to be constant which was stated before and these values are c_v =0.9, c_a =0.4, and c_h is equal to 1 when undercutting and equal to 0.6 when overcutting (Vlasblom 2005). These equations again are considered very basic and only give a rough estimate of the cutterhead cutting forces and if more precise estimates are desired then Equations 2.24, 2.25, and 2.26 can be used.

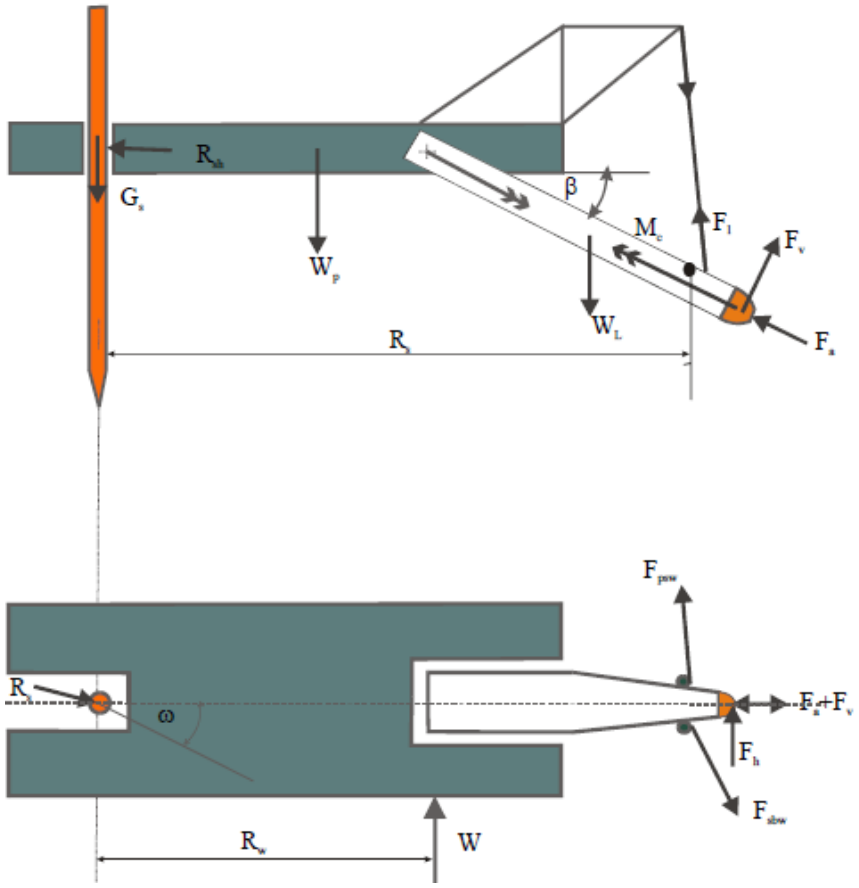

Figure 8: Free body diagram of cuttersuction dredge (Vlasblom 2005)

Finally, Glover (2002) determined all of the preliminary designs for a model dredging system for the Haynes Coastal Engineering Laboratory at Texas A&M University

College Station campus. These preliminary designs consisted of the designs for a structural system for a dredge-tow carriage model, laboratory setup of the dredge carriage, and all of the similitude calculations for all of the dredge carriage components. For the current research some of the preliminary calculations were reviewed so that they could be implemented into the current research. This review consists of how the forces on the dredge carriage ladder were determined. In Figure 9 the free body diagram of the articulating arm and cutterhead are shown. This demonstrates how the cutting force on the cutterhead are applied which is similar to the system that was used in previous studies. From this system of the free body diagram the static equilibrium equation were written for the articulating arm and cutterhead system. The equilibrium equations that were developed for the articulating arm and the cutter are shown by Equations 2.28 – 2.33 which Equations 2.28, 2.29, and 2.30 are summation of static forces in the x, y, and z directions and Equations 2.31, 2.32, and 2.33 are the summation of static moment forces in the x, y, and z directions. Now these equations can be used to do further calculations on the dredge carriage ladder.

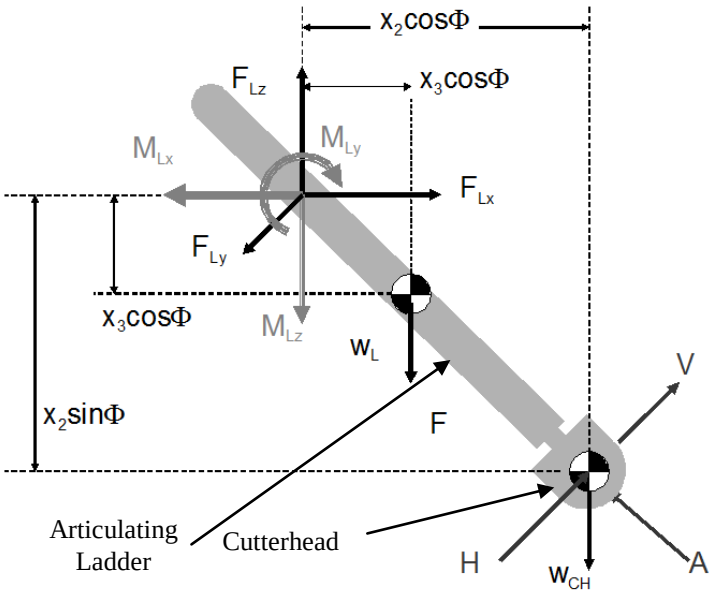

Figure 9: Free body diagram of articulating ladder (Glover 2002)

$$F_{LX} = -V \sin \Phi + A * \cos \Phi \quad (2.28)$$

$$F_{LY} = H \quad (2.29)$$

$$F_{LZ} = W_L + W_{CH} - V * \cos \Phi - A * \sin \Phi \quad (2.30)$$

$$M_{LX} = Hx_2 \sin \Phi \quad (2.31)$$

$$M_{LY} = Vx_2 \cos \Phi - W_L x_3 \cos \Phi - W_{CH} x_2 \cos \Phi \quad (2.32)$$

$$M_{LZ} = Hx_2 \sin \Phi \quad (2.33)$$

Now that the equilibrium static equations are known for the articulating arm and cutterhead, they can be used to determine the forces applied to the dredge carriage ladder. In Figure 10 the dredge carriage free body diagram is shown which shows all of the forces acting on the ladder from the articulating arm. So, a summation of forces can be applied to find the static equilibrium equations for the ladder and from those equations and Equations 2.28 – 2.33, the forces F_{AZ}, M_{PM}, and M_{CM} can be determined. So, this method of determining the static equilibrium equations will be implemented in the current cutting force research and will be discussed in the following chapters.

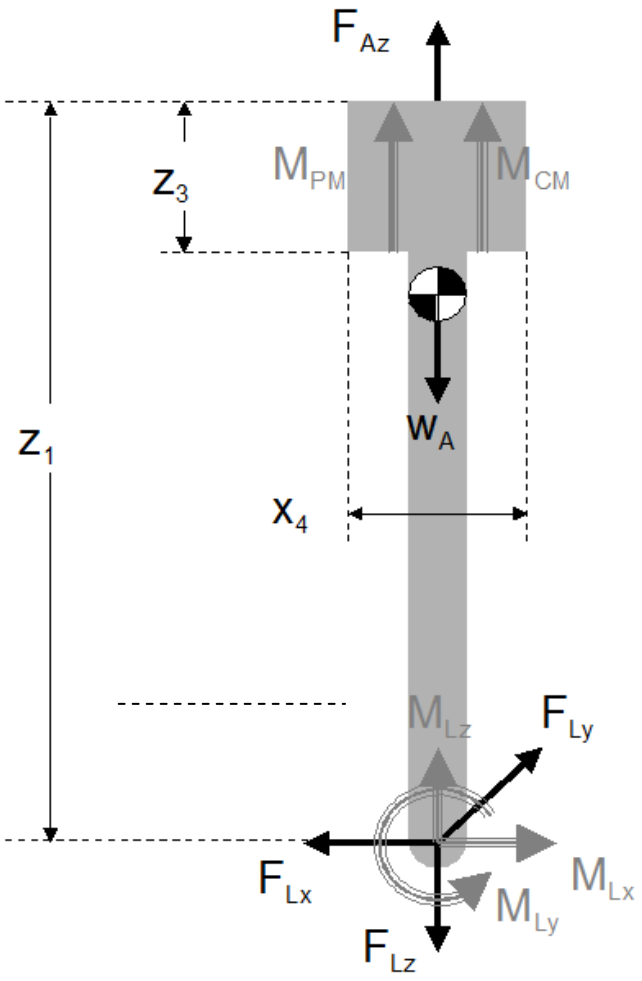

Figure 10. Free body diagram of ladder (Glover 2002)

CHAPTER III
FACILITY AND OVERVIEW OF DREDGE CARRIAGE MODEL

Forces induced on the cutterhead are very important which has been seen from the previous chapter, and these forces can be transmitted from the cutterhead up through the ladder to the ladder supports that could cause problems if not properly designed. Also, the cutting forces are significant when trying to design the swing winches and deciding what type of swing anchors to use. From this, it shows that forces on the cutterhead are important and these forces have demonstrated great interest for many researchers. This research topic has been researched by a number of researchers including S. A. Miedema, A.G. van Os, W. van Leussen, and W. J. Vlasblom which was reviewed extensively in the previous chapter.

The current cutting force research, which was performed at the Haynes Coastal Engineering Laboratory, considers an entirely new concept on how the forces on the cutterhead are determined. This concept takes into account the cutting forces acting in the vertical, horizontal, and axial directions of the entire cutterhead and not just on one blade of the cutterhead like what was done in previous studies. This concept entails using the dredge/tow carriage in the dredge/tow tank facility at Texas A&M University. The dredge tow tank, dredge carriage, and the force measuring and data acquisition systems are discussed in the following.

Dredge-Tow Tank

The construction of the Haynes Coastal Engineering Laboratory was started in August 2001 and was dedicated in June 2003 (Randall et al 2005). The Haynes Laboratory consists of a shallow water wave basin and the dredge/tow flume which are positioned side by side in the facility and both tanks have the capacity of 2,233 L/s (35,000 GPM) of water being pumped through them. A top and side view of the dredge/tow flume is shown in Figure 11 and all of the dimensions were taken from Randall et al (2005). The dredge/tow flume is oriented in the west to east direction and it is approximately 45.6 m (149.5 ft) in length and has a width of 3.66 m (12 ft). The dredge/tow flume has the capacity of a safe maximum water level of 3.05 m (10 ft). The flume is equipped with a sediment pit measuring 7.56 m (24.8 ft) in length and 3.66 m (12 ft) wide and a depth of 1.52 m (5 ft), also along the north flume wall there is an observation well where the sediment pit can be viewed when a test is in progress. The flume has a water diffuser on the west end which was mentioned earlier that could produce a flow of 2,233 L/s (35,000 GPM) if needed, and in the east end of flume there is a lower and upper weir which can be used to control the water level in the tank. Also, the shallow water wave basin and the dredge/tow flume are equipped with a collection tank that can be used to drain most of the water in the tanks in a matter of minutes if needed.

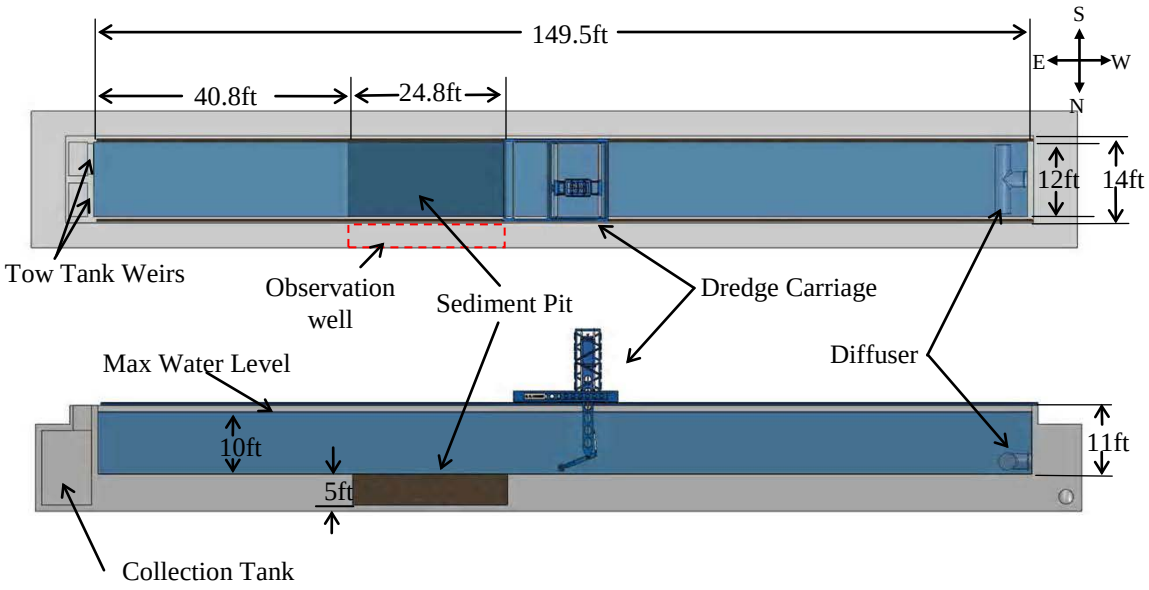

Figure 11. Tow tank description (dimensions in ft, divide by 3.28 for m)

Dredge Carriage

The dredge/tow carriage conceptual design was completed by Glover in 2002 and Glover and Randall in 2004, and the final design, construction of carriage, and installation in coastal facility was completed by Oilfield Electric Marine (OEM), Inc and Digital Automation and Control Systems, Inc. (DACS). In April of 2005 the dredge/tow carriage was delivered and installed in the Haynes Laboratory. The finalized dredge tow carriage is shown in Figure 12. In Figure 12 the locations of the ladder cradle, upper and lower ladder, articulating arm, and cutterhead are demonstrated. The dredge/tow carriage is oriented in a north, south, east, and west directions, and these directions are used to describe locations of instrumentation on the dredge carriage. The carriage is positioned on top of two guide rails (similar to that of a locomotive) at the top of the dredge/tow flume and these guide rails are oriented in the west to east direction.

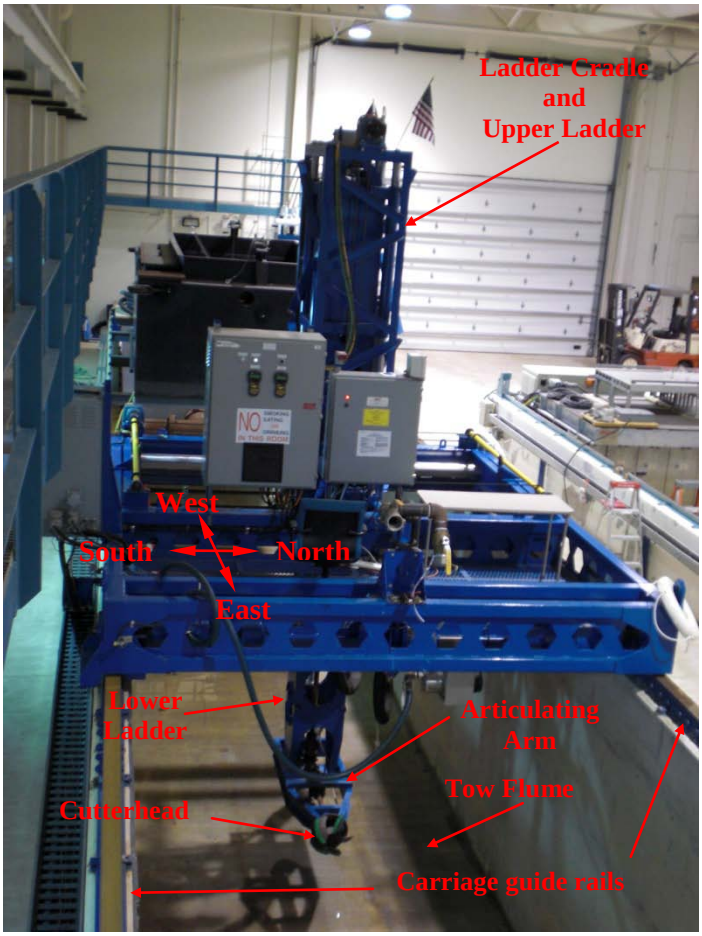

Figure 12. Prototype dredge carriage

The dredge carriage is considered to be 1:6 scale of a 0.609 m (24 in) prototype cuttersuction dredge, which means the carriage is equipped with a suction inlet of 0.102 m (4 in) and a discharge of 0.076 m (3 in). The carriage is equipped with a density gauge and a flow meter which are considered very useful when dredging is concerned, because using these two instruments, the production can be calculated for a dredge test along with other quantities. The carriage has the capacity of dredging at a ladder angle of 0 to 50 degrees, and has an estimated ladder weight of 909 kg (2,000 lb) which will be used to compare to the modeled ladder in the following. In Table 1 are further characteristics and capacities of the dredge/tow carriage. The dredge/tow carriage drive systems are controlled with digital variable frequency drives or by servo drives, which

are said to have accurate rates of acceleration and can maintain constant velocities (Randall et al 2005).

Table 1. Characteristics of dredge/tow carriage (Randall et al 2005)

Category	Characteristic
Maximum Carriage Speed	2 m/s (6.6 ft/s)
Distance to reach constant speed	3.1 m (10 ft)
Total Dredge/Tow Carriage Weight	4545 kg (10,000 lb)
Cradle Weight	1364 kg (3,000 lb)
Ladder Weight	909 kg (2,000 lb)
Carriage Power	Two 3.8 kW (5 hp) motors
Cutter Power	7.5 kW (10 hp)
Pump Power	14.9 kW (20 hp)
Side to Side Cradle Motor Power	1.1 kW (1.5 hp)
Vertical Ladder Motor Power	1.1 kW (1.5 hp)
Articulating Ladder Position Motor Power	0.5 kW (0.8 hp)
Dredge Pump Flow Rate	Maximum 1893 LPM (500 GPM)
Dredge Pump Size	10.4 cm (4 in), suction; 7.62 cm (3 in), discharge
Control System	Wireless LPC Automated and manual operation
Data Acquisition	Real-time display and data storage (Microsoft Entivity)
Swing Travel	1.6 m (5.3 ft) on either side of flume centerline
Ladder Angle	0 to 50 degrees from horizontal

For this current cutting force research the dredge/tow carriage was drawn with a program called SolidWorks 2009, which is a three dimensional modeling software that is capable of determining weight, center of gravity, moment of inertia etc. of parts and assemblies within the program. In Figure 13 is the side and front view of the final SolidWorks model of the dredge/tow carriage and this model will be used to describe the measurements of the different parts equipped on the prototype dredge carriage. The main base of the carriage is 5.1 m (16.74 ft) in length by 4.04 m (13.27 ft) wide and 0.515 m (1.688 ft) high, the cradle is (10 ft) high and the upper and lower ladder has a total length of 6.05 m (19.85 ft) which has a vertical stroke of approximately 137.2 cm (54 in). The main piece of the dredge/tow carriage is the articulating arm measuring 1.7526 m (5.75 ft) in length and is capable of pivoting on the lower ladder so the dredging angle can be set without a problem for testing, and the most important piece is

the model dredge cutterhead with a mean diameter of 30.48 cm (12 in) and a total length of 26.035 cm (10.25 in). For further review of the dredge/tow carriage measurements Figure 13 can be referenced.

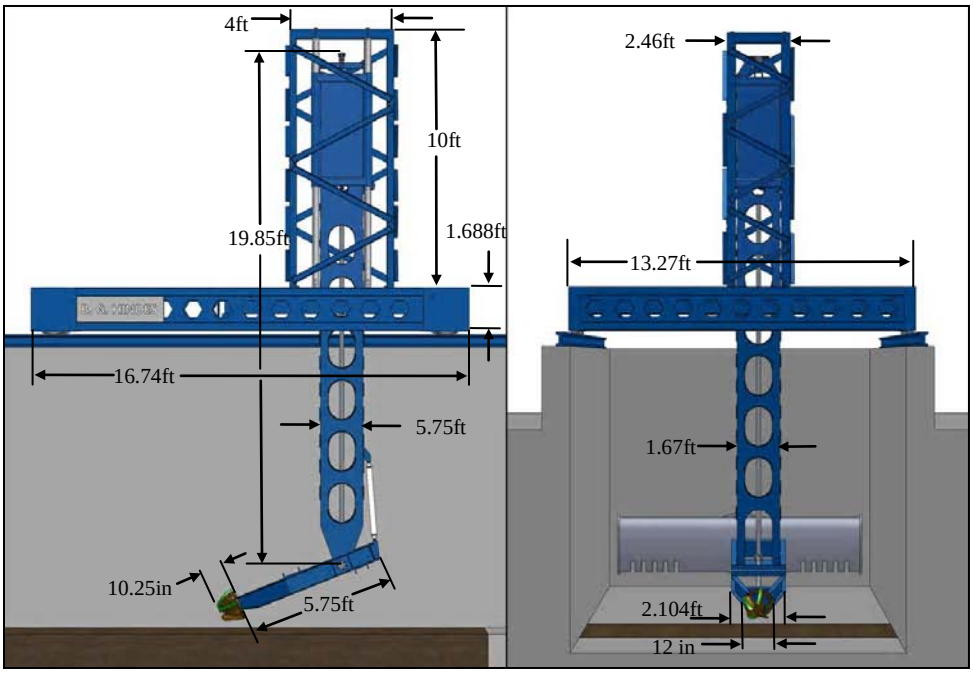

Figure 13. Plan and side view of dredge carriage (most dimensions are in ft, divide by 3.28 for m)

Carriage Force Measuring and Data Acquisition Systems

The dredge/tow carriage has the capacity of measuring forces that are produced by the upper and lower ladders and also capable of measuring the torque on the cutter shaft; however, for this cutting force study the torque sensor was not calibrated so the data couldn't be used. To measure forces on the ladder of the dredge carriage, the concept of using one dimensional load cells in various locations to get an accurate reading of the transmitted forces from the ladder system. The load cells were placed in locations that would keep the ladder as rigid as possible, so that the force readings could be measured accurately. The load cells that were used are a one dimensional 13.3 kN (3000 lb),

which were considered to have plenty of load capacity while doing a variety of testing for research projects. These load cells are Omega Engineering LC202-13.3 kN (3000 lb) gauges and have an accuracy of ± 0.25% which in this case is approximately 0.033 kN (7.5 lb) and the load cells have a ultimate over load of 300%, safe over load of 150%, and the output signal is 2 mV/V (Omega 2008). For the final design of the carriage, five of the 13.3 kN load cells were used and placed in the locations shown in Figure 14.

Load cell #1 was positioned where it would take most of the vertical load or weight of the ladder and this placement is shown in Figure 14 to be positioned in-between of the upper ladder and upper ladder cradle in the center of the ladder. Cell #2 is located on the upper south side of the middle of the ladder cradle and is oriented in a north to south direction which is assumed to take most of the load when a force in the north and south directions are applied to the cutterhead position. Cell #4 is positioned on the lower north side of the cradle and oriented in the north to south directions and it is assumed to take the same load as Cell #2. Cell #3 is located in the upper south-east corner oriented in a east to west direction and it is assumed to pick up load from torsional effect of the ladder and also pickup load when east or west forces are applied to the cutterhead. Finally, cell #5 is located on the lower north-west corner of the cradle oriented in a west to east direction and it is assumed that this load cell pick up the same loads as load Cell #3. In Figure 14 all of the load cell positions are shown, and also in the lower left-hand corner of the figure is a picture of the prototype position of the (3000 lb) load cell #5.

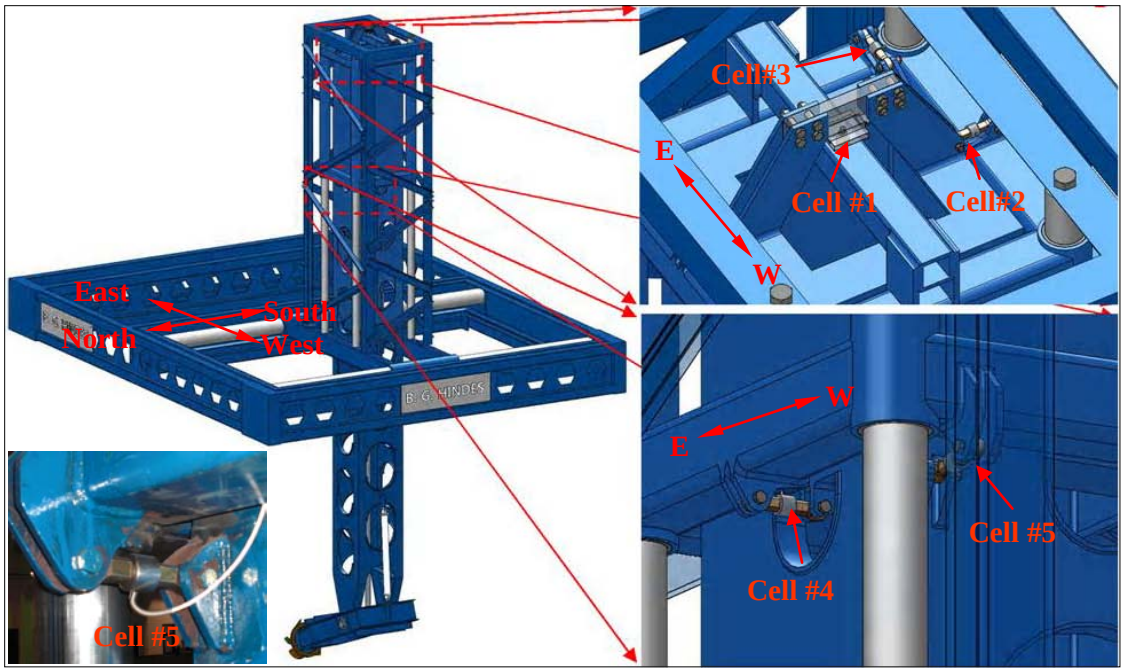

Figure 14. Description of load cell locations

The forces transducers are electronic sensors so a data acquisition is needed to record the data transmitted by the sensors. The dredge/tow carriage is equipped with a real-time display and data storage (Microsoft Entivity) systems (Randall et al 2005). The carriage interface is shown in Figure 15 and the interface consists of gauges for the vacuum and discharge pump pressures, and also consist of a density gauge that displays specific gravity and a velocity flow meter which displays feet per second. This interface also lets the user turn on the dredge pump or cutter drive motor at a click of the mouse. For the current research the five load cells were monitored while testing was in progress, and these gauges are shown in the upper right-hand corner of Figure 15. The force transducer gauges read a percentage of the maximum value of the load cells, which is approximately 13.3 kN (3000 lb), and these gauges have a range of ±100 percent. The negative represents or shows that the load cell is in compression and the positive means the load cell is in tension. The data from the load cells are gathered from the data acquisition system and then the PC stores the data in a text file, which can processed in

Matlab or Excel. This process of recording data is done at an interval of one Hz or one reading per second, so this gives plenty of data that can be used in a research experiment.

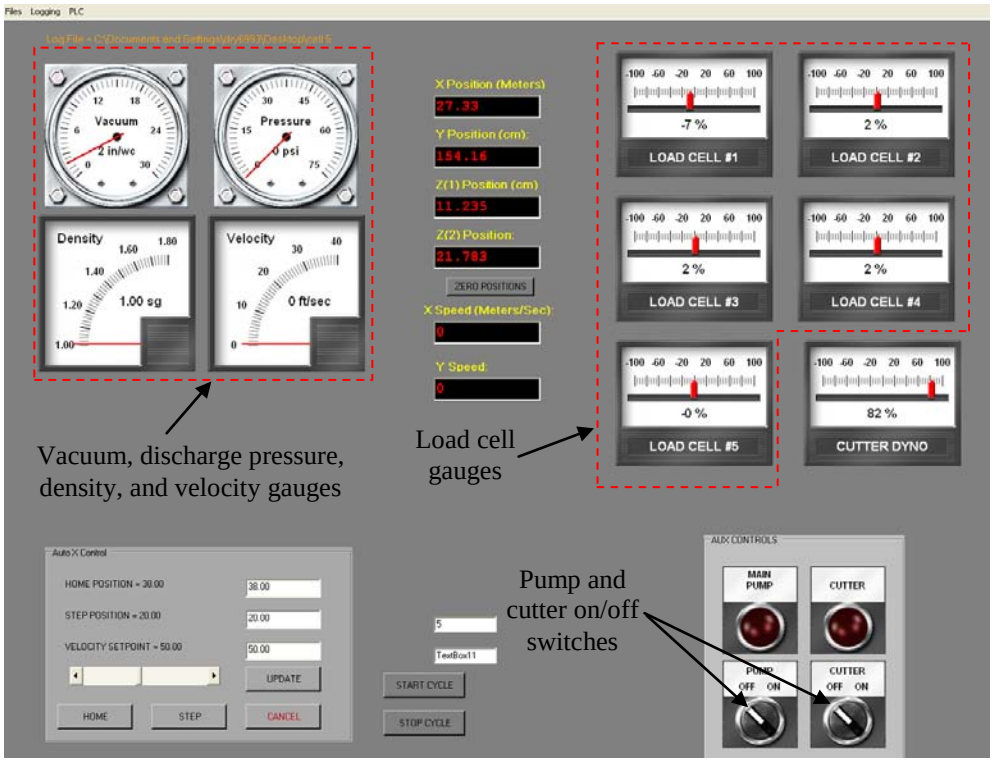

Figure 15. Interface of dredge carriage

CHAPTER IV
CALIBRATION PROCEDURE OF LOAD CELLS

For the current cutting force research a number of instruments on the dredge/tow carriage had to be calibrated to achieve optimum results. It is very important that instruments that are used in research are calibrated to a sufficient accuracy to achieve implemental results. On the dredge/tow carriage there are five load cells as seen in the last chapter, and these need to be calibrated. So, to be able to calibrate the five load cells on the carriage a procedure had to be developed for this calibration process. In the following, the procedure for the calibration of the five carriage load cells is developed and discussed in detail.

Calibration of Calibrator Cell

For the calibration of the five load cells another source of knowing the load on the carriage cells had to be known. This was done by using another load cell and this was an Omega Engineering LC202- 17.79 kN (4000 lb) one directional cell, and this cell has the same specifications as the LC-202- 13.3 kN cell. This cell is powered and the output (mV) recorded with a strain gauge indicator.

The calibration of the cell was accomplished using a 22.24 kN (5000 lb) laboratory scale. A 35.585 kN (8000 lb) come-along was used to apply the load to the load cell. In Figure 16 (left), it shows how the load cell, come-along, and lab scale were attached together and were linked together by 26.69 kN (3 ton) shackles and (3 ton) chain. In the figure it is shown that the configuration is attached to the floor by a floor anchor and the lab crane was used to secure the top of the calibration configuration. The load cell had to be calibrated in the tension and compression state and was done as follows. In Figure 16 (middle) the tension test is shown and consists of just applying load in the tension direction in approximately 0.889 kN (200 lb) increments until the maximum was reached of +17.79 kN (4000 lb). Now the final compression calibration was done and can be

seen in Figure 16 (right). This test was a little more difficult because a compression device had to manufactured, which is the blue device in Figure 16 and again readings at approximately 0.889 kN (200 lb) increments were recorded until the maximum load of the calibrator cell was reached.

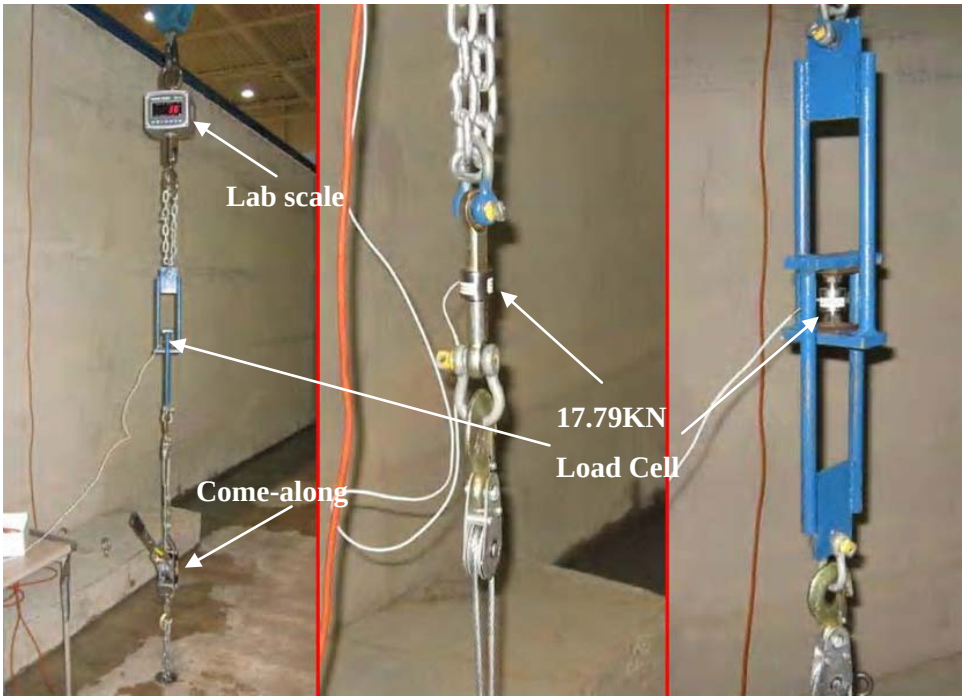

Figure 16. Calibration procedure for the calibrator cell

After the calibration was completed the data had to be processed to get the calibration equation that was needed. The Microsoft Office Excel program was used to produce Figure 17, which shows the millivolt output of the calibrator cell along the x-axis and the applied load (pounds, lb) along the y-axis. Using the trendline option in Excel a linear best fit line was fit to the tension and compression calibration data, and from this line, an equation is calculated by Excel and this is how calibration Equation 4.1 was developed. In Figure 17, it is shown that the tension and compression collected data for the calibrator cell is sufficient and this is confirmed by a R^2 value of 1.000. In Equation 4.1

the mV (millivolts) is the output of the strain gauge indicator and the Load (lb) (pounds) is the load that the cell is experiencing. So the calibrator cell is calibrated and the calibration equation is known, and now that this is completed, a process for determining the calibration equations for the carriage load cells can be developed.

$$\text{Load(lb)} = 172.9605 \times (\text{mV}) - 6.3004 \tag{4.1}$$

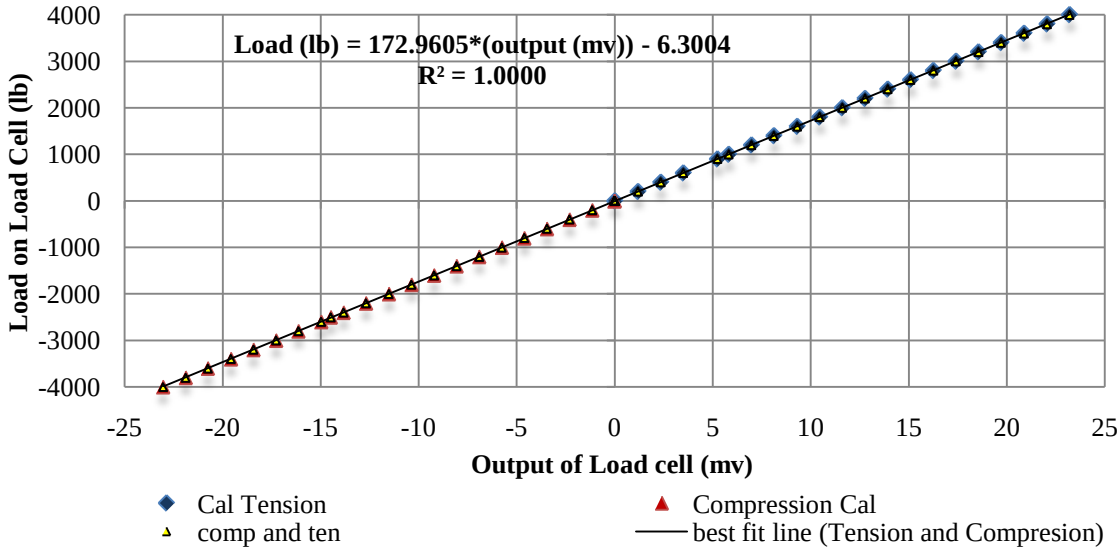

Figure 17. Calibration of calibrator cell

Calibration of Dredge Carriage Load Cells

Now that the calibrator cell is calibrated; the five load cells on the dredge carriage can be calibrated. The same type of procedure needs to be preformed for the carriage cells. The problem that was encountered was that the load cells on the carriage couldn't be taken off because they were hard wired to the carriage. Also the data acquisition system that is used for the carriage takes data as a percent (%) not in millivolts like the calibrator cell does. Since this was the case, a procedure had to be developed so that the carriage load cells could be calibrated on the carriage. So a calibration bracket shown in

Figure 18 was designed with the assumption that the two load cells, if put in line together, would read the same force. The simple concept of using a hydraulic jack was used to apply the force to get a tension and compression load by putting the jack in the lower quadrant to get a tension load and repeat the process by moving the jack to the upper quadrant to get a compression load on the cells, and this procedure is shown to the left of Figure 18. After the concept was confirmed, the calibration bracket was drawn using the SolidWorks modeling software. The bracket was constructed using 3.81 cm x 3.81 cm (1.5 in x 1.5 in) x 11 gauge A 992 steel square tubing for the support structure and 0.635 cm (1/4 in) flat-bar A36 steel was used for the eye-lets to connect to the tie-rod ends of the carriage load cell and the calibrator load cell. Using this model, a built in finite element model in SolidWorks was used to determine if the current design of the carriage calibration bracket was sufficient.

In Figure 18, the load applied and fixed restraints used in the calibration bracket analysis are shown, and using the built in finite element model it was found when a 4.89 kN (1100 lb) load was applied to the end of the tension (ten) and compression (comp) arm which is representing the maximum force that is applied with the a hydraulic jack, a large stress of 659 N/mm^2 (9,557 psi) was found at the location of the two eye-let connections and these maximum stress locations in Figure 18 are circled in red. To reduce the stress at these locations 4 pieces of 2.54cm x 30.48cm x 0.635cm (1in x12in x1/4in) A36 flat bar was welded on both sides of the tension and compression arms and on both sides of the lower outside bracket bar, and these added supports are shown in the right side of Figure 18. After these supports were added, the stress analysis was repeated and a maximum stress was reduced to 444.4 N/mm^2 (6,445 psi), which is a 32.6 percent decrease in maximum stresses. When both tests were run, a displacement analysis was also done to make sure that the deflections of the bracket were in safe working range. In the first test, a maximum deflection of 0.8305 cm (0.327 in) occurred at the end of the tension and compression bar, and for the second test, a maximum deflection of 0.739 cm (0.291 in) occurred at the same location which is shown in Figure 18. So the added

supports from the stress test analysis improved the maximum deflection by 11 percent, and from the stress and displacement analysis test, it is confirmed that the calibration bracket with the four extra supports are sufficient for the final design.

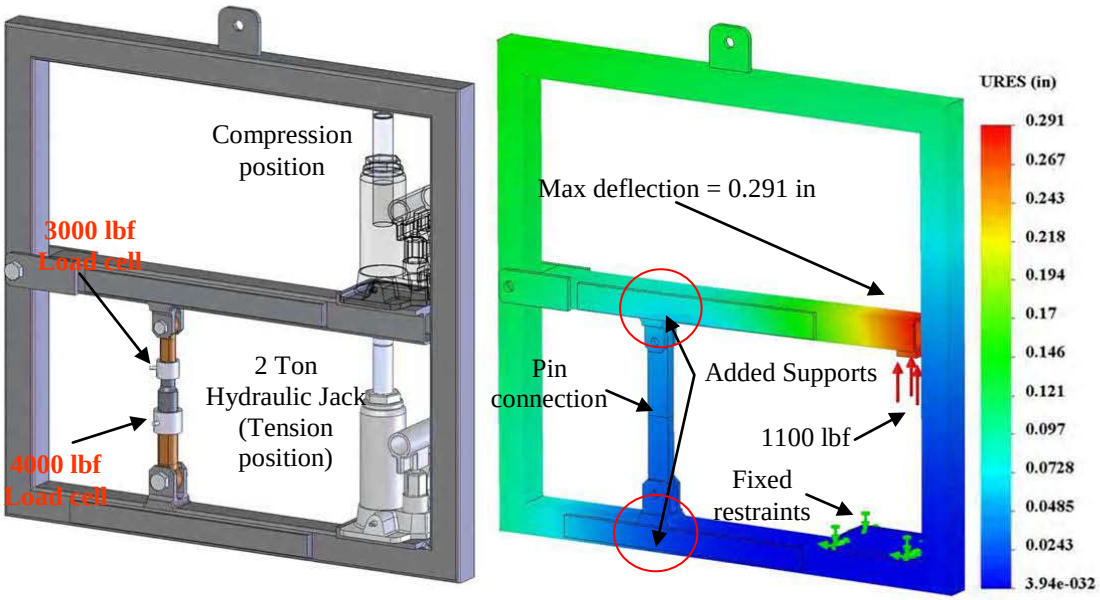

Figure 18. Preliminary design of carriage load cell calibration bracket (left), and SolidWorks displacement model of calibration bracket (right)

Now that the design was finalized the calibration bracket was fabricated and the final calibration bracket is shown in Figure 19, and from this figure it can be seen that it is identical to the drawing shown in Figure 18. Now that the calibration bracket is ready to be used to calibrate the carriage load cell, the setup was competed and shown in Figure 19, which shows the north side of the carriage and the procedure for calibrating the carriage load cells. In Figure 19 the tension calibration of the carriage load cell #4, and shows the final configuration of the carriage load cell, calibrator cell, and the hydraulic jack.

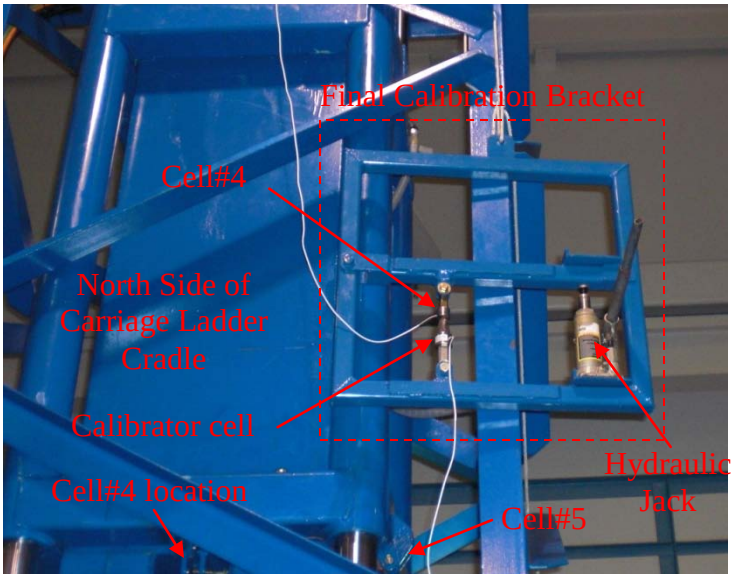

Figure 19. Final design of calibration bracket and carriage calibration procedure

The calibration procedure for calibrating the dredge carriage load cells was finished and then the calibration was started. The test consisted of applying load in approximately 0.889 kN (200 lb) increments up to the maximum of the 13.3 kN (3000 lb) load cell. This procedure was repeated for both the tension and compression situations for each of the five carriage load cells. After the data was obtained, Excel was used to plot the data for all of the load cells. The plotted test data are shown in Figure 20 and was generated using the percent (%) value from the data acquisition system of the dredge carriage for the x-axis and the y-axis is the converted output from the calibrator load cell. A linear best fit line was used to determine the calibration equation that is used to convert the test data that is obtained for the test procedure.

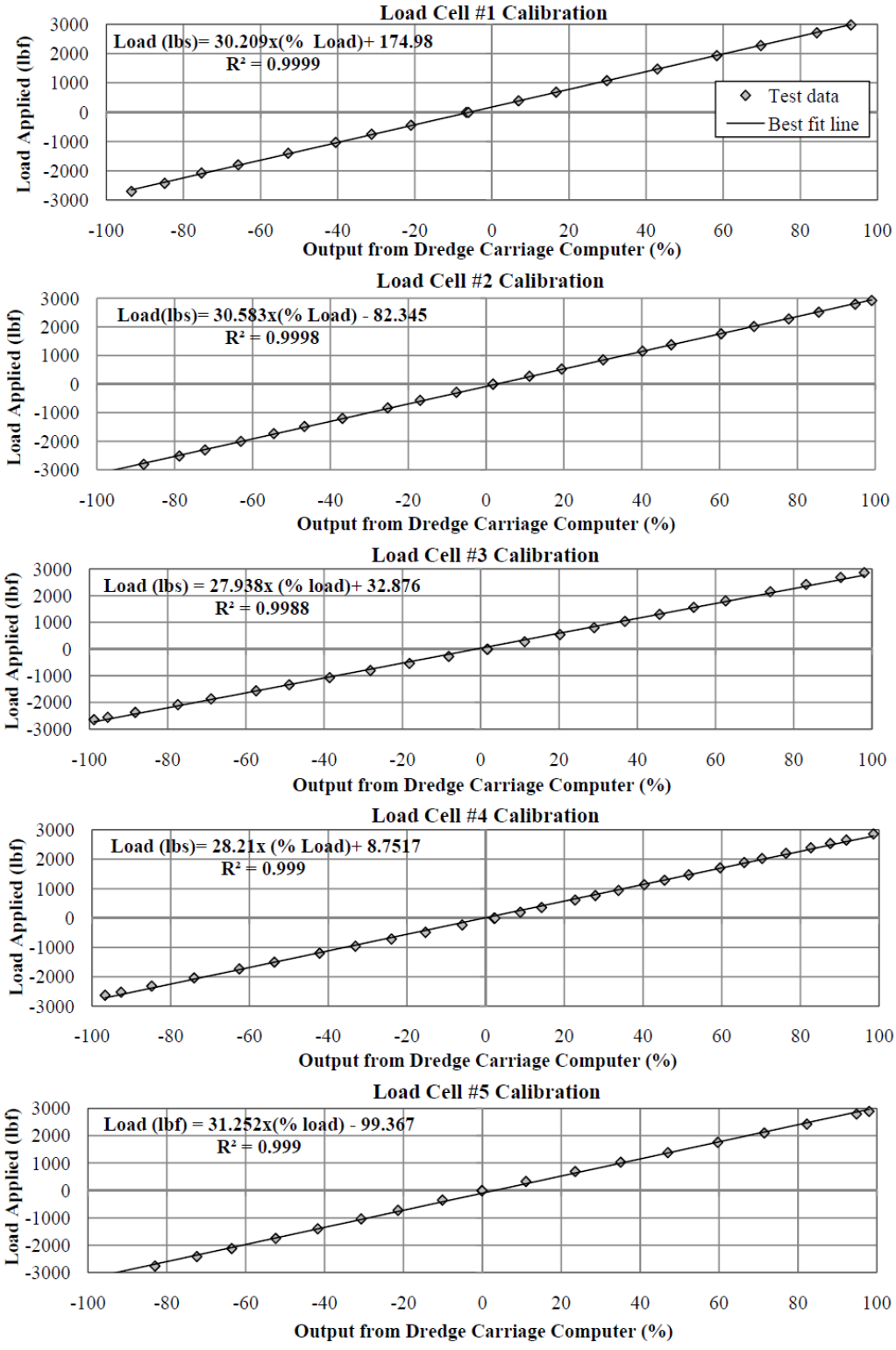

Figure 20. Calibration curves for all carriage load cells

Equations 4.2 through 4.6 are the calibration equations for the five carriage load cells and were generated using the best fit line discussed above. These equations are used to convert the raw data from the data acquisition system to know load in pounds. The raw data of the dredge carriage data acquisition system is in percent load, and that's why the only input variable for the five load cell equations are percent load. From Figure 20 it can be seen that all of the five calibration fits have a R^2 value very close to 1, which represent that the calibration curves have very little margin of error. The only gauge that was skewed a little was cell #5 on the compression side, but this can be corrected by recalibrating the compression side, however in this case the error is less than 5%, so the recalibration was not done. The calibration of the five load cells are completed and can now be used to convert data from the data acquisition system to known load in pounds (lbs).

$$\text{Cell \#1 load (lb)} = 30.209 \cdot (\%\ \text{load}) + 174.98 \tag{4.2}$$

$$\text{Cell \#2 load (lb)} = 30.583 \cdot (\%\ \text{load}) - 82.345 \tag{4.3}$$

$$\text{Cell \#3 load (lb)} = 27.938 \cdot (\%\ \text{load}) + 32.876 \tag{4.4}$$

$$\text{Cell \#4 load (lb)} = 28.21 \cdot (\%\ \text{load}) + 8.7517 \tag{4.5}$$

$$\text{Cell \#5 load (lb)} = 31.252 \cdot (\%\ \text{load}) - 99.367 \tag{4.6}$$

CHAPTER V
TESTING PROCEDURES FOR DETERMINING THE FORCES MEASURED BY THE CARRIAGE LOAD CELLS

Forces measured by the five carriage load cells using a known load applied on the dredge carriage cutterhead can be determined by three different methods. The first method is the actual laboratory tests that were done at the Haynes Coastal Engineering Laboratory. The second test consists of using a program called SolidWorks to determine loads in the five load cells. The last test method is the theoretical approach which assumes static loading on the dredge carriage ladder and uses the static equilibrium equations written for carriage ladder. From these three test methods, conclusions are made on how effective the research approach is for determining the cutting forces on the dredge cutterhead. The three tests are accomplished by applying a known load to the cutterhead to achieve results for the five load cells.

Laboratory Testing Procedure

The laboratory procedure was performed, to acquire data for the experimental results that are used to see how close the theoretical results compare, and this determines if the force reading in the five loads are adequate. The laboratory procedure consists of using the calibrator cell to read the load that was applied at the cutterhead. In the top left-hand corner of Figure 21 the pulling procedure is shown and this pulling procedure was completed for pulls in the south to north, north to south, east to west, and west to east directions. To apply the load, a 17.79 kN (4000 lb) come-along was used and was restrained by fixing one end to a tow tank floor anchor and the other end to the cutterhead. To get an accurate measurement of the applied force on the cutterhead; the pulling device was carefully place where it was parallel to the floor and perpendicular to the cutterhead. In doing this, the other procedures have improved repeatability and accuracy.

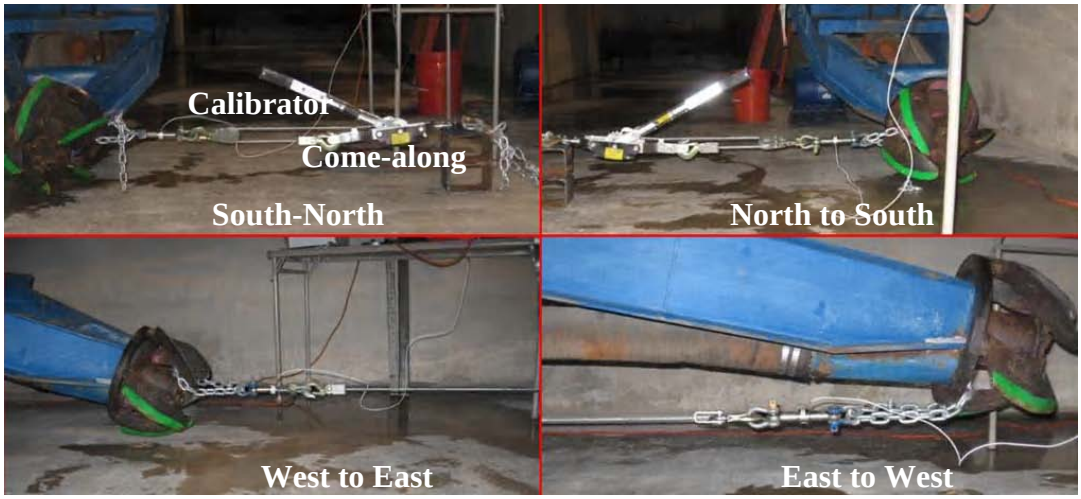

Figure 21. North, south, east, and west pull directions

The load on the cutterhead was applied in increments of approximately 0.45 kN (100 lb) up to 3.336 kN (750 lb) and was completed for each of the pull directions. For each of the pull increments, approximately 5 seconds of data was taken using the dredge carriage data acquisition system. The data were collected converted from percent load to pounds using the Equations 4.2, 4.3, 4.4, 4.5, and 4.6 which are the calibration equations obtained from the calibration process of the five load cells. For each of the pulls the articulating arm was set with a specific angle known as dredging angle (θ^o). On a prototype dredge the dredging angle corresponds to the digging depth which the ladder is set. For the dredge carriage, the articulating arm is set for a specified dredging angle shown in Figure 22, and the digging depth is adjusted by a vertical drive motor on the ladder. The laboratory test procedure was conducted for a dredging angle of 0^o, 11^o, and 22^o to compare how the forces in the five load cells corresponded to different dredging angles. From this testing procedure, the adequacy of the current cell configuration is determined.

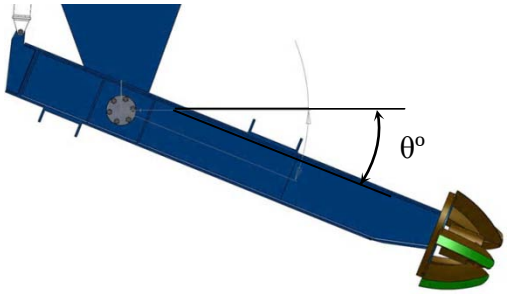

Figure 22. Dredging angle (θº) description

SolidWorks Program Procedure

For the SolidWorks procedure a model of the dredge carriage was drawn to scale to achieve good results from the program. The SolidWorks program is a three dimensional modeling software that has the ability of developing full scale models with the same dimensions and material property as the prototype structures. The SolidWorks program has a toolbox called Cosmosworks and is capable of doing a finite element analysis of a structure to achieve displacements, stress and strains, and loads in pins and bolted connections. The mesh for the finite element analysis had a global size of 3.05 cm (1.2 in) and has a tolerance of 0.15 cm (0.06 in). The setup is shown in Figure 23 which only considers the ladder and the articulating arm in the analysis because the other dredge carriage structure components are not needed to get the desired load in the load cells. The SolidWorks program settings are the linear static analysis tool. This analysis tool applies a load in small increments to get a true static analysis of the structure and to account for the deformation movement of the structure.

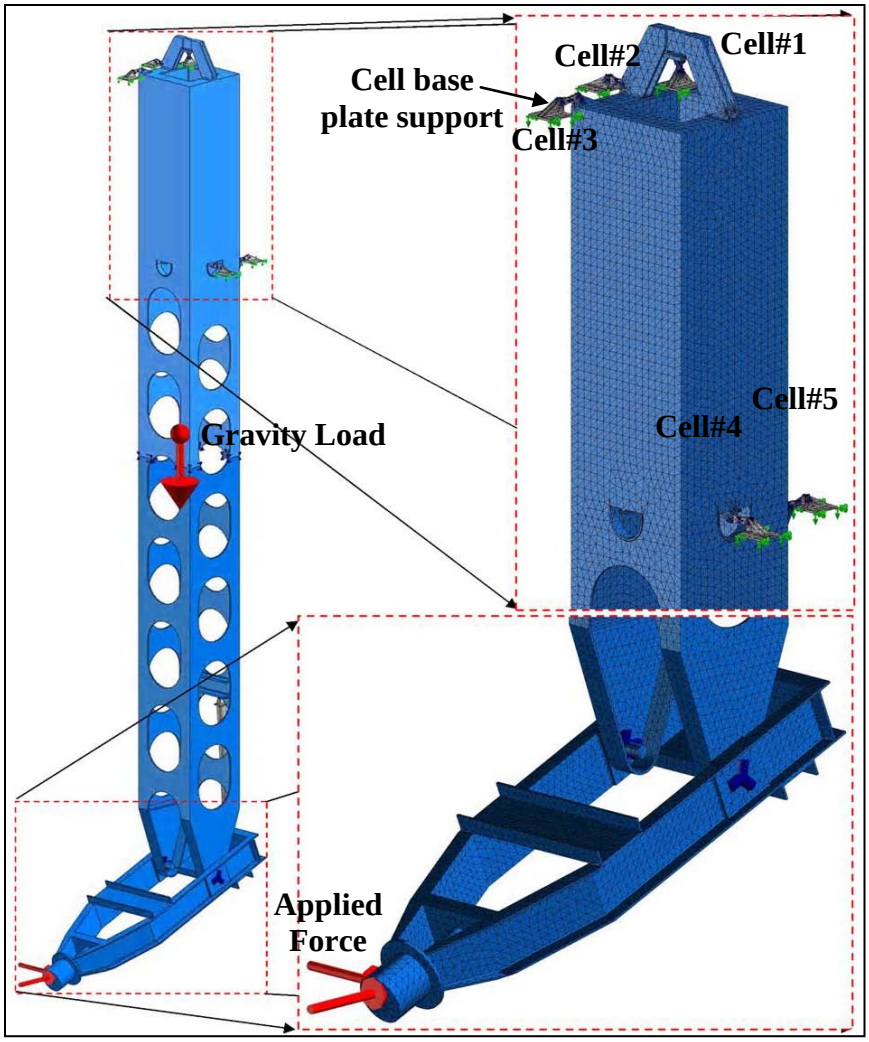

Figure 23. SolidWorks finite element model

The setup of the program consisted of applying pins where two parts are joined together, and for each through hole, two pins had to be used. To fully define the model, fifty two pins were used, and the load cell locations were replaced with a pin connection so the result of the axial load in the pin is considered to be the force which the load cell would be experiencing. In Figure 23, the cells restraint base plates are shown and this technique was used to replace the ladder cradle which takes the place of the restraints of the load cells. The five base plates shown in the figure are restrained in all six degrees of freedom and are shown by the green arrows in the figure. The gravity load of the

structure was applied to the center of gravity to take the gravitational effects of the structure into account. The same procedure was used in this test as was used for the laboratory testing procedure by applying load at the cutterhead location shown in Figure 23. The same directions of pulls and loads were used in this procedure as the laboratory test. The results from this procedure are discussed in the next chapter.

Ladder Force Equilibrium Equation Procedure

The third and final test was the theoretical analysis of the ladder structure to determine the forces in the five load cells by using static force equilibrium approach. For the equation development of the force equilibrium equations for the dredge carriage ladder, Equation 5.1 is used to determine these equilibrium equations (Riley and Sturges 1996). In Equation 5.1, it is assumed that only static loading is applicable to the ladder and dynamic affects are assumed to be negligible in this study of cutting forces on a dredge cutterhead.

$$\begin{aligned} &\sum \boldsymbol{F_x} = \mathbf{0} \quad \sum \boldsymbol{F_y} = \mathbf{0} \quad \sum \boldsymbol{F_z} = \mathbf{0} \\ &\sum \boldsymbol{M_x} = \mathbf{0} \quad \sum \boldsymbol{M_y} = \mathbf{0} \quad \sum \boldsymbol{M_z} = \mathbf{0} \end{aligned} \tag{5.1}$$

For Equation 5.1 a main coordinate system was considered to be located at the cell#1, which is the location at the top of the ladder. For the equation development, the sign convention used is shown in the top right corner of Figure 24. From the SolidWorks analysis, a large shear force was found at the cell #1 location. For this analysis, an assumption was made that the shear force at this location was in the plus or minus direction along the x axis and this direction depends on the pull direction of the applied load to the cutterhead. Therefore, the force was assumed to be in the positive x direction and is shown in Figure 24 as F_{c1x}. In Figure 24, the weight of the ladder and the articulating arm are described as W_{lad} and W_{aa}. The weight and the location of the center of gravities used for the W_{lad} and W_{aa} values were produced from the SolidWorks model of the dredge carriage.

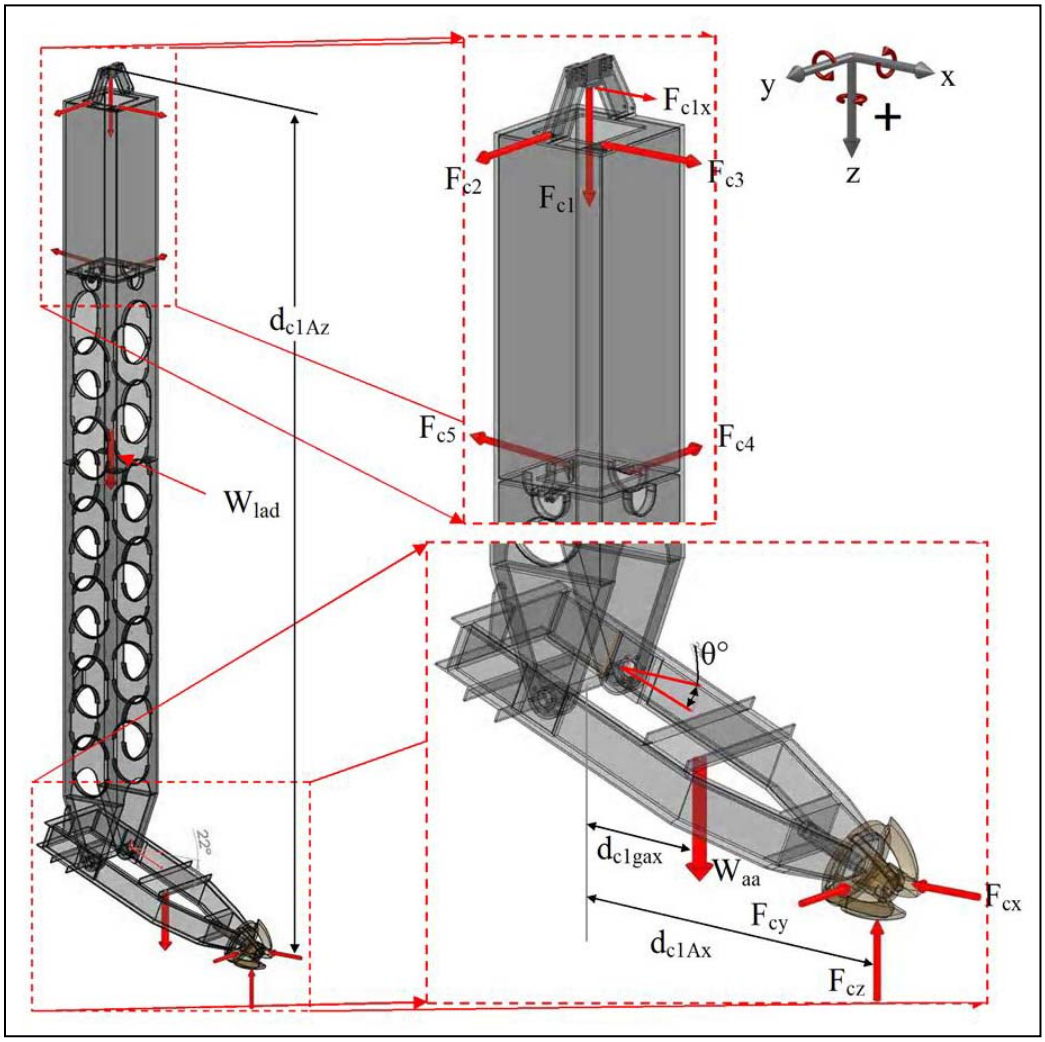

Figure 24. Free body diagram of dredge carriage ladder

The five forces in the load cells are described by F_{c1}, F_{c2}, F_{c3}, F_{c4}, and F_{c5}, and the subscript c# represents the cell number that it represents. In the summation of the equations the F_{c4} and F_{c5} values had to be split up in x and z components because the two cells weren't exactly perpendicular to the ladder. So the values were $F_{c4x}=F_{c4}\sin 89.9$, $F_{c4z}= F_{c4}\cos 89.9$, $F_{c5x} = F_{c5}\sin 84.9$, and $F_{c5z}= F_{c5}\cos 84.9$ and these were used for the equation formation. The axial, horizontal, and vertical cutting forces are describe by the

values F_{cx}, F_{cy}, and F_{cz} , and the location of the cutting forces were considered to be applied at the center of mass of the cutterhead shown in Figure 24. All of the forces have been described and now the summation of forces in the x, y, and z directions can be tabulated. The summation of moments for the ladder was taken at the location of cell#1 and from this position the distance to the center of mass of the articulating arm and distances to the cutterhead were determined. The distance from cell#1 to the center of mass of the articulating arm along the x-axis is shown in Equation 5.2, and this distance has the variable theta (θ) which represents the dredging angle that was described in the laboratory procedure test. The distance from cell#1 to the cutting force location are given by Equations 5.3 and 5.4, and these distances also are a function of the dredging angle (θ).

$$d_{c1gax} = 21.2992 * \cos(\theta - .5237) \tag{5.2}$$

$$d_{c1Ax} = 55.0212 * \cos(\theta - .4556) \tag{5.3}$$

$$d_{c1Az} = 234.56 + 55.021 * \sin(\theta - .4556) \tag{5.4}$$

Now that the distances for the center of mass for the articulating arm and cutting force locations have been defined, the summation of moments was taken about the x, y, and z axis. From the summation of forces and moments in the x, y, and z directions, six equations were formed and were used to determine forces in the five load cells. Equation 5.5 was substituted in Equation 5.6 to get the completed systems of equations for the carriage ladder system. From Equations 5.5 and 5.6, there are six equilibrium equations, and there are nine unknowns that have to be determined to get a fully defined system of equations.

$$A = \begin{bmatrix} 0 & 1 & 0 & 0 & -.0018 & -.089 & 0 & 0 & -1 & 1 & 1 \\ 1 & 0 & 0 & 1 & 0 & -.99 & -1 & 0 & 0 & 0 & 0 \\ 0 & 0 & 1 & 0 & -.999 & 0 & 0 & -1 & 0 & 0 & 0 \\ 0 & 0 & 0 & -9.3 & 0 & -9.09 & 0 & -d_{c1Ax} & 0 & 0 & 0 \\ 0 & 0 & -5.3 & 0 & 59.51 & 0.811 & 0 & d_{c1Az} & 0 & 0 & 0 \\ 0 & 0 & 0 & 5.25 & 0 & -60.76 & -d_{c1Az} & 0 & d_{c1Ax} & 0 & -d_{c1gax} \end{bmatrix} \quad (5.5)$$

$$A \times \begin{bmatrix} F_{c1x} \\ F_{c1} \\ F_{c2} \\ F_{c3} \\ F_{c4} \\ F_{c5} \\ F_{cx} \\ F_{cy} \\ F_{cz} \\ W_{lad} \\ W_{al} \end{bmatrix} = \begin{bmatrix} 0 \\ 0 \\ 0 \\ 0 \\ 0 \\ 0 \end{bmatrix} \quad (5.6)$$

To achieve results similar to the laboratory and SolidWorks procedure, Equations 5.5 and 5.6 had to be rearranged. Now to get results that can be compared to the other two testing procedures, the values F_{cx}, F_{cy}, and F_{cz} were considered as known variables. In assuming this, Equations 5.5 and 5.6 were rearranged and Equation 5.7 was developed, which has six unknowns and six equations, so in this form the system of equations can be solved to determine the shear force and all of the forces in the load cells. A program generated with MATLAB was used to solve the system of equations for the same loads that were applied to the cutterhead location in the other two testing procedures.

$$\begin{bmatrix} 0 & 1 & 0 & 0 & -.0018 & -.0888 \\ 1 & 0 & 0 & 1 & 0 & -.9960 \\ 0 & 0 & 1 & 0 & -.9999 & 0 \\ 0 & 0 & 0 & -9.25 & 0 & -9.089 \\ 0 & 0 & -5.25 & 0 & 59.5107 & .8111 \\ 0 & 0 & 0 & 5.25 & 0 & -60.756 \end{bmatrix} \times \begin{bmatrix} F_{c1x} \\ F_{c1} \\ F_{c2} \\ F_{c3} \\ F_{c4} \\ F_{c5} \end{bmatrix} = \begin{bmatrix} -W_{lad} - W_{aa} + F_{cz} \\ F_{cx} \\ F_{cy} \\ F_{cy}\, d_{c1Ax} \\ -F_{cy}\, d_{c1Az} \\ F_{cx}\, d_{c1Az} + W_{aa}\, d_{c1gax} \end{bmatrix} \quad (5.7)$$

CHAPTER VI
RESULTS

The data results for the laboratory, SolidWorks, and the equations procedures were all gathered, and Microsoft Excel was used to generate the graphs for all of the tests results. The data from all of the five load cells and tests are used to generate the graphs for each pull direction. From the testing procedures chapter, it was said that data was taken for the dredging angles of 0, 11, and 22 degrees, but for the results chapter, the results from the 22 degree tests for the laboratory, SolidWorks, and equations procedures were used. This decision was made because the results for the different dredging angles didn't have sufficient variability in the results, so the dredging angle of 22 degrees was chosen because it resembles a dredging angle of a prototype dredge.

North Pull Results

The north pull results for all of the procedures are reviewed first. In Figure 25, the output from the Excel spreadsheet is shown and the legend at the bottom of the figure gives the description of the meaning for each line. When looking at the configuration of each load cell on the ladder it can be seen visually that cell 2 and cell 4 should take most of the load when a force in the south to north direction is applied, and cells 3 and 5 should be picking up the torsional effect of the twisting of the ladder. In Figure 25, cells 2 and 4 are taking an applied load, but cells 3 and 4 are shown to be taking most of the load and cell 5 to be taking no load at all. This load on cell 4 is to be expected, but the load in cell 3 is not that obvious and cell 5 is being affected by the interference of cell 1 in the shear direction, which this shear effect is resisting the load and that load is considered to be applied to cell 5. In Figure 25, it can be seen that the results from the SolidWorks and the equations procedure have little error and can be considered to be very close. The cell 1 results show that the SolidWorks and equation procedures are close. However, the laboratory results show a different load rating, and this could be due

to the ladder shifting and redistributing the load in a different cell, but results from the procedure for cell 1 has a similar slopes as the other two procedures up to approximately 0.889 kN (200 lb) where the shift occurs which could be due to cradle ladder interference.

Now looking at cells 3, 4, and 5 which show a good result when the three procedures are compared, but when the applied load at the cutter reaches 1.779 kN (400 lb) and above the procedure results change drastically and the SolidWorks and equations results stay linear. Also, there is a sufficient difference in the offset of the procedure results with the other two procedures which can be corrected by taking the mean of the data and subtracting the mean out of the procedure results and this procedure is applied to the dredging data in the following chapter. This offset is also due to different loads applied. A shift occurs in cells 3 and 4 at 1.668 kN (375 lb), which could be caused with interference from the ladder cradle. The cell that has a good difference from the other two test is cell 2, which shows a great difference in slopes from the procedure results to the other two and could be because of interference of the ladder cradle again, but the other pulls are reviewed to make sure cell 2 is taking readings properly.

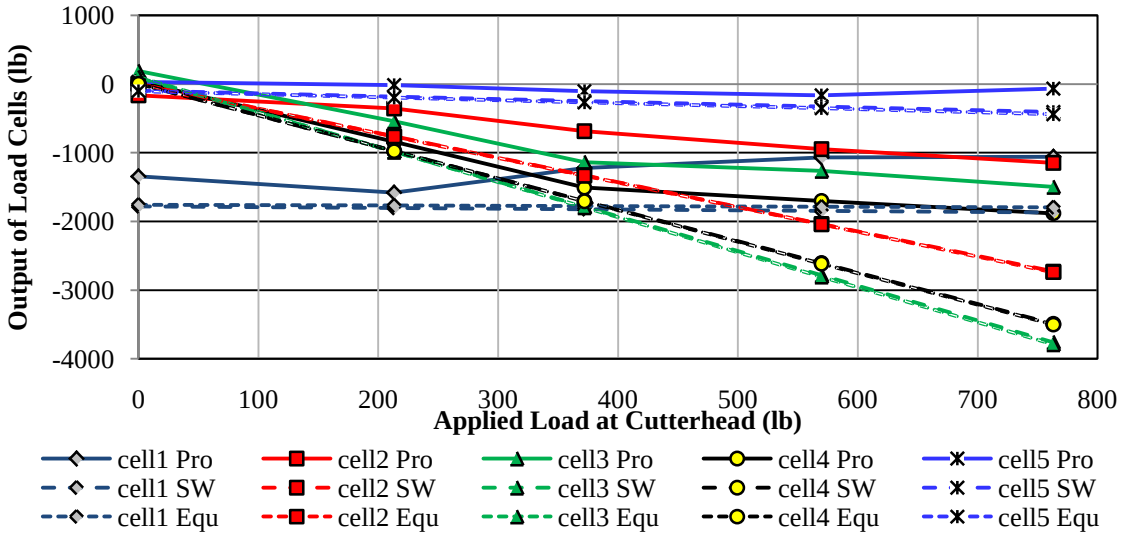

Figure 25. North pull results for all testing procedures

To better describe the ladder cradle interference that is stated above, a test from the SolidWorks procedure is used. This test contains a demonstration of deformation analysis of a south to north pull of a magnitude of 3.34 kN (750 lb) on the ladder supported by a substituted model ladder cradle and this demonstration is shown in Figure 26. The figure shows the amount of deflection that occurs when a force is applied to the cutterhead location shown. The ladder and ladder cradle have clearance of only approximately 0.635 cm (0.25 in) and from this deflection analysis it can be seen in Figure 26 that the ladder in the areas circled in red moves 0.762 cm (0.30 in) or more. This movement in the ladder is greater than the 0.635 cm clearance which is available and from this movement of the ladder binding can occur in the marked areas. This binding creates false readings in all of the load cells as seen in the results from the north pull.

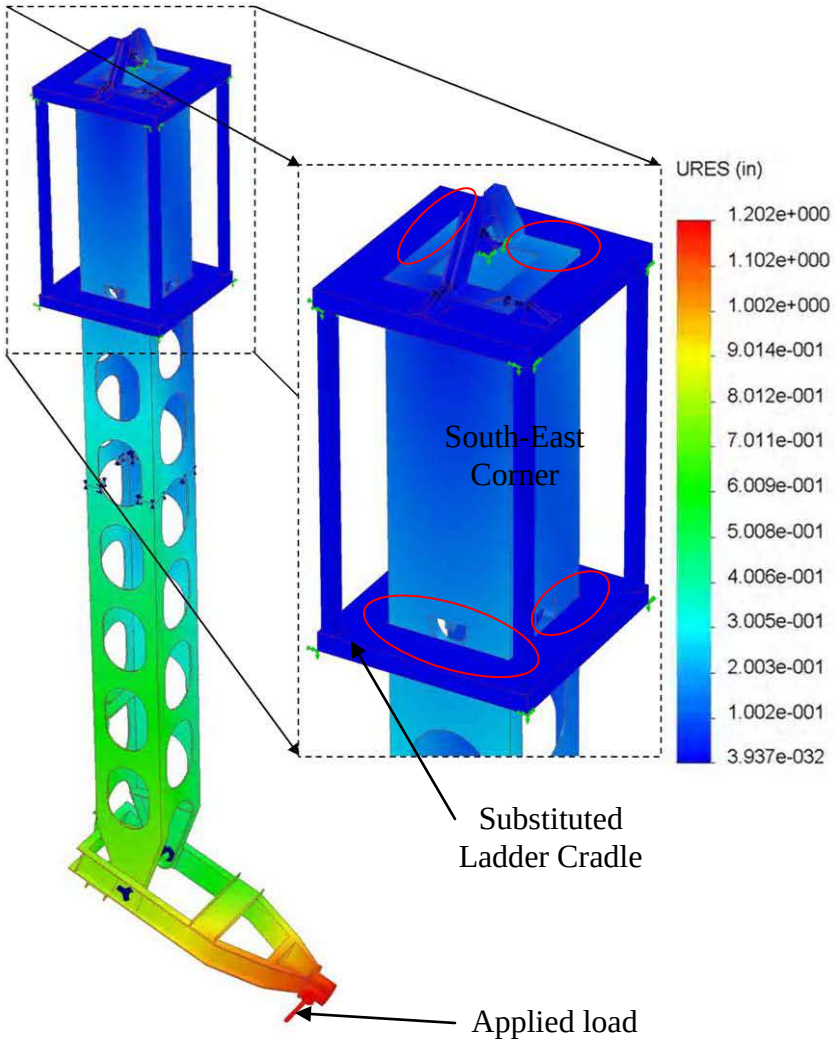

Figure 26. Demonstration of cradle ladder interference

South Pull Results

The south pull results are reviewed and conclusions drawn on the accuracy of the cells when considering cutting forces in the north to south direction. The results from the laboratory, SolidWorks, and equations procedures for the south pull have been graphed to show how accurate the cells are for each procedure. In Figure 27, results for cell 1 show they are similar to the north pull results in the beginning, but the slopes are different. In the south pull results of cell 1 the laboratory results better resembles the SolidWorks and equation results. For cell 1, the laboratory results are offset from the

other two because of variables in the laboratory; however this can be corrected when the cutting forces are calculated by taking the mean of the data and subtracting it. The results for cell 1 are reasonable and show that good results can be approximated. Again by visual inspection, cells 2 and 4 should be resisting the load of the south pull and cells 3 and 5 should be resisting the torsional affect for the twisting of the ladder. From the results, cell 4 readings are close, but cells 2 again are off considerably from the SolidWorks and equations results. In this pull test there is an irregularity at and above of applied load of 0.889 kN (200 lb) which is believe to be caused by ladder cradle interference. This pull test shows good results for cells 1, 3, 4, and 5, but cell 2 shows to have more error in this pull direction than in the north pull procedure and shifts occur in cells 3 and 4 at approximately 0.889 kN (200 lb) and are skewed above this applied load to the cutterhead.

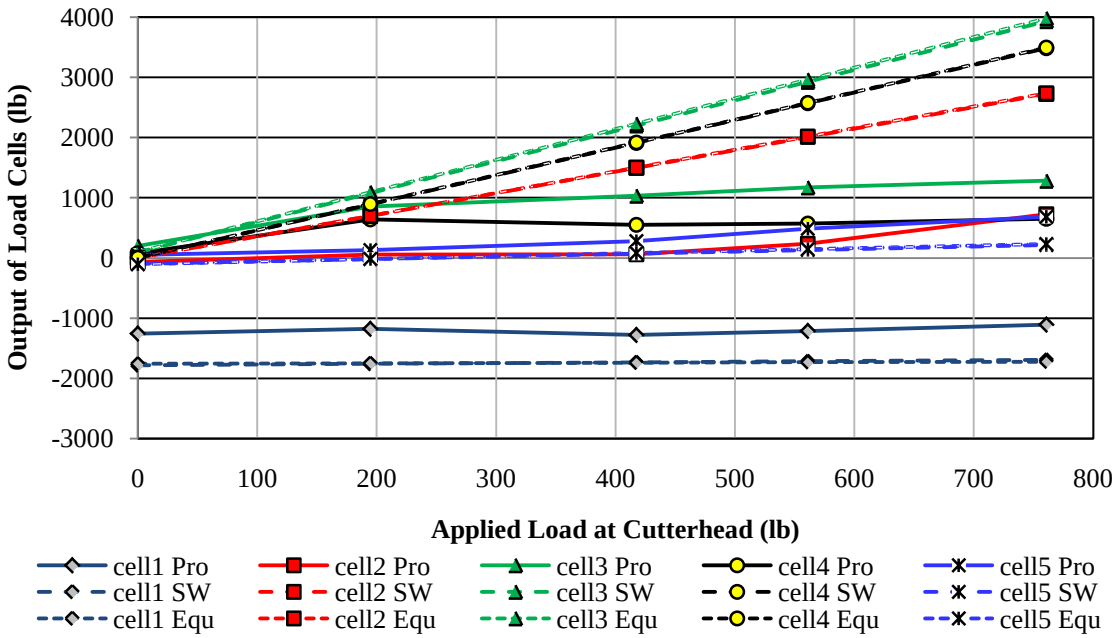

Figure 27. South pull results for all testing procedures

East Pull Results

The East pull results are now reviewed and conclusions drawn on the accuracy of the cells when considering cutting forces in the west to east direction. In Figure 28, cell 1 is shown to be reacting the same as the other two pulls and it is shown to be consistent with the SolidWorks and equations procedures. By visual inspection of the cells when a west to east pull is performed, it can be expected that cells 3 and 5 take most of the load. In Figure 28 this loading of cell 3 and 5 are to be expected and this shows that the two cells are working properly when a west to east load is applied to the cutterhead, but again a shift occurs around 0.889 kN (200 lb) which is again probably due to ladder-cradle binding. In Figure 28, the SolidWorks and equations results can't be seen due to the results from cell 4 covering them, and this is expected because when a west to east pull is applied these two cells should be reading approximately the same. The laboratory results for cell 2 show a small amount of offset and this could be due to a ladder shift or binding. The same shift in the reading occurred at the same applied load and again this is considered in the cutting forces calculation. For these pull tests, the results look to be accurate and show that good results can be expected when calculating cutting forces as long as cutting forces don't exceed 0.889 kN (200 lb).

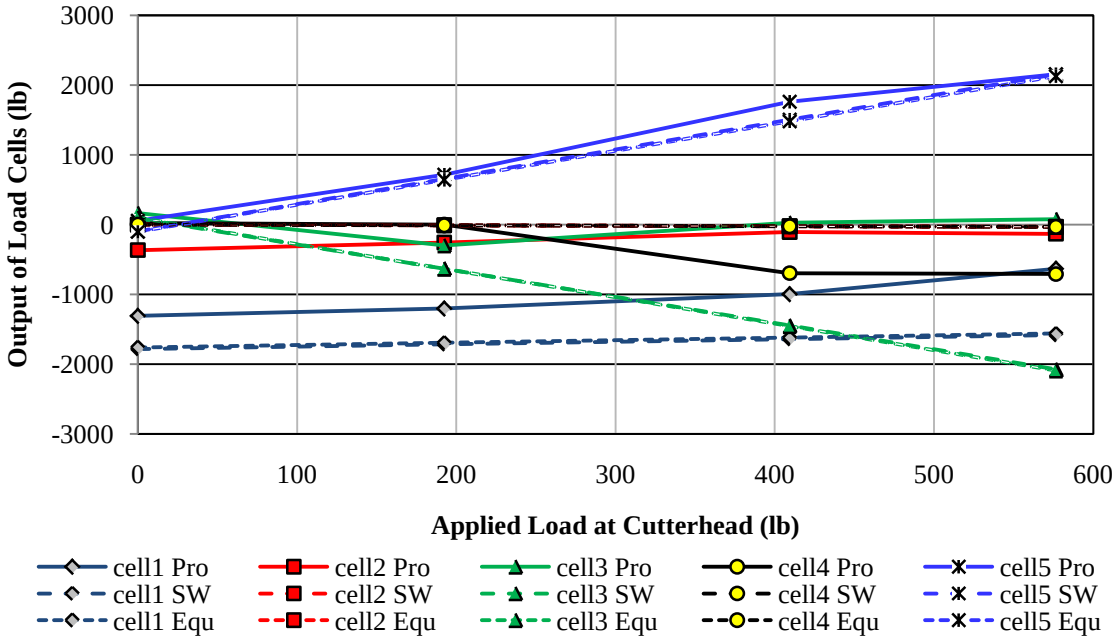

Figure 28. East pull results for all testing procedures

West Pull Results

Finally, the west pull results are reviewed and conclusions drawn on the accuracy of the cells when considering cutting forces in the east to west direction. In Figure 29, cell 1 is shown to be reacting slightly different than the other test, but this is due to a different starting or offset value than the other test and could be due again to ladder shift. In Figure 29, cell 3 and 5 have the same results as the east pull, but are oriented different do to the different pull direction. This test has the same similarity as the east pull and even has the same shift at the same loading as the other pull test. Again the results look appropriate and show that good results can be expected for the cutting force calculations if the cutting forces again don't exceed 0.889 kN (200 lb) because of the shift that occurs in all of the pull tests. Also, data from cell 2 is inspected carefully for the cutting force calculation in the next chapter.

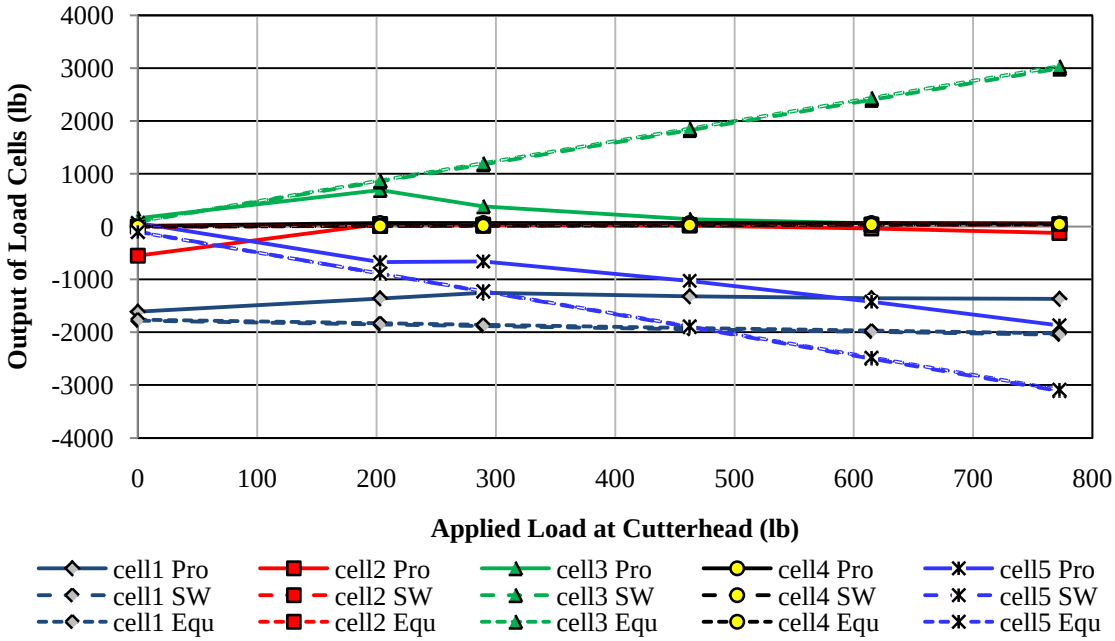

Figure 29. West Pull for all testing procedures

Conclusions

The laboratory, SolidWorks, and equations procedures show reasonable results on the cells working properly for the current load cell configuration. The results however show irregularities in the five loads when a force of approximately 0.889 kN (200 lb) and above are applied to the cutterhead in the north, south, east, and west pull directions, and from these shifts, it is believed that the ladder is moving too much and causing binding with the ladder cradle which cause these irregularities in the laboratory procedure data. These irregularities in data indicate that the current load cell configuration needs to be modified. Also, the results from cell 2 show that readings are sometimes skewed and inaccurate for the north and south pull directions, but in the east and west directions the gauge seems to be working properly for an applied load to the cutterhead between 0 – 0.889 kN (0-200 lb). This irregularity is taken into consideration when the cutting forces are being calculated. The results from the three procedures have produced favorable

results and shows that the cutting forces on the cutterhead can be approximated accurately if cutting forces again don’t exceed 0.889 kN (200 lb).

CHAPTER VII
CUTTING FORCE RESULTS FOR LABORATORY DREDGING TESTS

Equation Rearrangement to Determine Cutting Forces

The main results from all of this research testing of the dredge carriage are the actual results for the cutting forces on the cutterhead while doing a dredging test in the laboratory. Some assumptions have to be made for the cutting force results of F_{cx}, F_{cy}, and F_{cz} to be measured. These assumptions are that the forces in the loads cells correspond equally with the forces that are generated with the force equilibrium equations developed in the equilibrium equation procedure. So with this assumption, the forces that are recorded from the data acquisition system for a dredge test, can be converted using the calibration Equations 4.2, 4.3, 4.4, 4.5, and 4.6, and then these outputs are directly input into the force equilibrium equations to achieve the cutting forces at the center of mass at the cutterhead. From the equilibrium equations generated by the equation method, the assumption is that the loads in the five loads cells are known and the cutting forces and shear force in cell 1 are unknown. So Equations 5.5 and 5.6 were rearranged to get this configuration for F_{c1}, F_{c2}, F_{c3}, F_{c4}, and F_{c5} as known values and F_{c1x}, F_{cx}, F_{cy}, and F_{cz} as unknown values and this form of the system of equations is shown when Equation 7.1 is substituted into 7.2.

$$B = \begin{bmatrix} 0 & 0 & 0 & -1 \\ 1 & -1 & 0 & 0 \\ 0 & 0 & -1 & 0 \\ 0 & 0 & -d_{c1Ax} & 0 \\ 0 & 0 & d_{c1Az} & 0 \\ 0 & -d_{c1Az} & 0 & d_{c1Ax} \end{bmatrix} \tag{7.1}$$

$$B \times \begin{bmatrix} F_{c1xs} \\ F_{cx} \\ F_{cy} \\ F_{cz} \end{bmatrix} = \begin{bmatrix} F_{c1} + F_{c4}(.00175) - W_{lad} - W_{aa} \\ -F_{c3} + F_{c5}(.996) \\ -F_{c2} + F_{c4}(.9999) \\ F_{c3}(9.25) + F_{c5}(-9.0885) \\ F_{c2}(5.25) - F_{c4}(59.511) - F_{c5}(.81) \\ -F_{c3}(5.25) + F_{c5}(60.76) + W_{aa}\, d_{c1gax} \end{bmatrix} \tag{7.2}$$

Using Equations 7.1 and 7.2, the unknowns F_{c1xs}, F_{cx}, F_{cy}, and F_{cz} can be solved for each iteration (iteration is equal to one reading per sec). The dredge carriage data acquisition system records the gauge readings at 1 Hz or 1 reading per second as discussed in Chapter III. A dredging test for the dredge carriage is approximately between 100 sec and 400 sec depending on the criteria of the specific dredge test. So to get results for each iteration of a test, a program had to be developed to solve the system of equations for each iteration. The MATLAB program was used to develop a program that consists of the input of the acquired data from the test and a loop was formed to solve the system of equations for each iteration. The results were stored in a matrix where the data could be retrieved and transferred to an Excel spreadsheet and the cutting force data was used to generate graphical results. Using this program, results of the cutting forces induced on the dredge cutterhead was generated for a specific dredging test.

Dredging Test #1 Cutting Force Results

In the summer of 2008, two dredging test were completed using the dredge carriage. The parameters that need to be defined for these tests are the flowrate (LPM or GPM), swing speed velocity (cm/sec or in/sec), cutter advancement (cm or in), cutter RPM, and depth of cut (cm or in). The depth of cut is set visually by a scale on the side of the ladder and the flowrate and cutter RPM are set by inputting a percent value for each into the dredge carriage operating system. The parameters that are automated for these two specific tests are the swing speed velocity, cutter advancement, number of cuts, and distance travel for each cut. This automation was done by John Henriksen and was input into the operating system of the dredge carriage. The cutter advancement, swing speed

velocity, and swing direction is described in Figure 30, and this figure shows how a dredging test is performed. Two tests were used for the research on forces induced on the cutterhead. When the tests were in progress the data was taken for the five load cells on the carriage and this is the data that are used in the cutting forces research.

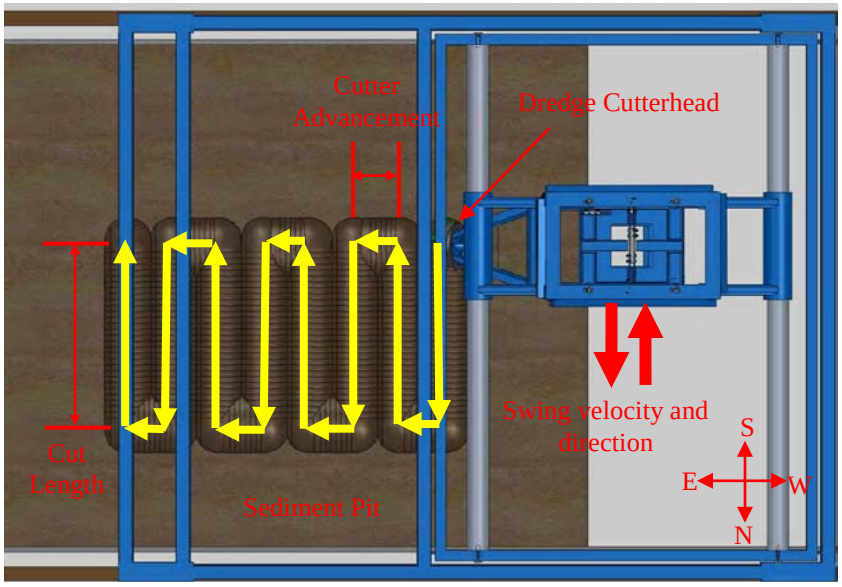

Figure 30. Description of laboratory dredging test (top view of dredge carriage)

The first dredging test observed is test#1 which consists of a cutter RPM of 86, flowrate of 1135.5 LPM (300 GPM), and depth of cut of 20.32 cm (8 in). The cutter advancement and swing speed velocity were calculated by using data from Figure 31 which shows the swing position and cutter advancement position. From the data, an average cutter advancement was calculated to be approximately 36.83 cm (14.5 in) and swing speed velocity was calculated to be approximately 2.29 cm/s (0.905 in/s).

The output of the program for the cutting forces of test 1 are shown in Figure 31, which shows the values for F_{cx} (Axial Cutting Force), F_{cy} (Horizontal Cutting Force), and F_{cz} (Vertical Cutting Force). The dredging test consists of eight cuts which are

demonstrated in Figure 30 and this is also shown by how many cutter advancements are made. The cutting forces correspond to the directions of loads on the cutterhead shown in Figure 24. F_{cx}, F_{cy}, and F_{cz} are all shown to be in the negative direction relative to the coordinate system in upper right-hand corner of Figure 24. In Figure 31 the same cutting force directions are used, and if the cutting forces are negative, that means that the assumed forces are in the opposite direction than they are in Figure 24.

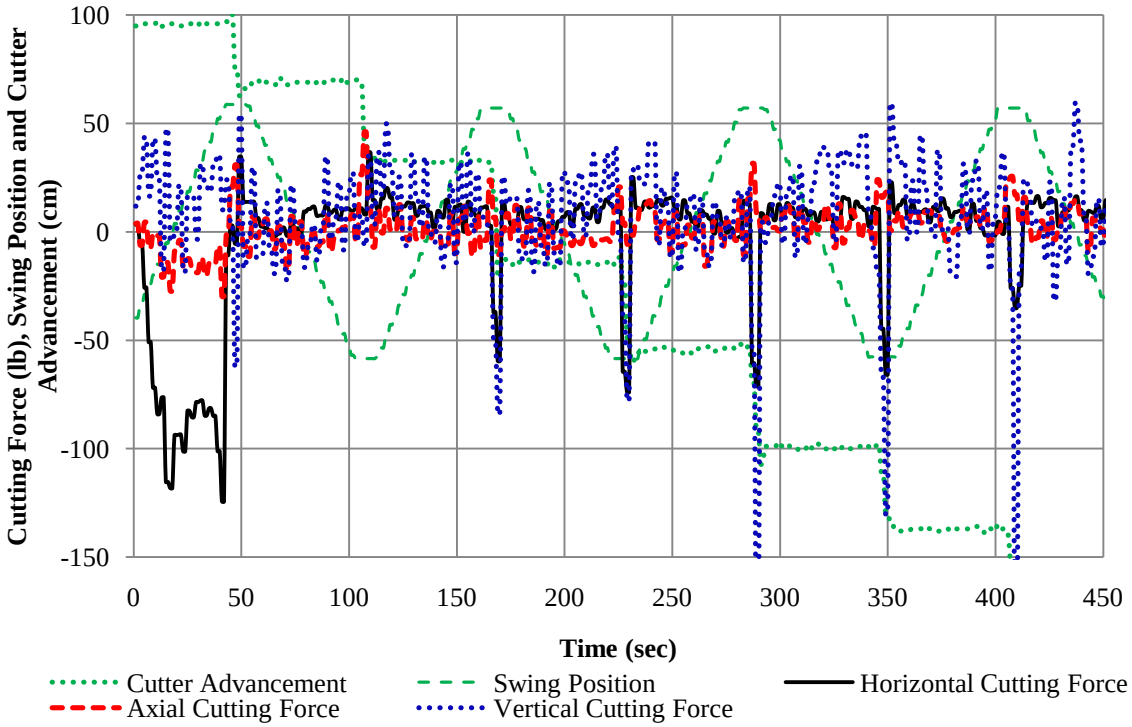

Figure 31. Calculated cutting forces for summer 2008 test#1

In Figure 31, the swing position is shown to have a positive or negative slope which depends on the direction of swing. This direction of swing is very important because this determines if overcutting or undercutting is occurring. For the dredge carriage the cutterhead rotates counterclockwise when viewed from the front and this defines overcutting when the cutterhead moves from a north to south direction, and undercutting

is defined by the cutterhead moving in the south to north direction and this can be observed in Figure 32. So in Figure 31 when the swing positions slope is negative overcutting is occurring, and when the slope is positive undercutting is occurring. The overcutting and undercutting have a significant effect on the forces induced on the dredge cutterhead. So now that the cutting force directions and the description of overcutting and undercutting for the dredge carriage have been defined, some observations can be made about the graphical cutting force data in Figure 31.

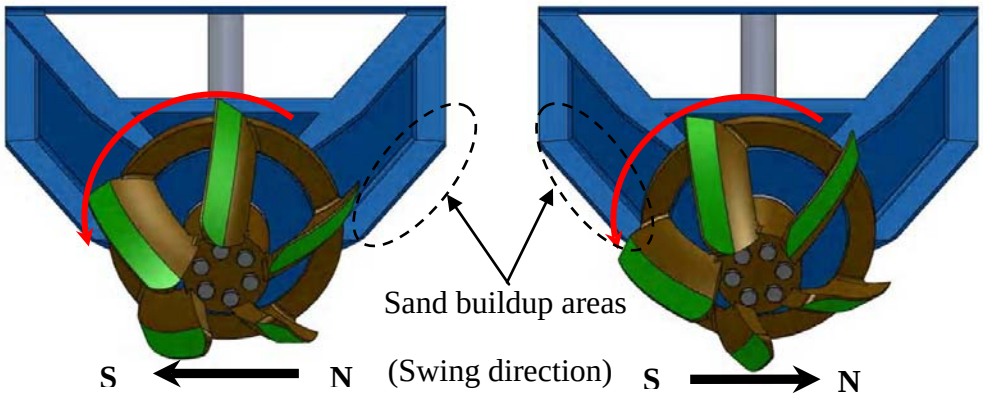

Figure 32: Demonstration of overcutting (left), and undercutting (right)

The first thing that needs to be considered is to determine if the shift that was determined by the procedure results occurs in the dredging test 1. To determine if the shift occurs Figure 31 is used to determine if a 0.889 kN (200 lb) and above force are experienced in the test. Looking at Figure 31, it can be seen that a 0.889 kN force is not experienced in the test, so the cutting forces can be assumed to be accurately calculated. For the calculation of the cutting forces, the mean of the cutting data for cell 1 was calculated and subtracted so the data would fit the equation procedure better and by doing this the results for F_{cx} and F_{cz} were shifted to the zero line and the forces weren't affected. This modification was done by taking the mean value of cell 1 from the test data, and this mean was subtracted from the total weight (W_{lad}+ W_{aa}) that was used for the equation

formation, and then the output was added to the mean weight to get a value that is more closely related to the weight used to form the equations. This data modification procedure was performed for all five load cell data sets so an improved cutting force result could be calculated from the cutting force program.

In Figure 31, it can be seen that a large horizontal cutting force was experienced, and this is due to the buildup of sand on the articulating arm which caused the elevated cutting force and this buildup area can be seen in Figure 32, but when the cutter advances the cutting force diminishes and this situation isn't experienced again for the rest of the cuts. This is because the articulating arm is free of the weight of the sand because the articulating ladder is in the first cutting path which the sand has already been removed. This buildup of sand on the articulating arm was visually observed for the dredging test and the force on the ladder confirms the experience of the sand buildup. In Figure 31, it can be seen that when the cutterhead advances between cuts, a jump in the axial load is experienced. This jump is to be expected because the cutterhead is getting pushed through the sediment, and the forcing of the sand is reacting on the cutterhead which leads to this jump in the axial load on the cutterhead. In Figure 31, cut 2 is shown to have gradual upward slope and for cut 3 a gradual downward slope of the cutting forces are shown, and this is due to the slight sand buildup and due to overcutting for cut 2 and undercutting for cut 3.

In the advancement into cut 4, a noticeable change was observed in the horizontal and vertical cutting forces and this continued through the rest of the cutter advancements. This shift in horizontal and vertical cutting forces could be due to the binding of the ladder in the cradle or could be due to the cell 1 location taking load in the shear direction. This shift will be observed in the following to see if the same situation occurs in test 2 cutting force results. However, this shift only occurs when the cutter is advanced and when the side cutting begins the force dissipates and returns to forces similar to cuts 2 and 3. This shift could also be from the shift that occurred when a force

of 0.889 kN (200 lb) was applied at the location of the cutter seen in chapter VI. So the cutting forces for test 1 have shown approximate results and have shown that cutting forces can be determined using this method of cutting force research, however further conclusion will be drawn when test 1 results are compared to test 2 results.

Dredging Test #2 Cutting Force Results

The second dredging test consists of all the same parameters as dredging test 1 and this helps in confirming that the cutting forces obtained from test 1 are sufficient. For this test the same automation program was used and no changes were made, so the swing position and cutter advancement position are the same as test 1 and can be confirmed by Figure 33. In Figure 33, the results for the cutting forces for test 2 are shown and can now be compared to the results from test 1. In Figure 33, cut 1 shows that the same thing occurs when the first cut is done and this is due to the same situation observed in test 1 which is sand buildup on the articulating arm. So cut 1 shows that the similar situation occurs in test 1 and this confirms that a large horizontal cutting force is experienced due to sand buildup. Figure 33 shows that when the carriage advances between cuts, a large axial force is experienced and this same phenomena was experienced in test 1.

However, when the cutter advances to cut 4 the same phenomena isn't experienced as from test 1 where horizontal and vertical cutting forces jumped significantly, but there are slight jumps when cutter advances into cut 4 and cut 8. The last thing that was observed for test 1 was undercutting and overcutting issue and for test 2 it can be seen that for cut 2 there is slightly upward slope of the cutting forces and for cut 3 a downward slope is observed for the cutting forces. The cuts 4 through 8 have the same variation in cutting forces as observed in cuts 3 and 4. This shows that the cutting forces can be calculated approximately for two repeated dredging test. However, the pull results of the laboratory, SolidWorks, and equation procedures and the cutting force

results for test 1 and 2 shows there are some irregularities in the cutting force procedure, but further conclusions will be drawn after the two dredging test are compared further.

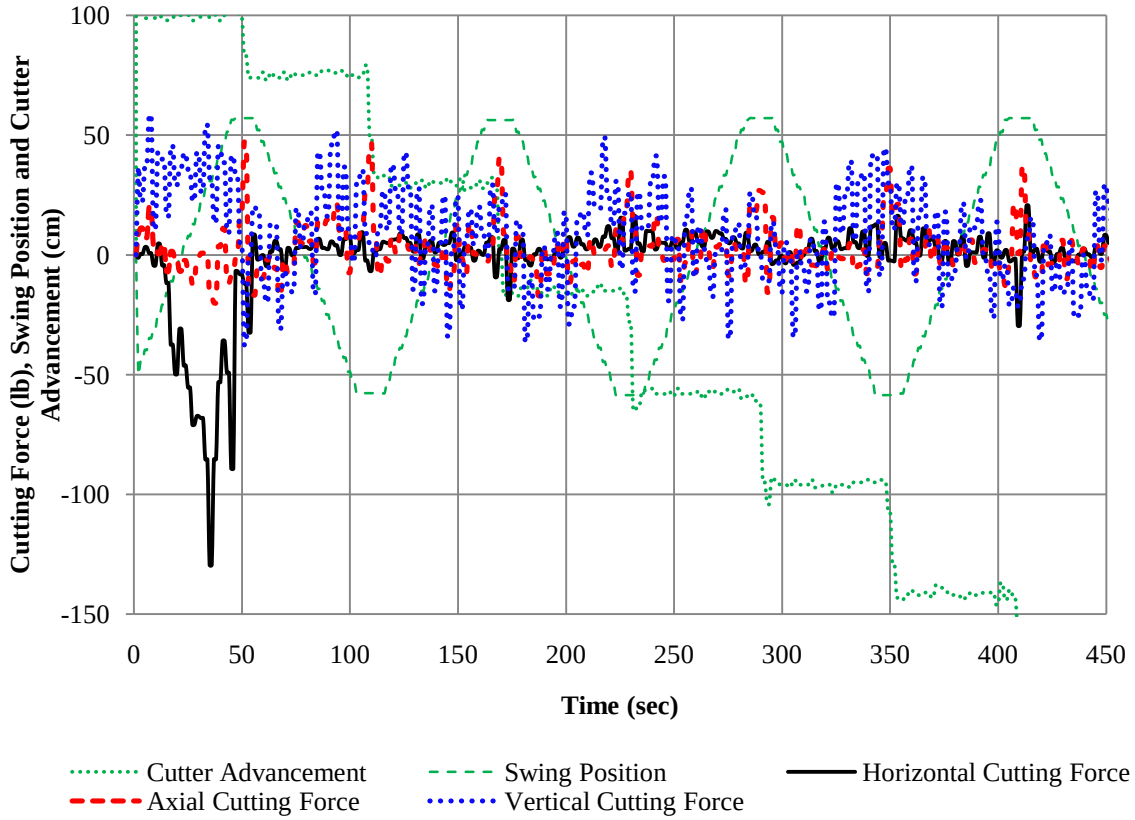

Figure 33. Calculated cutting forces for summer 2008 test#2

Test 1 and 2 Comparison

This section gives an enhanced overview of how the cutting forces vary for the horizontal, axial, and vertical cutting forces between to identically repeated dredging test. This overview determines if the current configuration of the load cells on the dredge carriage are performing properly. The following comparison involves splitting the horizontal, axial, and vertical cutting forces results up into three different graphs so

that each individual cutting force can be compared for test 1 and test 2 results by overlaying the two tests on each other.

So the first cutting force that is compared is the horizontal cutting forces from test 1 and test 2 and this is shown in Figure 34. This figure shows the same axis for the cutting forces, but the y-axis for the cutter advancement and swing position is shown on the right-hand side of Figure 34 and these two variables are the same for each test because test 1 and 2 were computer automated and have the same repeatability. As discussed above it can be seen that the first cuts of the two tests are closely related. In cutter advancement one and two, a slight difference in the two tests is observed because test 1 rises at these two advancement positions and test 2 decreases slightly. When advancements 3 through 6 are observed it can be seen that test 1 has sufficient increase in force and test 2 only decreases slightly. Looking at the advancement into cut 8 it can be seen that the two test horizontal cutting forces are almost identical. When cuts 2 through 8 are compared, it can be said that some variations occur and when comparing these two tests it can be seen that they have some significant irregularities when the two horizontal cutting forces are observed. These irregularities could be due to the current configuration of location cell 1, because cell 1 is not mounted so that it can rotate in the direction of the movement of the ladder and this is why a large shear force is observed at this location. Also, in the procedure results chapter, shifts in cell 4 occurred and cell 2 showed to have a large error in the laboratory data, and data from these two cells are the two main contributors in the calculation of the cutting force in the horizontal direction. When taking all of the contributions of possible errors in the horizontal force calculation it can be said that the current configuration of the load cells on the carriage have an elevated irregularity in the pull procedure results and the horizontal cutting force results shown in Figure 34. From this comparison of horizontal cutting forces it can be said that the current load cell configuration needs to be modified so that more accurate results for cutting forces can be determined.

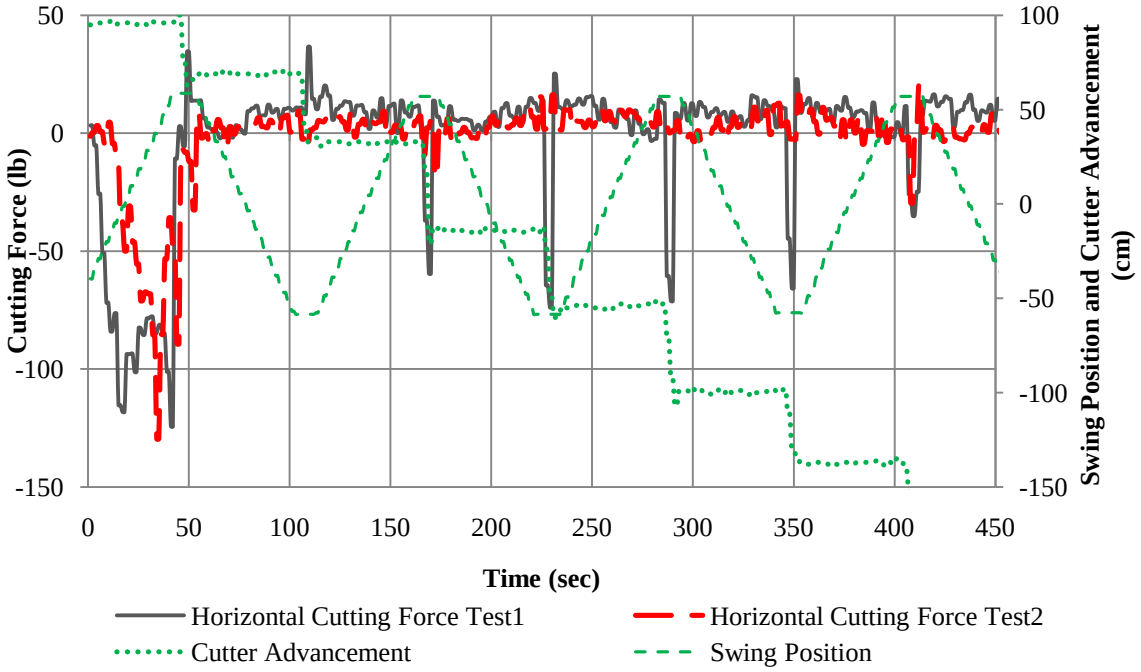

Figure 34. Test #1 and #2 horizontal cutting forces overlayed

The second comparison is the cutting forces in the axial direction shown in Figure 35. Figure 35 is setup identically to Figure 34 expect for the different force data. In cut 1 the axial cutting force shows the same variations for each of the tests. In the movement of the cutter when advancing, the advancements 1 through 7 are almost identical when the two tests are compared. This cutting force result shows that the axial force is more accurate than the horizontal cutting force because the axial cutting forces doesn't have significant irregularities imbedded in the cutting force data. However, this accuracy can be confirmed because in the east and west pull results from results chapter that showed cells 3 and 5 to be working properly and the data from these two gauges are used mostly to calculate the axial cutting force. The axial force comparison shows that the current load cell configuration is sufficient when calculating this cutting force.

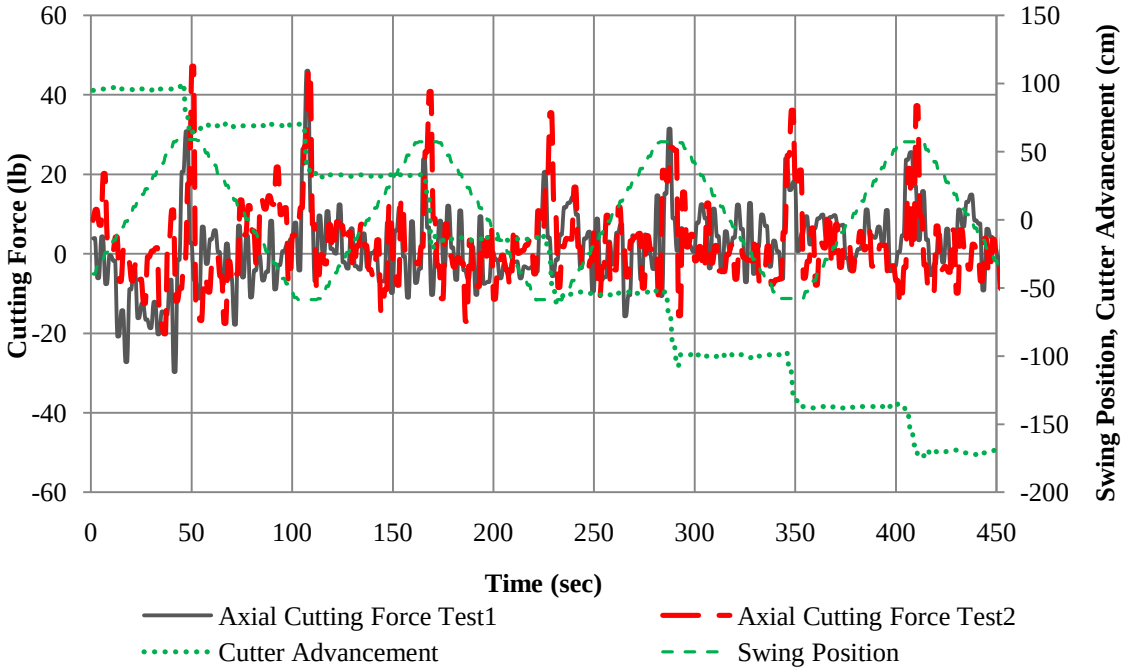

Figure 35. Test #1 and #2 axial cutting forces overlaid

The last test comparison is the vertical cutting forces for the two dredging tests. Figure 36 show the overlaid results for the vertical cutting forces for tests 1 and 2. Looking at the figure it can be said that cut 1 of test 1 and 2 show no similarities in cutting forces, but when cuts 2 through 8 are observed it can be said that the two tests are more closely related than cut 1. However, as said in the results section of test 1 and 2 above, when the cutter advances through the sediment significant irregularities are experienced in the cutter advancements 3 through 7 for test 1. So this compassion of the vertical cutting forces shows that readings from cell 1 are irregular when the cutter advances. So it is confirmed that the cell 1 location needs to be modified so that improved vertical cutting forces can be determined.

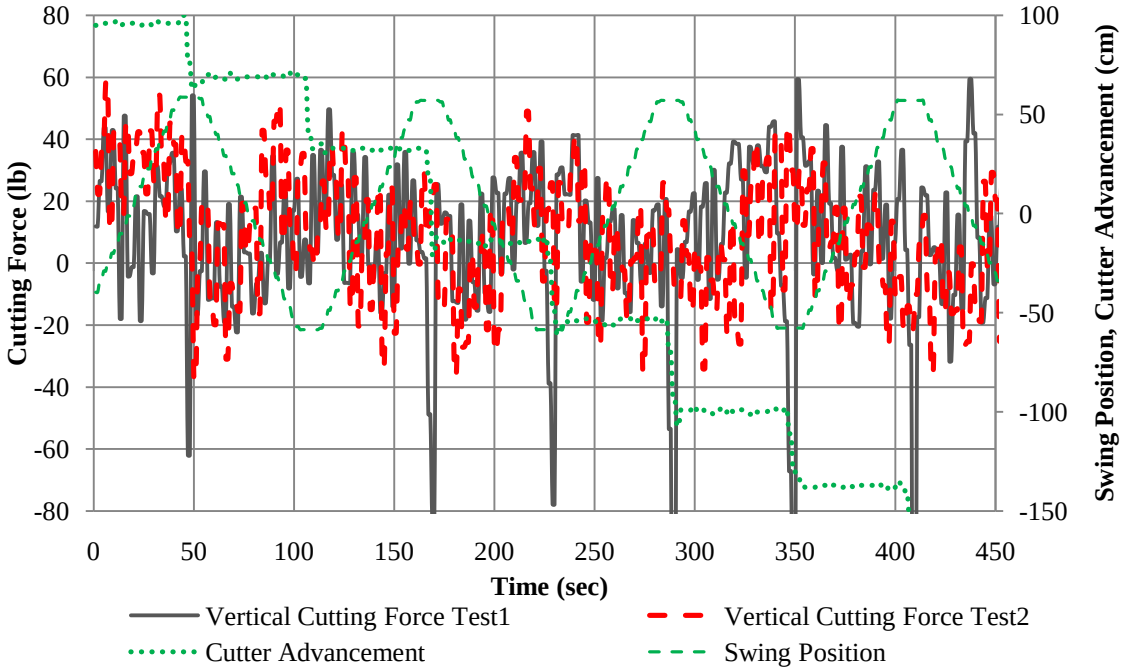

Figure 36. Test #1 and #2 vertical cutting forces overlaid

Conclusions

From this results section, the equations from the equation procedure have been rearranged so the cutting forces for a dredging test could be calculated and from this the systems of equations in Equations 7.1 and 7.2 were developed. Thus, the raw data from the carriage have been converted by using the calibration equations developed for the five load cells and the output from these equations were input into the program developed using MATLAB and the cutting forces were calculated and graphed for the two dredging tests done in the summer of 2008. The results for the axial cutting force are shown to be accurate and good results were calculated. The results for the horizontal and vertical cutting forces showed that irregularities were imbedded in the force data which caused spikes in the results for these to cutting forces. So from the procedure results chapter and the information gather in this chapter, it can be said that the current load cell configuration needs to be improved so that more accurate cutting forces can be determined.

CHAPTER VIII
DREDGE CARRIAGE LADDER REDESIGN

In the chapters of the procedure results and the dredging test results have shown that there are significant irregularities in the data that was presented in these two chapters. From these irregularities in the data collected from the current load cell configuration shows that the dredge carriage ladder moves to significantly which causes binding in the ladder cradle and shifts or irregularities occur in the load cell data. From these shifts it has been confirmed that the current load cell configuration needs to be modified. This modification requires redesigning the way that load cell 1 is mounted to the carriage ladder and a new load cell configuration to improve the rigidity of the carriage ladder which involves moving the current load cells to different locations to determined if the deformation of the ladder can minimized.

Redesign of Cell Location #1

The redesign cell 1 location is needed because the load cell that is used for this location is a one-directional force transducer which means that the sensor can only record readings in one direction. The current configuration is shown in the left side of Figure 37 that shows what direction the load cell takes a reading and also shows the shear force that was found in the direction shown from the SolidWorks pull procedure in the previous chapters. This current cell configuration also doesn't have the ability to reposition if the ladder shifts in any direction. Since the cell doesn't have the degrees of freedom needed to move with the movement of the ladder then if testing continues the cell will eventually will be damaged.

So to keep from damaging the cell in the future, the current configuration was redesigned using the SolidWorks program and can be seen in the right of Figure 37. This redesign involved using the same concept that was used for cells 2, 3, 4, and 5 which uses a simple concept of two tie-rod ends attached to each end of the load cell.

With this concept, if the ladder moves in any direction the load cell can move with the ladder without being damaged. Also the top load cell ladder bracket had to be redesign, so that the tie-rod concept could be installed without the ladder being repositioned from the current configuration. The lower tie-rod is attached to the ladder cradle by a designed base plate that can be easily removed by removing two 0.9525 cm x 1.905 cm (3/8 in x3/4 in) bolts if maintenance to the top load cell is needed.

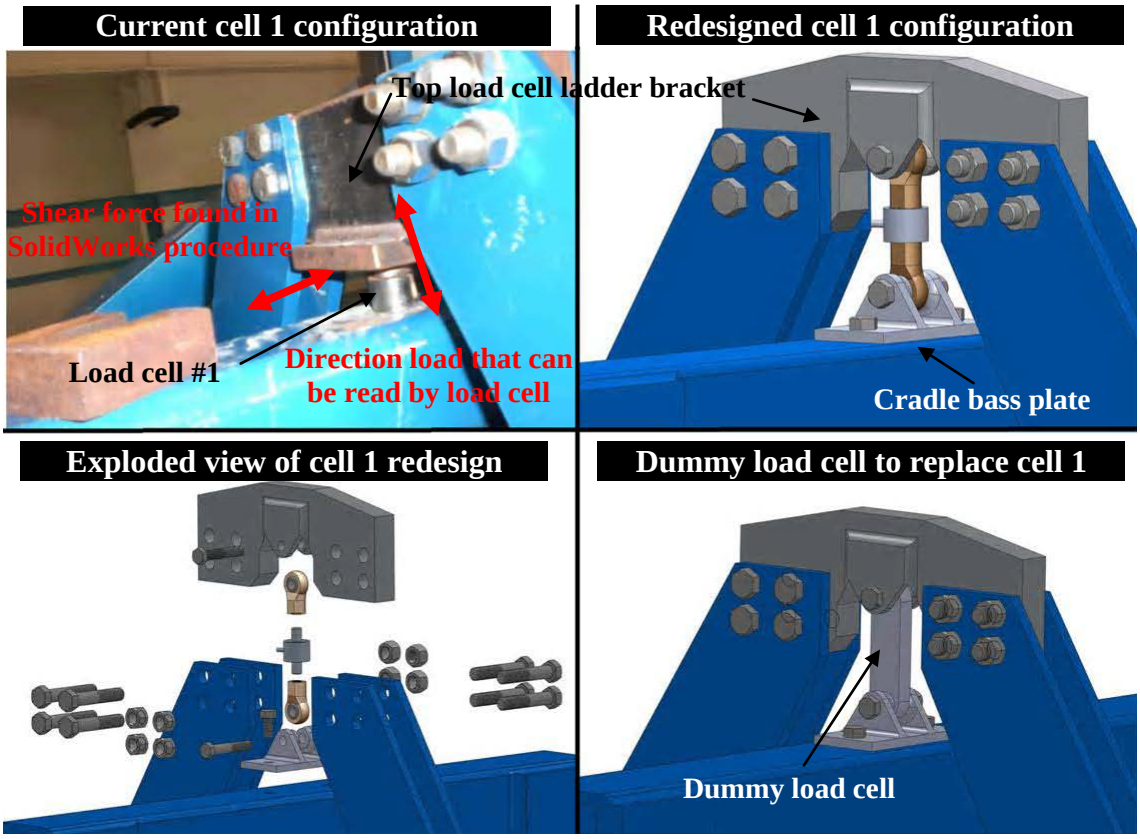

Figure 37. Load cell #1 redesign

An exploded view of the redesigned cell 1 location can be seen in the lower left-hand corner of Figure 37. This shows how the base plate, tie-rod ends, and load cell can be removed without any effort. This simple removal concept was implemented because

when the dredge carriage is on standby or no test are being preformed then cell 1 can be replaced by a dummy cell which is just a piece of 1.27 cm x 2.54 cm (½ in x 1in) A36 flat bar and this is done because load cell 1 has the weight of the dredge ladder on it constantly so this procedure is done to keep from damaging the load cell. This dummy cell has all of the same dimensions as the tie-rod ends and the load cell assembly and this was done to have easy installation and removal of the dummy load cell. In the lower right-hand corner of Figure 37, the installed dummy load cell is shown.

Design for Ladder Position of Load Cell #6

The second thing that needed to be corrected was the large movement of the carriage ladder inside the cradle. The Cosmosworks finite element model of SolidWorks was used again to determine the displacements of the carriage ladder so that a more rigid load cell configuration could be found. Using this program, the cells 2, 3, 4, and 5 were positioned in several different configurations and the displacement program was run for all of the different load cell configurations. From the analysis all of the configurations that were tested showed the same results or significantly worse deflections as the current load cell configuration. From these results it was determined that another degree of freedom had to be restrained to get a decrease in deflection of the ladder. To restrain the carriage ladder further, a sixth load cell has to be added to get the rigidity that is needed to decrease the deflection of the ladder.

To add another load cell to the ladder, a location had to be chosen for the placement of the sixth load cell. It was determined that moving the cells 2, 3, 4, and 5 didn't help the deflection of the ladder so the current configuration of the load cells was not changed. To determine a location to place the sixth load cell the SolidWorks model of the carriage ladder was used again. So to perform the deflection test using Cosmosworks, the sixth cell had to be added to the model and then the test could begin. The pulling procedure that was performed in the chapter V was repeated for applied load in 1.11 kN (250 lb)

increments up to a total applied load of 3.34 kN (750 lb) and the same north, south, east, and west pulling directions were used.

In determining the location where the sixth load cell should be placed, some preliminary test were done to determine if the placement of the cell would be on the upper ladder where cells 1, 2 and 3 are located or on the lower ladder where cells 4 and 5 are located. The preliminary tests were run and it was confirmed that the placement of the sixth load cell would be more beneficial if it was placed on the lower ladder along with cells 4 and 5. So a full analysis was done with the sixth load cell being placed in the lower ladder position and from this location four different tests were conducted with the locations of cell 6 in the positions described in Table 2. Using these locations of cell 6, analysis was performed to find the deflections of the ladder and the forces of every load cell.

Table 2. Design location of load cell #6

Redesign of Testing of Ladder	
Test #	**Placement location of load cell #6**
Current Configuration	No changes were made to ladder
Testing #1	Cell#6 located on lower Southeast corner oriented in north to south direction
Testing #2	Cell#6 located on lower South-east corner oriented in east to west direction
Testing #3	Cell#6 located on lower South-west corner oriented in north to south direction
Testing #4	Cell#6 located on lower South-west corner oriented in east to west direction

Results of Displacement Analysis of Dredge Ladder

Using the finite element model in SolidWorks the deflections of the dredge carriage ladder were calculated. These calculated deflections are used in determining the location of the sixth load cell. When running the SolidWorks it was determined that the major deflections were occurring at the cutterhead location which is expected because that is the location where the force is being applied. So the same pulling procedures were

completed, and the maximum displacements were recorded for the gravity load and all pulling directions in the increment stated above. Using these maximum displacement data four graphs were generated for the north, south, east, and west pulling directions. These graphs include the results for all four tests that are described in Table 2, and the figures were used to compare results for the four tests and where the cell 6 should be placed.

The first displacement results that were compared are the north pull redesign data shown in Figure 38. It can be seen that the maximum deflections occur for the current configuration which is expected and the data shows a dislocation at an applied load of 1.11 kN (250 lb) and after this location the slope of the displacement data becomes steeper, which at the 1.11 kN (250 lb) applied force the gravity load of the ladder keeps the ladder from moving significantly. Test 3 location shows a linear deflection when the cutterhead is loaded and also has a 45.9 percent decrease in deflection when compared to the current configuration. The locations for tests 2 and 4 almost identical and only have a difference of 0.25 percent difference and both test have a decrease of 63.6 percent in deflection from the current configuration. The last and largest decrease in deflection is test 1 which had a decrease of 65.8 percent. The results from all four test show very good improvement in decreasing the deflection the ladder.

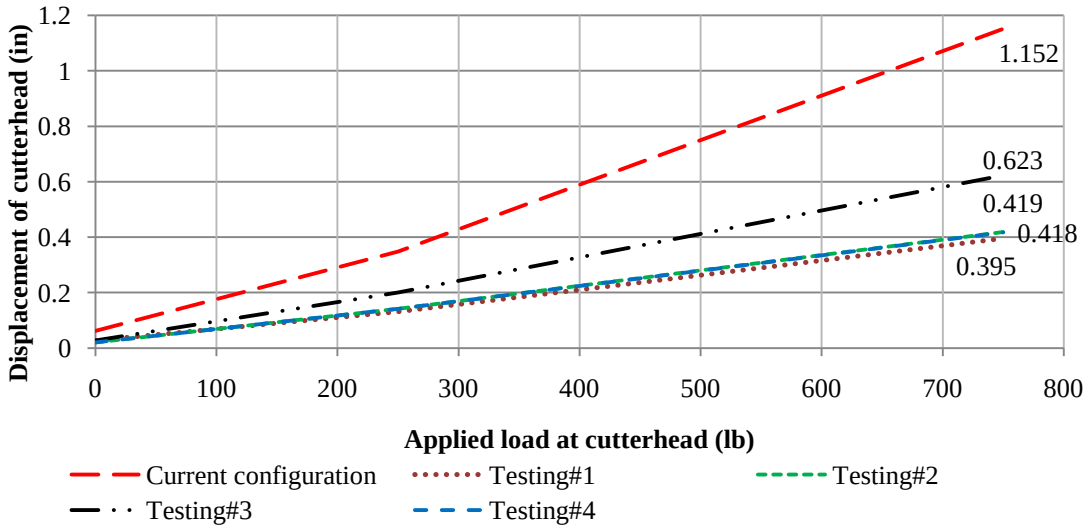

Figure 38. North pull redesign displacement data

The next pull direction compared is the results from the south pull procedure shown in Figure 39. This pull direction shows an increase in deflection of the current configuration from the north pull, but this data has no dislocation in the data and test 1, 2, 3, and 4 also have no dislocations which means as the force is applied at the cutterhead a linear deflection occurs for all tests. Test 3 shows an improvement in deflection of 48.3 percent, however this is isn't comparable to test 1, 2, and 4 because these three tests show an approximate decrease in deflection of 67 percent. These three tests locations show that the three are almost identical and cell 6 could be placed in anyone of the three locations.

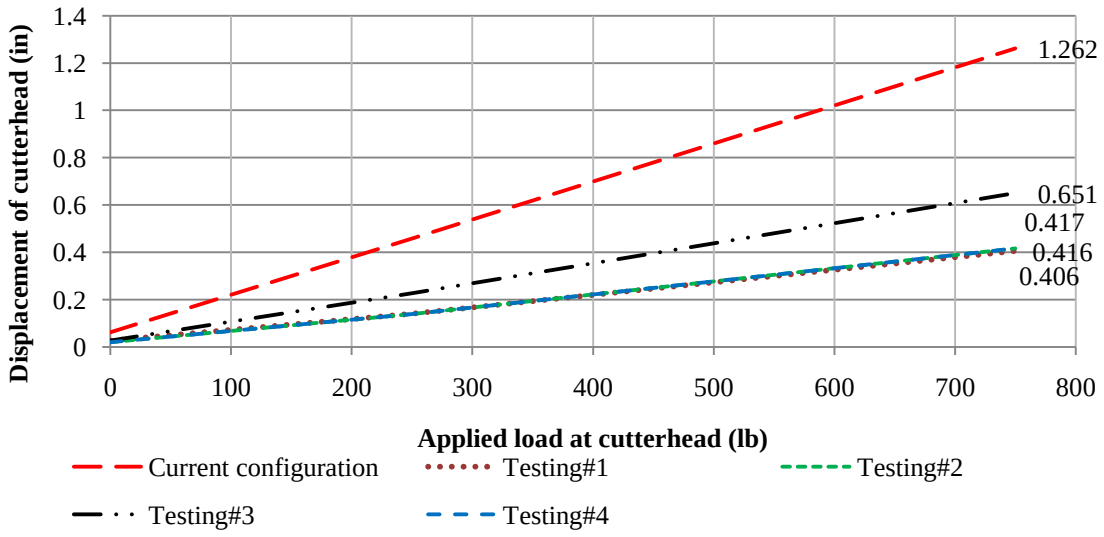

Figure 39. South pull redesign displacement data

Then next pull direction compared are the results from the east pull procedure shown in Figure 40. This pull direction shows and even larger maximum deflections in the current configuration when compared to the north and south pull displacement results. For this pull direction results show a shift in every test condition at approximately 1.11 kN (250 lb) and at this location and above the slope for every displacement test becomes slightly steeper and the meaning of this shift was discussed in the north pull results. Test 1 and 3 shows a decrease in deflection of 76 and 72 percent which is a dramatic decrease but test 2 and 3 shows better results of 90 percent decrease for both. The results for these pull direction tests show that test positions 2 and 4 are the best positions for the placement of cell 6.

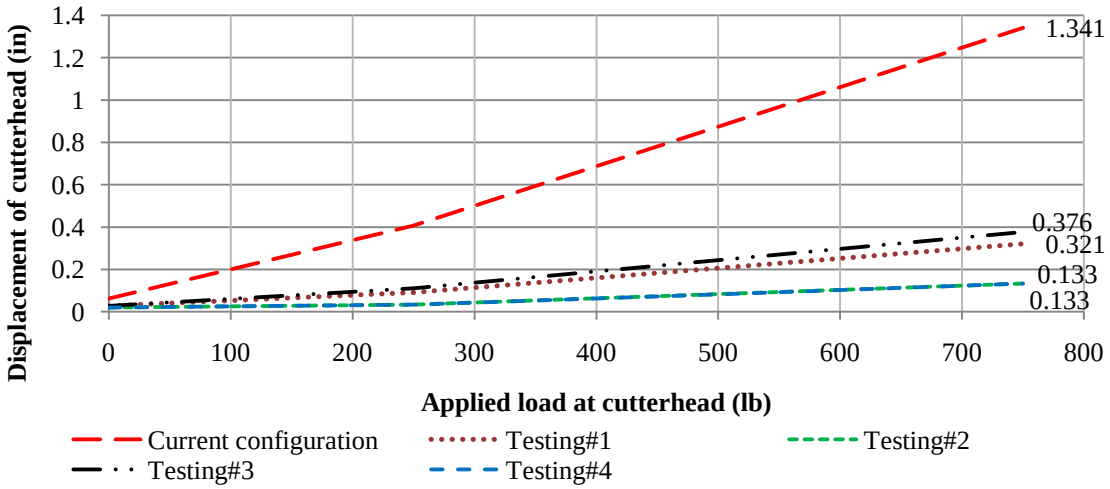

Figure 40. East pull redesign displacement data

The final pull direction compared is the results from the west pull procedure shown in Figure 41. This pull direction shows an even further increase in deflection for the current configuration and for these result no shifts occur. Test 1 and 3 have almost identical decrease in deflections to the east pull direction of 75 and 71 percent and tests 2 and 4 shows a decrease of 88 percent for both. This pull displacement results also show that cell positions would be sufficient for the placement of cell 6.

From the displacement testing procedure, a conclusion can be drawn on the placement of cell 6. All of the pull procedure results for testing positions 1, 2, 3, and 4 shows significant decreases in deflection of the dredge carriage ladder. However the results from this displacement analysis section supports that the testing positions 2 and 4 would be the best locations for the sixth load cell.

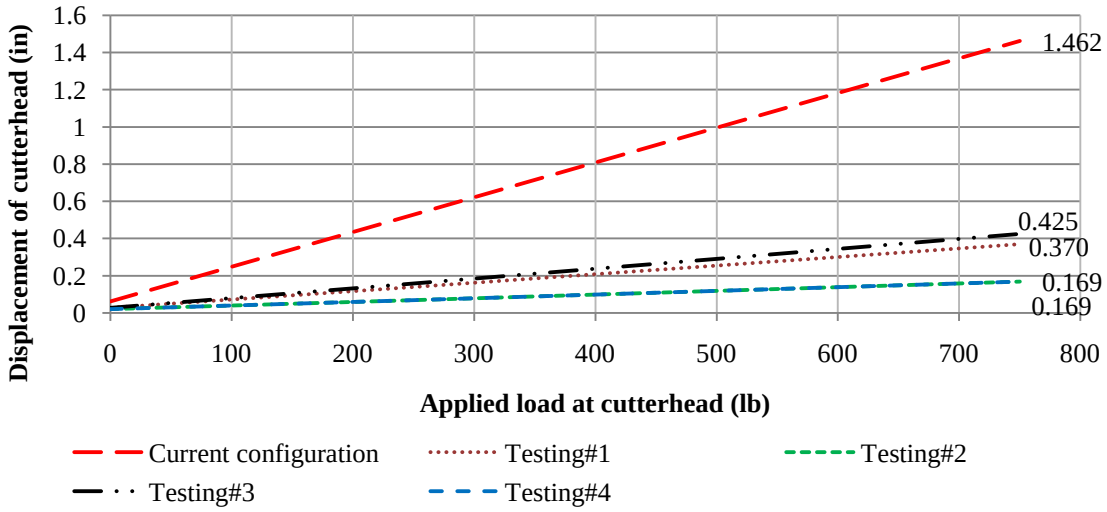

Figure 41. West pull redesign displacement data

Results of Forces on All Load Cells

To get further support in the best location position for cell 6, the loading in all load cells is used and this loading in the load cell were recorded when the displacement results were being generated. It is known that the safe maximum of the load cells that are used on the carriage ladder are approximately 13.34 kN (3000 lb), but as stated in chapter III the omega load cells have a 150 percent safe overload and a 300 percent maximum overload. The safe maximum is used to compare the forces in all six load cells. Also, the shear force at the cell 1 location is compared between the current configuration and new configurations. In Table 3 the current configuration results for the shear force and all load cell forces are given for the same pulling procedure used in the displacement results section. From these current configuration results conclusions can be made on the improvements that are made when placing cell 6 in the locations described in Table 2. In Table 3, the maximum value for the load cells were exceeded 5 times with a maximum overload of 118.8 percent, and the shear at the cell 1 location shows that a significant problem in the current configuration is relevant.

Table 3. Current configuration results for load cells and shear force

	Shear force in x dir (lb)	cell 1 load (lb)	cell 2 load (lb)	cell 3 load (lb)	cell 4 load (lb)	cell 5 load (lb)
Gravity load	**-187.75**	-1781.4	1.3848	91.85	1.385	-96.282
North Pull 250	**972.63**	-1810.4	-893.04	-1170	-1143.2	-198.15
North Pull 500	**2133**	-1839.4	-1787.5	-2431.8	-2287.8	-300.03
North Pull 750	**3293.4**	-1868.5	-2681.9	**-3693.7**	**-3432.4**	-401.9
South Pull 250	**-1348.1**	-1752.4	895.81	1353.7	1146	5.5899
South Pull 500	**-2508.5**	-1723.3	1790.2	2615.5	2290.6	107.46
South Pull 750	**-3668.9**	-1694.3	2684.6	**3877.4**	**3435.2**	209.33
East Pull 250	**1473.9**	-1694.8	-13.18	-846.61	-13.182	880.8
East Pull 500	**3135.6**	-1608.2	-27.746	-1785.1	-27.75	1857.9
East Pull 750	**4797.3**	-1521.6	-42.311	-2723.5	-42.317	2835
West Pull 250	**-1849.4**	-1868	15.95	1030.3	15.952	-1073.4
West Pull 500	**-3511.1**	-1954.6	30.515	1968.8	30.52	-2050.5
West Pull 750	**-5172.8**	-2041.2	45.08	2907.2	45.087	**-3027.5**

The first test that is compared is the testing for location 1 for cell 6, and the results for this test location are shown in Table 4. For this test there are 13 values that exceed the safe maximum of the load cells and the maximum load is marked in gray and exceeds the safe maximum by 112 percent. However, when the shear force is evaluated, it shows an average decrease in load of 97.2 percent. This reduction in the shear force is very significant because this means that the loads that are recorded from a dredging test will be more accurate.

Table 4. Testing 1 redesign load cell and shear force tests results

	Shear force in y dir (lb)	cell 1 load (lb)	cell 2 load (lb)	cell 3 load (lb)	cell 4 load (lb)	cell 5 load (lb)	cell 6 load (lb)
Gravity load	-14.463	-1792.8	16.758	-112.18	-229.44	-112.69	-231.7
North Pull 250	-46.795	-1787.5	-831.42	-112.18	74.627	-112.69	1202.8
North Pull 500	-79.127	-1782.2	-1679.6	-112.18	378.7	-112.69	2637.4
North Pull 750	**-111.46**	-1776.9	-2527.8	-112.18	682.76	-112.69	**4071.9**
South Pull 250	17.869	-1798.1	864.93	-112.18	-533.51	-112.69	-1666.2
South Pull 500	50.201	-1803.4	1713.1	-112.18	-837.58	-112.69	**-3100.8**
South Pull 750	82.533	-1808.7	2561.3	-112.18	-1141.6	-112.69	**-4535.3**
East Pull 250	17.427	-1649.6	-23.144	754.87	1811.4	1009.5	1816.8
East Pull 500	49.317	-1506.4	-63.046	1621.9	**3852.2**	2131.7	**3865.3**
East Pull 750	81.207	-1363.2	-102.95	2489	**5893**	**3253.9**	**5913.8**
West Pull 250	-46.353	-1935.9	56.659	-979.22	-2270.3	-1234.9	-2280.2
West Pull 500	-78.243	-2079.1	96.561	-1846.3	**-4311.1**	-2357.1	**-4328.7**
West Pull 750	**-110.13**	-2222.3	136.46	-2713.3	**-6351.9**	**-3479.3**	**-6377.2**

The next test that is compared is testing for location 2 for cell 6 and the results for this test location are shown in Table 5. This test location only has 3 values that exceed the safe maximum of the load cell. The maximum is mark in the table and this value only exceeds the limit by 12.7 percent which is a considerable difference than the results shown for testing 1. When the shear force for test 2 and the current configuration are compared, a decrease of 96.9 percent is experienced, which is slightly lower from the results of test 1, but is still a significant improvement.

Table 5. Testing 2 redesign load cell and shear force tests results

	Shear force in y dir (lb)	cell 1 load (lb)	cell 2 load (lbf)	cell 3 load (lb)	cell 4 load (lb)	cell 5 load (lb)	cell 6 load (lb)
Gravity load	-14.912	-1780.1	17.064	-114.35	2.1523	0.72907	115.08
North Pull 250	-70.322	-1867	-803.67	-101.48	-1124.2	-700.55	-595.85
North Pull 500	-125.73	-1953.9	-1624.4	-88.602	-2250.5	-1401.8	-1306.8
North Pull 750	**-181.14**	-2040.8	-2445.1	-75.727	**-3376.8**	-2103.1	-2017.7
South Pull 250	40.498	-1693.3	837.79	-127.23	1128.5	702.01	826.01
South Pull 500	95.908	-1606.4	1658.5	-140.11	2254.8	1403.3	1536.9
South Pull 750	**151.32**	-1519.5	2479.3	152.98	**3381.1**	2104.6	2247.9
East Pull 250	-13.874	-1768.7	13.944	771.1	0.069654	120.35	-901.3
East Pull 500	-12.837	-1757.3	10.824	1656.5	-2.013	239.98	-1917.7
East Pull 750	-11.799	-1745.9	7.7044	2542	-4.0956	359.6	-2934.1
West Pull 250	-15.95	-1791.6	20.184	-999.8	4.2349	-118.89	1131.5
West Pull 500	-16.987	-1803	23.304	-1885.3	6.3176	-238.52	2147.8
West Pull 750	-18.025	-1814.4	26.424	-2770.7	8.4002	-358.14	**3164.2**

The next test that is compared is testing for location 3 for cell 6, and the results for this test location are shown in Table 6. For this test there are 17 values that exceed the safe maximum of the load cells. The maximum load is marked in gray and exceeds the safe maximum by 165.5 percent which is an even large increase than the maximum in testing 1. The average shear force for this test decreased by 95.5 percent when compared to the current configuration, however when the number of exceeded loads and the value for

maximum loads shows that this load cell configuration is exceedingly worse than the testing locations 1 and 2 and even the current configuration.

Table 6. Testing 3 redesign load cell and shear force tests results

	Shear force in y dir (lb)	cell 1 load (lb)	cell 2 load (lb)	cell 3 load (lb)	cell 4 load (lb)	cell 5 load (lb)	cell 6 load (lb)
Gravity load	-11.386	-1786.8	16.504	-112.21	236.94	-112.73	231.79
North Pull 250	-88.884	-1831.7	-800.45	-112.21	-2339.5	-112.73	-1199.9
North Pull 500	-166.38	-1876.7	-1617.4	-112.21	**-4916**	-112.73	-2631.5
North Pull 750	**-243.88**	-1921.7	-2434.3	-112.21	**-7492.5**	-112.73	**-4063.1**
South Pull 250	66.112	-1741.8	833.45	-112.21	2813.4	-112.73	1663.4
South Pull 500	143.61	-1696.8	1650.4	-112.21	**5389.9**	-112.73	**3095.1**
South Pull 750	**221.11**	-1651.9	2467.4	-112.21	**7966.4**	-112.73	**4526.7**
East Pull 250	-41.882	-1715.5	18.724	754.83	-1840.1	1009.5	-1816.7
East Pull 500	-72.378	-1644.1	20.945	1621.9	**-3917.2**	2131.7	**-3865.2**
East Pull 750	**-102.87**	1572.8	23.165	2488.9	**-5994.3**	**3253.9**	**-5913.6**
West Pull 250	19.11	-1858.1	14.284	-979.25	2314	1234.9	2280.3
West Pull 500	49.606	-1929.4	12.064	-1846.3	**4391.1**	-2357.1	**4328.7**
West Pull 750	80.102	-2000.7	9.8434	-2713.3	**6468.1**	**-3479.4**	**6377.2**

The final test that is compared is testing for location 4 for cell 6 and the results for this test location are shown in Table 7. This testing location results are compared to the results for test 2, it can be seen that the results are almost identical and from the evaluation nothing needs to be compared.

Table 7. Testing 4 redesign load cell and shear force tests results

	Shear force in y dir (lb)	cell 1 load (lb)	cell 2 load (lb)	cell 3 load (lb)	cell 4 load (lb)	cell 5 load (lb)	cell 6 load (lb)
Gravity load	-14.911	-1780	17.064	-114.29	2.153	0.72907	-115.01
North Pull 250	-70.415	-1866.9	-803.56	-101.41	-1124.1	-700.55	595.92
North Pull 500	-125.92	-1953.7	-1624.2	-88.536	-2250.4	-1401.8	1306.8
North Pull 750	**-181.42**	-2040.6	-2444.8	-75.66	**-3376.7**	-2103.1	2017.8
South Pull 250	40.593	-1693.1	837.69	-127.16	1128.4	702.01	-825.94
South Pull 500	96.096	-1606.3	1658.3	-140.04	2254.7	1403.3	-1536.9
South Pull 750	**151.6**	-1519.4	2478.9	-152.91	**3381**	2104.6	-2247.8
East Pull 250	-14.006	-1768.6	14.097	771.16	0.090698	120.35	901.36
East Pull 500	-13.101	-1757.1	11.13	1656.6	-1.9716	239.98	1917.7
East Pull 750	-12.196	-1745.7	8.1625	2542.1	-4.0338	359.6	2934.1
West Pull 250	-15.816	-1791.4	20.031	-999.74	4.2152	-118.89	-1131.4
West Pull 500	-16.722	-1802.9	22.998	-1885.2	6.2775	-238.52	-2147.8
West Pull 750	-17.627	-1814.3	25.965	-2770.6	8.3397	-358.14	**-3164.1**

Conclusion from Displacement and Load Cell Force Results

From the displacement analysis and the load cell force results, the location of the sixth load cell can be determined. The displacement and force results section show that the testing 1 and 3 locations have larger displacements and significant forces in the load cells when compared with testing 2 and 4 results. From this evaluation the placement of the sixth load cell would be sufficient at the locations for testing 2 and 4. However due to cell installation difficulties the position for testing 4 is chosen for the placement of the sixth load cell.

Application of Force Equilibrium Equations to Redesigned Configuration

Now that the position for the sixth load cell has been determined and due to this redesign of the ladder, the force equilibrium equations have to be recalculated. The same method used in chapter V for the equilibrium equations procedure is used. The free body diagram of the redesigned carriage ladder is shown in Figure 42. This figure is similar to Figure 24 but the force for cell 6 (F_{c6}) was added and also the location for cell 1 changed. Using the SolidWorks finite element model again it was determined that the shear force that was found in chapter V had changed directions due to the addition of

cell 6 and now this shear force is oriented along the y-axis and this is shown in Figure 42. The only distance that was change was d_{c1Az} and this new distance is given by Equation 8.1. The only difference between Equations 5.4 and 8.1 is the value 234.56 was changed to 236.185, and this change was due to the location of cell 1 being changed in the redesign. All other distances and forces are identical as the ones shown in Figure 24.

$$d_{c1AzR} = 236.185 + 55.021 * \sin(\theta - .4556) \tag{8.1}$$

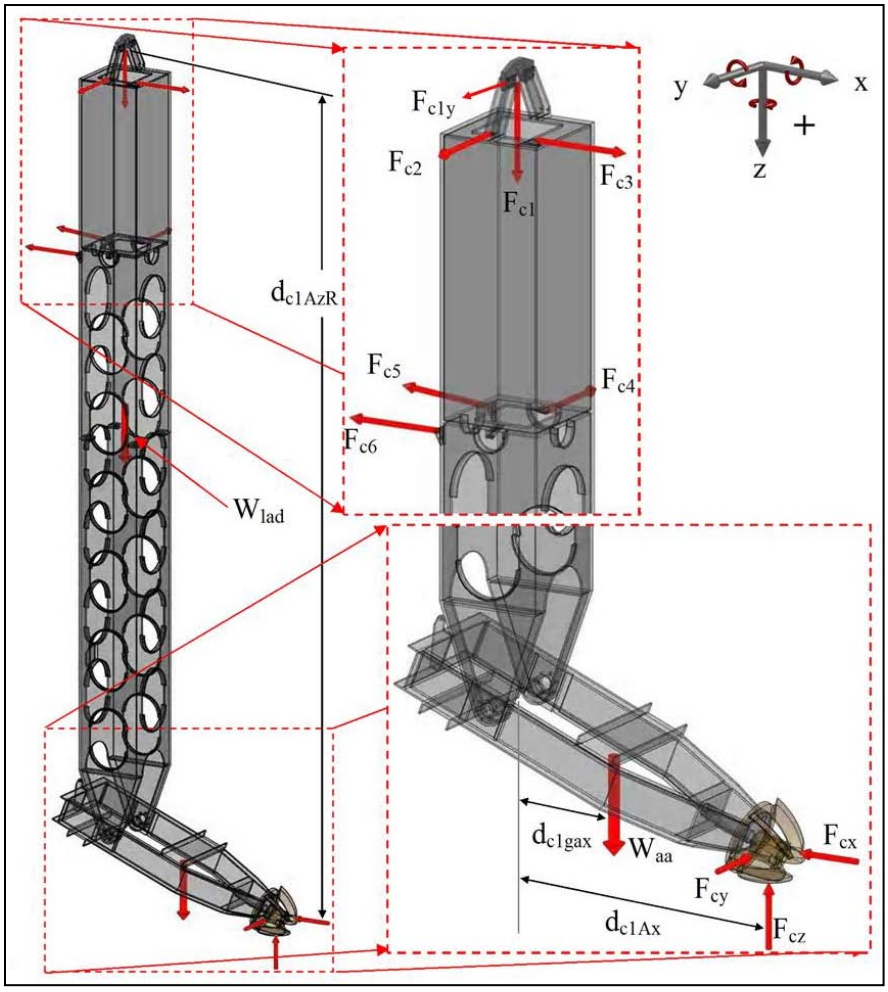

Figure 42. Free body diagram of redesigned ladder

Now that all of the changed variables in the free body diagram have been defined, Figure 42 can be used to develop the redesigned force equilibrium equations for the ladder. This equation formulation uses Equation 5.1 to determine the loads in the new load cell configuration. Using Equation 5.1, the summation of forces were taken in the x, y, and z directions and the summation of moments were taken about the x, y, and z axis. From this summation of forces and moments, the equilibrium equations for the redesigned dredge carriage ladder were determine, and this system of equations are expressed when Equation 8.2 is substituted into Equation 8.3. In this system of equations there are 12 unknowns, but this systems of equations are only a summary of all the forces acting on the carriage ladder.

$$C = \begin{bmatrix} 0 & 1 & 0 & 0 & -.0018 & -.089 & 0 & 0 & 0 & -1 & 1 & 1 \\ 0 & 0 & 0 & 1 & 0 & -.996 & -1 & -1 & 0 & 0 & 0 & 0 \\ 1 & 0 & 1 & 0 & -.999 & 0 & 0 & 0 & -1 & 0 & 0 & 0 \\ 0 & 0 & 10 & -9.25 & 0 & -9.89 & 9.13 & 0 & -d_{c1Ax} & 0 & 0 & 0 \\ 0 & 0 & -6.875 & 0 & 61.14 & .8116 & 0 & 0 & d_{c1AzR} & 0 & 0 & 0 \\ 0 & 0 & 0 & 6.875 & 0 & -62.37 & -61.7 & -d_{c1AzR} & 0 & d_{c1Ax} & 0 & -d_{c1gax} \end{bmatrix} \quad (8.2)$$

$$C \times \begin{bmatrix} F_{c1y} \\ F_{c1} \\ F_{c2} \\ F_{c3} \\ F_{c4} \\ F_{c5} \\ F_{c6} \\ F_{cx} \\ F_{cy} \\ F_{cz} \\ W_{lad} \\ W_{aa} \end{bmatrix} = \begin{bmatrix} 0 \\ 0 \\ 0 \\ 0 \\ 0 \\ 0 \end{bmatrix} \quad (8.3)$$

So by using the Equations 8.2 and 8.3 the six unknown load cell forces can be solved under one assumption. To determine forces in the six load cells when a known force is applied at the cutterhead location, Equations 8.2 and 8.3 have to be rearranged where

F_{c1}, F_{c2}, F_{c3}, F_{c4}, F_{c5}, and F_{c6} are set as unknown values and F_{cx}, F_{cy}, F_{cz}, W_{lad}, and W_{aa} as known values. To be able to determine a solution for the unknowns above, it has to be assumed that the shear force F_{c1y} is assumed to equal zero and from this assumption Equation 8.4 can be substituted into Equation 8.5. This assumption that the shear force equals zero is based on the results from testing 4 in the design of a new location for cell 6 which had a reduction in shear force of 96 percent when compared to the current cell configuration.

$$D = \begin{bmatrix} 1 & 0 & 0 & -.00175 & -.0889 & 0 \\ 0 & 0 & 1 & 0 & -.996 & -1 \\ 0 & 1 & 0 & -.9999 & 0 & 0 \\ 0 & 0 & -9.25 & 0 & -9.0889 & 9.125 \\ 0 & -6.875 & 0 & 61.141 & .8116 & 0 \\ 0 & 0 & 6.875 & 0 & -62.377 & -61.688 \end{bmatrix} \tag{8.4}$$

$$D \times \begin{bmatrix} F_{c1} \\ F_{c2} \\ F_{c3} \\ F_{c4} \\ F_{c5} \\ F_{c6} \end{bmatrix} = \begin{bmatrix} -W_{lad} - W_{aa} + F_{cz} \\ F_{cx} \\ F_{cy} \\ F_{cy}\, d_{c1Ax} \\ -F_{cy}\, d_{c1AzR} \\ F_{cx}\, d_{c1AzR} - F_{cz}\, d_{c1Ax} + W_{aa}\, d_{c1gax} \end{bmatrix} \tag{8.5}$$

Figure 43 was generated to show that Equations 8.4 and 8.5 are correct. In the development of these two equations it was assumed that the shear force at the cell 1 location was zero, and in Figure 43, the cell 2 data for the equations procedure shows that it is off by approximately 0.889 kN (200 lb) which this error is due to that assumption.

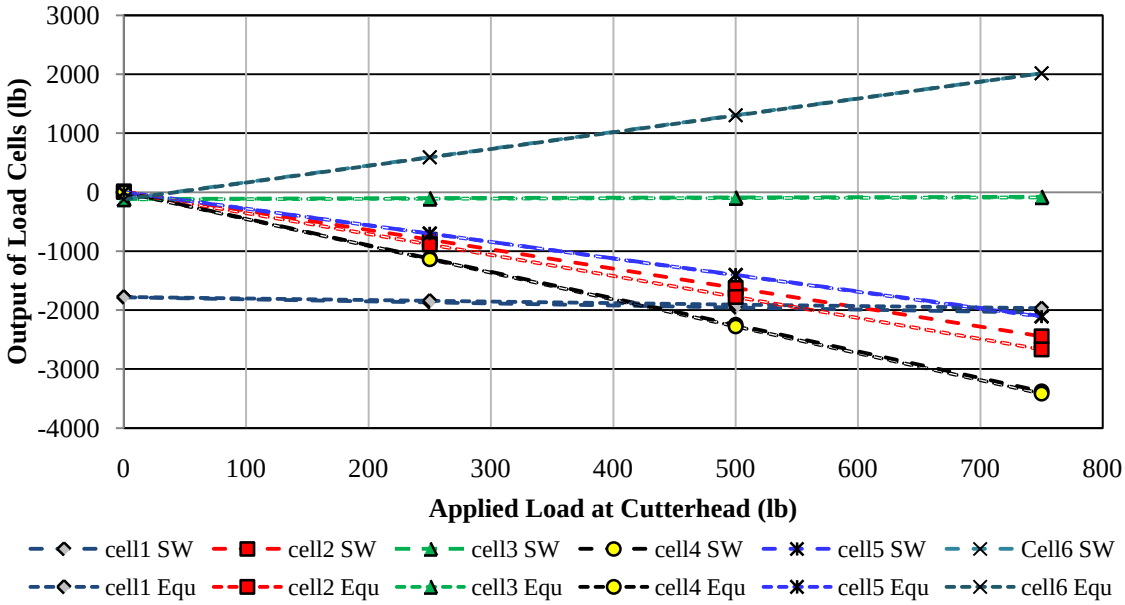

Figure 43. Redesign results for north pull direction

The final application of this system of equations shown in Equations 8.2 and 8.3 is developing a system of equations where F_{cx}, F_{cy}, F_{cz}, and F_{c1y} are unknown and the variables F_{c1}, F_{c2}, F_{c3}, F_{c4}, F_{c5}, F_{c6}, W_{lad}, and W_{aa} are known's. This system of equations is developed again by using Equations 8.2 and 8.3 and is shown when Equation 8.6 is substituted into Equation 8.7. In this system the variable F_{c1y} can be determined because there are only four unknowns and six equations. So using this system of equations expressed by Equation 8.6 and Equation 8.7, the cutting force F_{cx}, F_{cy}, and F_{cz} can be determined. Since the shear force ($F_{c1y)}$ can be calculated using these two equations it can be determined that accurate cutting forces can be calculated.

$$E = \begin{bmatrix} 0 & 0 & 0 & -1 \\ 0 & -1 & 0 & 0 \\ 1 & 0 & -1 & 0 \\ 0 & 0 & -d_{c1Ax} & 0 \\ 0 & 0 & d_{c1AzR} & 0 \\ 0 & -d_{c1AzR} & 0 & d_{c1Ax} \end{bmatrix} \tag{8.6}$$

$$E \times \begin{bmatrix} F_{c1y} \\ F_{cx} \\ F_{cy} \\ F_{cz} \end{bmatrix} = \begin{bmatrix} -F_{c1} + F_{c4}(.00175) + F_{c5}(.0888) - W_{lad} - W_{aa} \\ -F_{c3} + F_{c5}(.996) + F_{c6} \\ -F_{c2} + F_{c4}(.9999) \\ F_{c3}(9.25) + F_{c5}(9.0885) - F_{c6}(9.125) \\ F_{c2}(6.875) - F_{c4}(61.141) - F_{c5}(.8116) \\ -F_{c3}(6.875) + F_{c5}(62.377) + F_{c6}(61.688) + W_{aa}\, d_{c1gax} \end{bmatrix} \quad (8.7)$$

CHAPTER IX
APPLICATION OF LABORATORY MODEL CUTTING FORCES TO A PROTOTYPE CUTTERSUCTION DREDGE

The current cutting force research has shown that cutting forces can be estimated using the dredge carriage. From the estimation of cutting forces, these forces can be applied to a prototype cuttersuction dredge cutterhead. Froude scaling was used to find the similitude relationships for dredging swing speed and for cutter rotational velocities (Glover 2004). The swing speed relationship between a model and a prototype cuttersuction dredge is given by Equation 9.1 and the rotational velocities similitude is given by Equation 9.2, both of these equations were taken from Glover (2004). These two equations are used to scale up the swing speed and the cutterhead RPM that was used in the dredging test that were done in the summer 2008. In Equations 9.1 and 9.2 the D_{cutter} is the diameter of the cutterhead in inches and the g is the gravitational constant.

$$\left[\frac{V_{swing}}{\sqrt{gD_{cutter}}}\right]_{model} = \left[\frac{V_{swing}}{\sqrt{gD_{cutter}}}\right]_{prototype} \tag{9.1}$$

$$\left[N_{cutter}\sqrt{\frac{D_{cutter}}{g}}\right]_{model} = \left[N_{cutter}\sqrt{\frac{D_{cutter}}{g}}\right]_{prototype} \tag{9.2}$$

The main similitude relationship for the current cutting force research is the scaling of the cutting force shown in Equation 9.3. In Equation 9.3 the variable $F_{cutting}$ is the cutting force that the cutterhead is experiencing. This equation is used to scale the model cutting forces F_{cx}, F_{cy}, and F_{cz} up to cutting forces that would be applied to a prototype dredge cutterhead.

$$\left[\frac{F_{cutting}}{(D_{cutter})^3}\right]_{model} = \left[\frac{F_{cutting}}{(D_{cutter})^3}\right]_{prototype} \tag{9.3}$$

The dredge carriage is considered to be model of a 24 inch cuttersuction dredge which has been described in chapter III as a scale ratio of 1:6 which is considered a 4 inch model cuttersuction dredge. This scale ratio is used to represent the diameter (d_{cutter}) of the cutterhead in Equations 9.1, 9.2, and 9.3. Using Equations 9.1 and 9.2 the swing speed and cutterhead RPM for the model test are scaled and the output for the swing speed = 0.056 m/s (2.217 in/s) and cutterhead rotation speed = 35 RPM. Using Equation 9.3, the horizontal, vertical and axial cutting forces data from the model dredging test #2 were scaled up to a 24 inch prototype cuttersuction dredge and the results from this scaling are shown in Figure 44. The cutting force axis in the figure is in kips in which one kip is 1000 lb and the cutter advancement and swing position axis is in feet (ft). From the data shown in Figure 44, the swing winches, ladder, ladder supports, anchor cables and anchors, and cutterheads can all be designed to restrain these cutting forces.

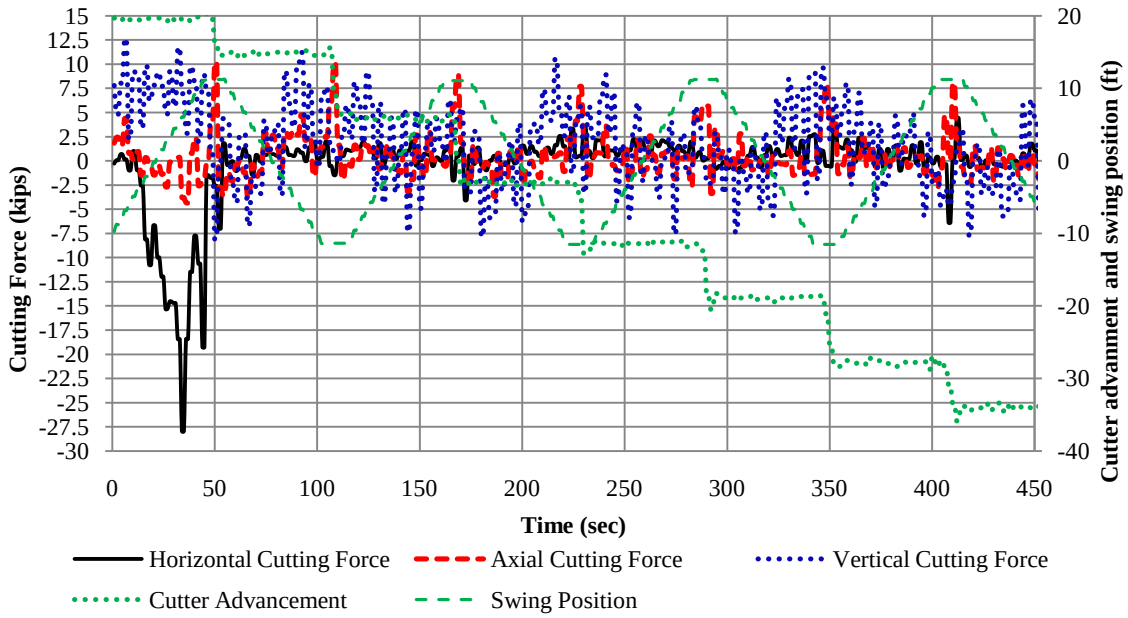

Figure 44. Prototype scaled cutting forces from model dredging test #2

CHAPTER X
SUMMARY AND CONCLUSIONS

The cutterhead of the cuttersuction dredge has been researched extensively from a range of basic concepts to concepts involving very mathematically detailed calculations. This was the case when the previous cutting force research evaluation was performed. The previous cutting force procedures evaluated include: Turner (1996), Miedema (1987) and (1989), Van Os and Van Leussen (1987), and Vlasblom (1998) and (2005). The cutting force calculation concepts from these researchers were evaluated and studied extensively and for this evaluation it was determined that some concepts are similar to the current cutting force research but for the most part the current cutting force research is a new concept of determining global forces generated by a dredge cutterhead.

This thesis topic of cutting forces on a laboratory cuttersuction dredge introduces an entirely different concept in determining cutting forces. This concept of determining cutting forces takes into account a more practical approach than previous cutting force studies. The current cutting force research involves using the dredge carriage located at the Haynes Laboratory at the Texas A&M University College Station campus. The dredge carriage is equipped with five load cells located on the ladder system and from this force measuring system it is assumed that forces on the cutterhead can be measured. This thesis showed the procedure for calibrating the load cells on the dredge carriage, and from the calibration, equations the force measured by the load cells can be determined. This concept of determining cutting forces on the cutterhead employed a laboratory pulling procedure on the dredge carriage ladder system, and the loads in the five load cells were recorded. This same procedure was also conducted using the three-dimensional modeling software called SolidWorks. These two methods were compared with theoretical calculations developed by using static equilibrium equations for the ladder system. From this comparison the current cutting force research concept was shown to be an applicable concept in determining cutting forces on the cutterhead.

However, some irregularities were found in the data which could mean that the current load cell configuration wasn't optimum for measuring the cutting forces.

In the summer of 2008, two dredging tests were performed and test data was recorded for the five load cells. Using the rearranged equilibrium equations, a solution for the cutting forces acting in the x, y, and z directions on the cutterhead and the shear force at the cell 1 location were determined. Using this cutting force calculation method, the data from the five load cells were used to determine the forces acting in the x, y, and z directions on the cutterhead in one second intervals (one Hz). From the two 450 second tests, it was determined that the current load configuration need to be redesigned due to irregularities in the data recorded for the five load cells.

A full analysis was completed to determine the problem areas in the current configuration. It was determined that the cell #1 location needed to be modified and also a sixth load cell needed to be added. This redesign involved changing the way that the location of cell #1 was configured and also a redesign was needed to determine a load cell configuration that kept the carriage ladder stable and as rigid as possible. The load cell #1 location was redesigned using the same concept used in the mounting of the other four cells. It was confirmed that a sixth load cell was needed to make the ladder more rigid so that accurate cutting force results could be obtained. The placement location for the sixth load cell was determined and from this new load cell configuration the new force equilibrium equations were developed and shown to be accurate.

The final procedure used is showing the similitude of the cutting force results from the dredging test #2 for a prototype 0.61 m (24 in) cutter suction dredge. The swing speed and rotational speed of the dredging test was used to determine the prototype swing speed and rotational speed of the cutter. The final calculation done was using the cutting force results from the dredging model test and scaling the forces up to a 0.61 m (24 in) prototype cuttersuction dredge.

Now that the ladder load cell arrangement has been redesigned, the new design of the load cell configuration has shown to be working properly. This method of determining the cutting forces on a dredge cutterhead using the dredge carriage has been confirmed to be accurate and very useful for future dredge cutting force research. In future cutting force research using this cutting force calculation, the variables of the different swing speeds, depth of cut, cutter RPM, flowrates, dredging angles, and types of material can be extensively evaluated. This thesis research topic of laboratory cutting forces on a dredge cutterhead has shown accurate results and from these research results a number of studies can be accomplished in the future.

REFERENCES

Glover, G. J. (2002) “Laboratory Modeling of Hydraulic Dredges and Design of Dredge Carriage for Laboratory Facility.” Master’s Thesis, Ocean Engineering Program, Civil Engineering Department, Texas A&M University, College Station, TX.

Glover, G. J. and Randall, R. E. (2004) “*Scaling of Model Hydraulic Dredges with Application to Design of a Dredge Modeling Facility*”, Journal of Dredging Engineering, Western Dredging Association (WEDA), Vol. 6, No. 2, pp 15-35.

Herbich, John B. (2000) “*Handbook of Dredging Engineering*.” Second Edition. McGraw-Hill Companies, Inc: New York.

Miedema, S.A. (1987) "The Calculation of the Cutting Forces When Cutting Water Saturated Sand, Basic Theory and Applications for 3-Dimensional Blade Movements with Periodically Varying Velocities for in Dredging Usual Excavating Elements." Doctoral thesis, Delft University, The Netherlands.

Miedema, S.A. (1989) "On the Cutting Forces in Saturated Sand of a Seagoing Cutter Suction Dredge". Proceedings of the World Dredging Congress. WODCON XII, Orlando, Florida.

Omega Engineering, Inc. (2008) “LC202 Miniature Universal Load Cells.” 03 Mar. 2009 http://www.omega.com/Pressure/pdf/LC202.pdf

Randall, R E., deJong, P., Sonye, S., Krippner, N., and Henriksen, J. (2005) “Laboratory Dredge Carriage for Modeling Dredge Operations.” Ocean Engineering Program, Civil Engineering Department, Texas A&M University, College Station, TX, 2005.

Riley, William F. and Sturges, Leroy D. (1996) “*Engineering Mechanics Statics*.” Second Edition. John Wiley & Sons, Inc: New York.

“*SolidWorks 2008-2009 for Windows*.” (2009): Dassault Systèmes, Santa Monica, CA.

Turner, Thomas M. (1996) “*Fundamentals of Hydraulic Dredging*.” Second Edition. American Society of Civil Engineers Press (ASCE Press) Reston, Virginia.

Van Os, A.G and Van Leussen, W. (1987) "*Basic Research on Cutting Forces in Saturated Sand*". Journal of Geotechnical Engineering, Vol. 113, No.12, pp. 1501-1516.

Vlasblom, W.J. (1998) “Relation Between Cutting-, Sidewinch-, and Axial Forces for Cutter Suction Dredgers.” *Proceedings of the 15th World Dredging Congress*, WODCON XV, Las Vegas, NV, pp. 275-291.

Vlasblom, W. J. (2005) “Cutter Suction Dredge.” http://www.dredging.org/documents/ceda/downloads/vlasblom3-the-cutter-suction-dredger.pdf

APPENDIX

Five Cell Configuration Force Calculation Programs

To get the equation results that were used in chapter VI a program called Matlab was used. This program was developed so the loads in the five load cells could be determined if a known load was applied at the location of the cutterhead. Below in Figure A.1 is the complete program for determining these forces in the five load cells.

```
%This is a program to calculate the loads in the five load cells for the
%  5 load cell configuration
%This program is used to check SolidWorks calculation and experimental
%  data results
format short
clc;
clear;
theta=22;   %Units are in Degrees (this angle can be change depending
%on dredging angle)
s=pi/180;   %Conversion factor from degrees to radians
%-------------------------------------------------------------------------

Fcx=0;   %Cutting force along x-axis ((+) west pull, (-) East pull
         %Units are in pounds (lb))
Fcy=0;   %Cutting force along y-axis (North Pull is (+), and South pull (-)
         %Units are in pounds (lb))
Fcz=0;   %Cutting force along z-axis (Units are in pounds (lb))
%-------------------------------------------------------------------------
Waa=339.4;  %Weight of Articulating arm and dredge cutterhead
%(Units are in pounds (lb))
Wlad=1429;  %Weight of Upper and lower ladder (Units are in lb)
%-------------------------------------------------------------------------
R1=-Fcz*55.0212*cos(theta*s-.4556*s)+Fcx*(234.56+55.0212*sin(theta*s-...
    .4556*s))+Waa*21.2992*cos(theta*s-.5237*s);
Equmatrix=[0 1 0 0 -.00175 -.0888;1 0 0 1 0 -.996;0 0 1 0 -.9999 0;...
    0 0 0 -9.25 0 -.996*9.125;0 0 -5.25 0 +(.9999*59.5+.00175*9.5)...
    .08889*9.125;0 0 0 5.25 0 -(.08889*10.5+.996*60.0625)];
knownforces=[-Waa-Wlad+Fcz;Fcx;Fcy;Fcy*55.0212*cos(theta*s-.4556*s);...
    -Fcy*(234.56+(55.0212)*sin(theta*s-.4556*s));R1];
%-------------------------------------------------------------------------
%Solution to unknowns
format bank
Sol1=(Equmatrix\knownforces)'%This gives the solution to the top shear
%  force and the five load cells in this order: Shear force, Cell#1,
%  Cell#2, Cell#3, Cell#4, and Cell#5
```

Figure A.1. Load cell force calculation program for five cell configuration

In this program there are several input variables that can be change to the specifics of a desired test. In line 8 the input for the dredging angle can be adjusted from 0 to 50 degrees and these set angle are because they are the capable working angle of the dredge carriage. In lines 13, 15, and 17 the variables that can be changed are underlined in red. These values are the forces that can be applied to the cutterhead location. Lines 23 through 29 are the system of equation developed in the equation procedure and is shown by Equation 5.7. Line 33 is the equation the gives the results starting with shear force at the cell1 location, cell 1 force, cell 2 force, cell 3 force, cell 4 force, and cell 5 force. In the program on lines 13, 15, and 17 describes what needs to be changed to change the direction of load on the cutterhead.

The next program that was used in the cutting force research was the cutting force calculator for the five cell configuration. This program was developed so the cutting forces in the x, y, and z directions could be solved. The main part of this program is the system of equation that was used. The systems of equations that are generated when Equation 7.1 is substituted into Equation 7.2 are the system of equations shown in Figure A.2 on lines 72 through 79.

This program is a little different than the one shown in Figure A.1 because this program loads a text file that has all of the load cell data in it from a dredging test. This is done by input the exact file name of the text file in line 11, also this text file must be in the same folder as this cutting force calculator program file. On line 13 the name of the text file must be inputted in the location underlined in red. In lines 19 and 20 the n and t values can be changed to adjust the axis on the cutting force results plot. The values in lines 23 through 26 are the outputs from the program shown in Figure A.1 and these values do not change. The process described in chapter VI of taking the mean and subtracting it was done so that more precise calculations could be made and this process is shown on lines 29 through 45. The calibration equations developed in chapter IV are inputted in lines 56 through 64 and these equations take the raw data loaded by lines 48

through 52 to calculate the forces in the load cells in pounds. Lines 65 through 85 is a solver for determining cutting forces and this solver solves the cutting force system of equations for each second of the dredging test.

On lines 87 and 88 there is an equation that can be used to show the cutting forces in the command window of Matlab. From the command window you can copy and paste the data into a text file and then Microsoft excel can be used to import the data and then plot of the cutting forces can be generated. However the program in Figure A.2 is used generate a figure that shows the swing position, advancement position, and the cutting force in the x, y, and z directions and this is done by the code on lines 90 through 111.

```
1         %CUTTING FORCE CALCULATOR FOR FIVE LOAD CELL CONFIGURATION
2 %Cutting Forces in the five load cells are known
3 %This program is used to check SolidWorks calculation and experimental data)
4 %Dredging Angle
5 format short
6 clc;
7 clear;
8 clf;
9 %--------------------------------------------------------------------------
10           %VALUES THAT NEED TO BE CHANGED FOR THE SPECIFIC TEST
11 load MACAUG27.txt %The title of the dredging test text file goes here
12                 %Lettering at the top of the text file needs to be deleted
13 data=MACAUG27;  %This has to be the same name as the text file name
14 theta=22; %Units are in Degrees (Dredging angle depends on dredging test)
15 %--------------------------------------------------------------------------
16 Waa=339.4;  %Weight of Articulating arm and dredge cutterhead
17 %(Units are in pounds (lb))
18 Wlad=1429;  %Weight of Upper and lower ladder (Units are in lb)
19 n=100;   %This value can be changed to adjust the axis
20 t=300; % t can be changed to adjust the plotted axis
21 %--------------------------------------------------------------------------
22  %THIS IS THE LOAD IN THE 4 LOAD CELLS WHEN NO LOAD IS APPLIED AT CUTTER
23 F22=1.53;
24 F33=100.28;
25 F44=1.53;
26 F55=-102.06;
27 %--------------------------------------------------------------------------
28              %TAKES MEAN OF THE RAW DATA
29 W1=mean(data(n:length(data),7));
30 F2=mean(data(n:length(data),8));
31 F3=mean(data(n:length(data),9));
32 F4=mean(data(n:length(data),10));
33 F5=mean(data(n:length(data),11));
34 %--------------------------------------------------------------------------
35 Fc1=30.2091*(W1)+174.9756;
36 F2a=30.5827*(F2)-82.3436;
37 F3a=27.9397*(F3)+32.4884;
38 F4a=28.21*(F4)+8.7501;
39 F5a=31.2517*(F5)-99.3691;
40 %--------------------------------------------------------------------------
41 Wadj=Waa+Wlad+Fc1;
42 F2adj=F2a-F22;
43 F3adj=F3a-F33;
44 F4adj=F4a-F44;
45 F5adj=F5a-F55;
46 %--------------------------------------------------------------------------
47            %LOADING OF THE RAW DATA FROM THE DREDGE CARRIAGE
48 Fc1raw=data(n:length(data),7); %Percent(%) load in Cell#1
49 Fc2raw=data(n:length(data),8); %Percent(%) load in Cell#2
50 Fc3raw=data(n:length(data),9); %Percent(%) load in Cell#3
51 Fc4raw=data(n:length(data),10); %Percent(%) load in Cell#4
52 Fc5raw=data(n:length(data),11); %Percent(%) load in Cell#5
```

Figure A.2. Five cell configuration cutting force calculator

```
swpost=data(n:length(data),15)-70; %Position of cutter in swing direction
%-------------------------------------------------------------------------
                    %CALIBRATION EQUATIONS
Fc1a=30.2091*(Fc1raw)+174.9756-Wadj; %Load Cell#1 force
                                     %(Units are in pounds (lb))
Fc2a=30.5827*(Fc2raw)-82.3436-F2adj; %Load Cell#2 force
                                     %(Units are in pounds (lb))
Fc3a=27.9397*(Fc3raw)+32.4884-F3adj; %Load Cell#3 force
                                     %(Units are in pounds (lb))
Fc4a=28.21*(Fc4raw)+8.7501-F4adj;    %Load Cell#4 force
                                     %Units are in pounds (lb))
Fc5a=31.2517*(Fc5raw)-99.3691-F5adj; %Load Cell#5 force
                                     %(Units are in pounds (lb))
%-------------------------------------------------------------------------
        %CALCULATION OF CUTTING FORCES FOR EACH INTERATION
s=pi/180;   %Conversion factor from degrees to radians
format bank
for k=1:length(Fc1a)
    Fc1=Fc1a(k);Fc2=Fc2a(k);Fc3=Fc3a(k);Fc4=Fc4a(k);Fc5=Fc5a(k);
        Equmatrix=[0 0 0 -1;1 -1 0 0;0 0 -1 0;0 0 -55.0212*...
            cos(theta*s-.4556*s) 0;0 0 (234.56+55.021*sin(theta*s-...
            .4556*s)) 0;0 -(234.56+55.021*sin(theta*s-.4556*s))...
            0 55.0212*cos(theta*s-.4556*s)];
    knownforces=[-Fc1+Fc4*.00175+Fc5*.0888-Wlad-Waa;-Fc3+Fc5*.996;...
        -Fc2+Fc4*.9999;Fc3*9.25+Fc5*(-9.0885);Fc2*5.25-Fc4*...
        59.5107+Fc5*.8111;-Fc3*5.25+Fc5*60.7556+Waa*...
        21.2992*cos(theta*s-.5237*s)];
    %Solutions of Unknowns
    Sol1=Equmatrix\knownforces;
    Fcx(k)=Sol1(2);
    Fcy(k)=Sol1(3);
    Fcz(k)=Sol1(4);
end
%-------------------------------------------------------------------------
%Cutdata=[Fcx',Fcy',Fcz',data(n:length(data),3)*100-1925,...
    %data(n:length(data),15)-70]
%-------------------------------------------------------------------------
     %PLOTTING OF Fcx, Fcy, Fcz, Swing Position, and Cutter Advancement
y=[1:(length(Fcx(1:t)))];
r=t+n-1;

plot(y,data(n:r,15)-70,'g:','linewidth',2); %Swing Position plot
hold on
plot(y,data(n:r,3)*100-1925,'g-.','linewidth',2); %Advancement plot
plot(y,Fcz(1:t),'b:','linewidth',2); %Cutting force in z direction plot
hold on
plot(y,Fcx(1:t),'r--','linewidth',2); %Cutting force in x direction plot
plot(y,Fcy(1:t),'k','linewidth',2); %Cutting force in y direction  plot
axis([0 t -150 100]);
grid on;
xlabel('TIME (sec)','fontsize',12);
ylabel('Cutting Force (lbf)','fontsize',12);
```

Figure A.2. Continued

```
105 ylabel('Cutting Force (lbf), Swing Position and Cutter Advancement (cm)',...
106     'fontsize',12);
107 legend('Vertical Cutting Force','Axial Cutting Force',...
108     'Horizontal... Cutting Force',1);
109 legend('Swing Position','Cutter Advancement','Vertical Cutting Force',...
110     'Axial Cutting Force','Horizontal Cutting Force',1);
111 hold off
```

Figure A.2. Continued

Six Cell Configuration Force Calculations

This cell configuration was developed from the redesign of the ladder in chapter VIII. Since the ladder configuration was change so were the program shown in Figures A.1 and A.2. So the program in Figure A.1 was modified, and from the modification, the program in Figure A.3 was developed. In this program, all of the input variables are the same as the program shown in Figure A.1, but the system of equations is different. Since the ladder was redesigned the system of equations changed and these equations were developed in chapter VIII and are shown in Equations 8.4 and 8.5. So the system of equations used for the five cell configuration was deleted and the system of equations shown in Equation 8.5 was inputted into the program in lines 22 through 28. This was the only change that was needed to be done to get results for the six load cell when a known load is applied to the cutterhead.

```
 1 %This is a program to calculate the loads in the six load cells for the
 2 %  six load cell configuration
 3 %This program is used to check SolidWorks calculations and experimental
 4 %  data resutls
 5 format short
 6 clc;
 7 clear;
 8 theta=22;   %Units are in Degrees (this angle can be change depending
 9 %on dredging angle)
10 s=pi/180;   %Conversion  factor from degrees to radians
11 %---------------------------------------------------------------------------
12 Fcx=0;   %Cutting force along x-axis ((+) west pull, (-) East pull
13         %Units are in pounds (lb))
14 Fcy=0;   %Cutting force along y-axis (North Pull is (+), and South pull (-)
15         %Units are in pounds (lb))
16 Fcz=0;   %Cutting force along z-axis (Units are in pounds (lb))
17 %---------------------------------------------------------------------------
18 Waa=339.4;  %Weight of Articulating arm and dredge cutterhead
19 %(Units are in pounds (lb))
20 Wlad=1436;  %Weight of Upper and lower ladder (Units are in lb)
21 %---------------------------------------------------------------------------
22 R1=-Fcz*55.0212*cos(theta*s-.4556*s)+Fcx*(236.185+55.0212*sin(theta*s-...
23     .4556*s))+Waa*21.2992*cos(theta*s-.5237*s);
24 Equmatrix=[1 0 0 -.00175 -.0888 0;0 0 1 0 -.996 -1;0 1 0 -.9999 0 0;...
25     0 0 -9.25 0 -9.0889 9.125;0 -6.875 0 61.14148 .8116 0;...
26     0 0 6.875 0 -62.37669 -61.6875];
27 knownforces=[-Waa-Wlad+Fcz;Fcx;Fcy;Fcy*55.0212*cos(theta*s-.4556*s);...
28     -Fcy*(236.185+(55.0212)*sin(theta*s-.4556*s));R1];
29 %---------------------------------------------------------------------------
30 %Solution to unknowns
31 format bank
32 Sol1=(Equmatrix\knownforces)'%This gives the solution to the six load
33 %cells in this order: Cell#1, Cell#2, Cell#3, Cell#4, Cell#5 and Cell#6
```

Figure A.3. Load cell force calculation program for six load cell configuration

The final program developed was the cutting force calculator for the ladder six load cell configuration. For this program several things needed to be added to accommodate the addition of the sixth load cell. The first thing added was the results from the gravity load analysis of the six load cell configuration in SolidWorks, and the results are shown on lines 23 through 27. Next all equations for the data modification process for cell 6 had to be added and this is shown on lines 35, 42, 49, and 57. The calibration equation for cell 6 had to be determined and after it was determined it was input into line 72. The final modification was to input the system of equations from Equation 8.6 and 8.7 into lines 81 through 88, and lines 89 through 120 didn't change. Now this program can be used to determine cutting forces for the redesigned six load cell configuration.

```
1          %CUTTING FORCE CALCULATOR FOR SIX LOAD CELL CONFIGURATION
2  %Cutting Forces in the five load cells are known
3  %This program is used to check SolidWorks calculation and experimental data)
4  %Dredging Angle
5  format short
6  clc;
7  clear;
8  %clf;
9  %-------------------------------------------------------------------------
10            %VALUES THAT NEED TO BE CHANGED FOR THE SPECIFIC TEST
11 load MACAUG27.txt  %The title of the text file goes here
12                    %Lettering at the top of the text file needs to be delete
13 data=MACAUG27;  %This has to be the same name as the text file name
14 theta=22;   %Units are in Degrees (Dredging angle depending on dredging test
15 %-------------------------------------------------------------------------
16 Waa=339.4;  %Weight of Articulating arm and dredge cutterhead
17 %(Units are in pounds (lb))
18 Wlad=1436;  %Weight of Upper and lower ladder (Units are in lb)
19 n=1;   %n=1 for test#1 and n=16 for test#2
20 t=450; % t can be can be changed to adjust the plotted axis
21 %-------------------------------------------------------------------------
22  %THIS IS THE LOAD IN THE 5 LOAD CELLS WHEN NO LOAD IS APPLIED AT CUTTER
23 F22=17.064;
24 F33=-114.29;
25 F44=2.153;
26 F55=0.729;
27 F66=-115.01;
28 %-------------------------------------------------------------------------
29              %TAKES MEAN OF THE RAW DATA
30 W1=mean(data(n:length(data),7));
31 F2=mean(data(n:length(data),8));
32 F3=mean(data(n:length(data),9));
33 F4=mean(data(n:length(data),10));
34 F5=mean(data(n:length(data),11));
35 F6=mean(data(n:length(data),##)); %Data column needs to be inputted into ##
36 %-------------------------------------------------------------------------
37 Fc1=30.2091*(W1)+174.9756;
38 F2a=30.5827*(F2)-82.3436;
39 F3a=27.9397*(F3)+32.4884;
40 F4a=28.21*(F4)+8.7501;
41 F5a=31.2517*(F5)-99.3691;
42 F6a=??+??; %Calibration equation needs to be inputted into ##+or-##
43 %-------------------------------------------------------------------------
44 Wadj=Waa+Wlad+Fc1;
45 F2adj=F2a-F22;
46 F3adj=F3a-F33;
47 F4adj=F4a-F44;
48 F5adj=F5a-F55;
49 F6adj=F6a-F66;
50 %-------------------------------------------------------------------------
51             %LOADING OF THE RAW DATA FROM THE DREDGE CARRIAGE
52 Fc1raw=data(n:length(data),7); %Percent(%) load in Cell#1
```

Figure A.4. Six cell configuration cutting force calculator

```
Fc2raw=data(n:length(data),8); %Percent(%) load in Cell#2
Fc3raw=data(n:length(data),9); %Percent(%) load in Cell#3
Fc4raw=data(n:length(data),10); %Percent(%) load in Cell#4
Fc5raw=data(n:length(data),11); %Percent(%) load in Cell#5
Fc6raw=data(n:length(data),##); %Percent(%) load in Cell#6
    %Data column needs to be inputted in ##
swpost=data(n:length(data),15)-70; %Position of cutter in swing direction
%-------------------------------------------------------------------------
                    %CALIBRATION EQUATIONS
Fc1a=30.2091*(Fc1raw)+174.9756-Wadj; %Load Cell#1 force
                                     %(Units are in pounds (lb))
Fc2a=30.5827*(Fc2raw)-82.3436-F2adj; %Load Cell#2 force
                                     %(Units are in pounds (lb))
Fc3a=27.9397*(Fc3raw)+32.4884-F3adj; %Load Cell#3 force
                                     %(Units are in pounds (lb))
Fc4a=28.21*(Fc4raw)+8.7501-F4adj;    %Load Cell#4 force
                                     %Units are in pounds (lb))
Fc5a=31.2517*(Fc5raw)-99.3691-F5adj; %Load Cell#5 force
                                     %(Units are in pounds (lb))
Fc6a=##+or-##-F6adj;                 %Load Cell#6 force (Units in (lb))
        %Calibration equations need to be inputted in ##+or-##
%-------------------------------------------------------------------------
         %CALCULATION OF CUTTING FORCES FOR EACH INTERATION
s=pi/180;   %Coversion factor from degrees to radians
format bank

for k=1:length(Fc1a)
    Fc1=Fc1a(k);Fc2=Fc2a(k);Fc3=Fc3a(k);Fc4=Fc4a(k);Fc5=Fc5a(k);Fc6=Fc6a;
        Equmatrix=[0 0 0 -1;0 -1 0 0;1 0 -1 0;0 0 -55.0212*...
            cos(theta*s-.4556*s) 0;0 0 (236.185+55.021*sin(theta*s-...
            .4556*s)) 0;0 -(236.185+55.021*sin(theta*s-.4556*s))...
            0 55.0212*cos(theta*s-.4556*s)];
    knownforces=[-Fc1+Fc4*.00175+Fc5*.0888-Wlad-Waa;-Fc3+Fc5*...
        .996+Fc6;-Fc2+Fc4*.9999;Fc3*9.25+Fc5*(9.0885)-Fc6*9.125;Fc2*...
        6.875-Fc4*61.141-Fc5*.8116;-Fc3*6.875+Fc5*62.37669+Waa*...
        21.2992*cos(theta*s-.5237*s)+Fc6*61.675];
    %Solutions of Unknowns
    Sol1=Equmatrix\knownforces;
    Fc5x(k)=Sol1(1);
    Fcx(k)=Sol1(2);
    Fcy(k)=Sol1(3);
    Fcz(k)=Sol1(4);
end
%-------------------------------------------------------------------------
%Cutdata=[Fcx',Fcy',Fcz',data(n:length(data),3)*100-1925,...
    %data(n:length(data),15)-70]
%-------------------------------------------------------------------------
     %PLOTTING OF Fcx, Fcy, Fcz, Swing Position, and Cutter Advancement
y=[1:(length(Fcx(1:t)))];
r=t+n-1;
plot(y,data(n:r,15)-70,'g:','linewidth',2); %Swing Position plot
hold on
```

Figure A.4. Continued

```
105 plot(y,data(n:r,3)*100-1925,'g-.','linewidth',2); %Advancement plot
106 plot(y,Fcz(1:t),'b:','linewidth',2); %Cutting force in z direction plot
107 hold on
108 plot(y,Fcx(1:t),'r--','linewidth',2); %Cutting force in x direction plot
109 plot(y,Fcy(1:t),'k','linewidth',2); %Cutting force in y direction  plot
110 axis([0 t -150 100]);
111 grid on;
112 xlabel('TIME (sec)','fontsize',12);
113 ylabel('Cutting Force (lbf)','fontsize',12);
114 ylabel('Cutting Force (lbf), Swing Position and Cutter Advancement (cm)',...
115     'fontsize',12);
116 legend('Vertical Cutting Force','Axial Cutting Force',...
117     'Horizontal... Cutting Force',1);
118 legend('Swing Position','Cutter Advancement','Vertical Cutting Force',...
119     'Axial Cutting Force','Horizontal Cutting Force',1);
120 hold off
```

Figure A.4. Continued

Drawing of Dredge Redesigned Parts

From the redesign of the cell 1 location some modifications were done to account for the new concept of mounting cell 1. These modifications involved redesigning the upper load cell bracket and this was done by using the program SolidWorks. In Figure A.5 is a fully dimensioned 3 orthographic view of the final design of the new upper load cell bracket. Also this redesigned involves designing a base plate bracket for cell 1, and this was done so the end of cell 1 could be attached to the ladder cradle. In Figure A.6 the final design of the base plate bracket is shown and in the figure the plate is fully dimensioned so that it can be manufactured. The final modification needed was to design a dummy load cell so that the cell 1 sensor could be removed and replaced with this dummy cell. In Figure A.6, the final design and all dimensions are shown so the dummy cell could be manufactured.

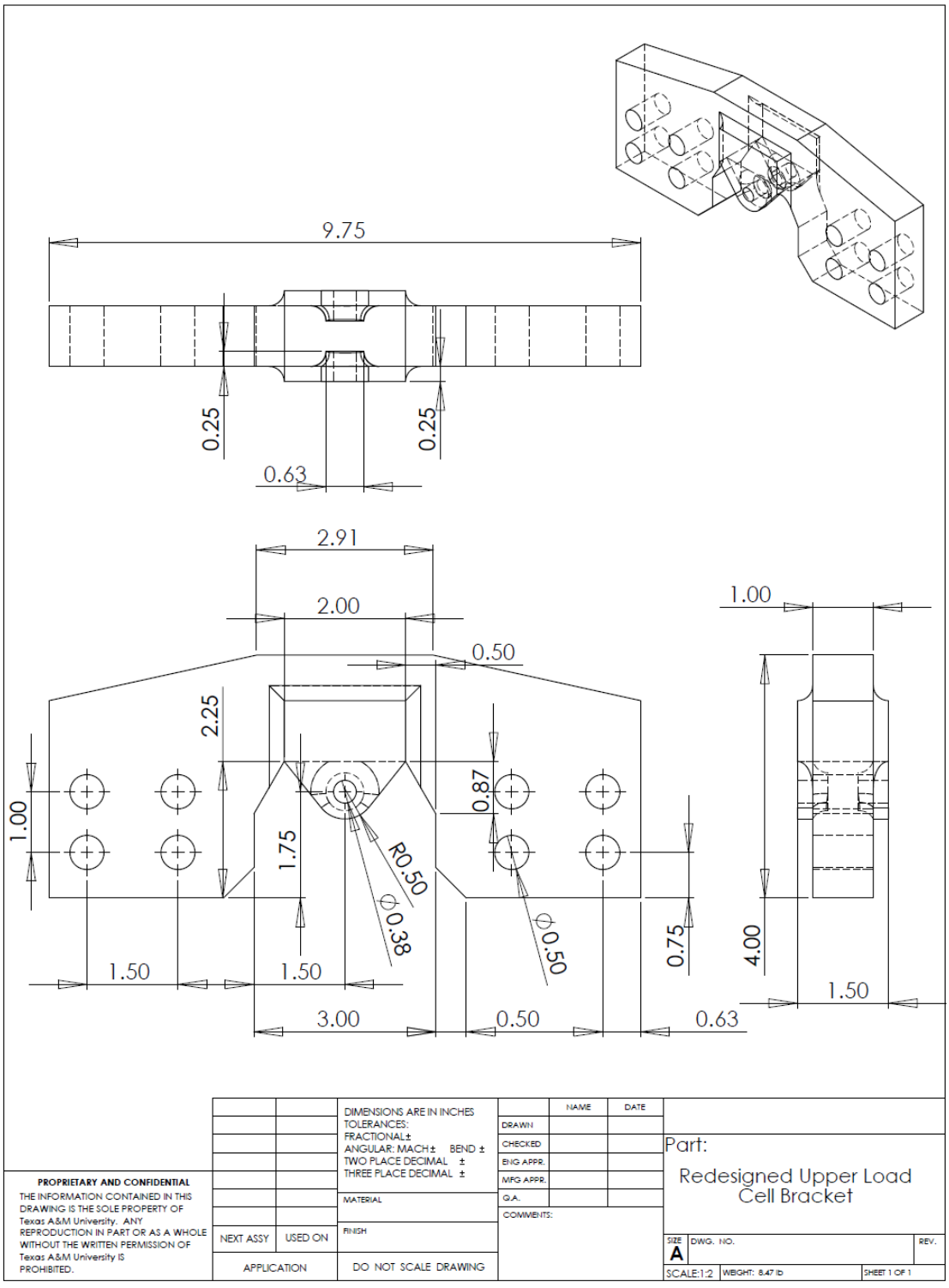

Figure A.5. Dimensioned redesign upper load cell bracket (dimensions are in inches)

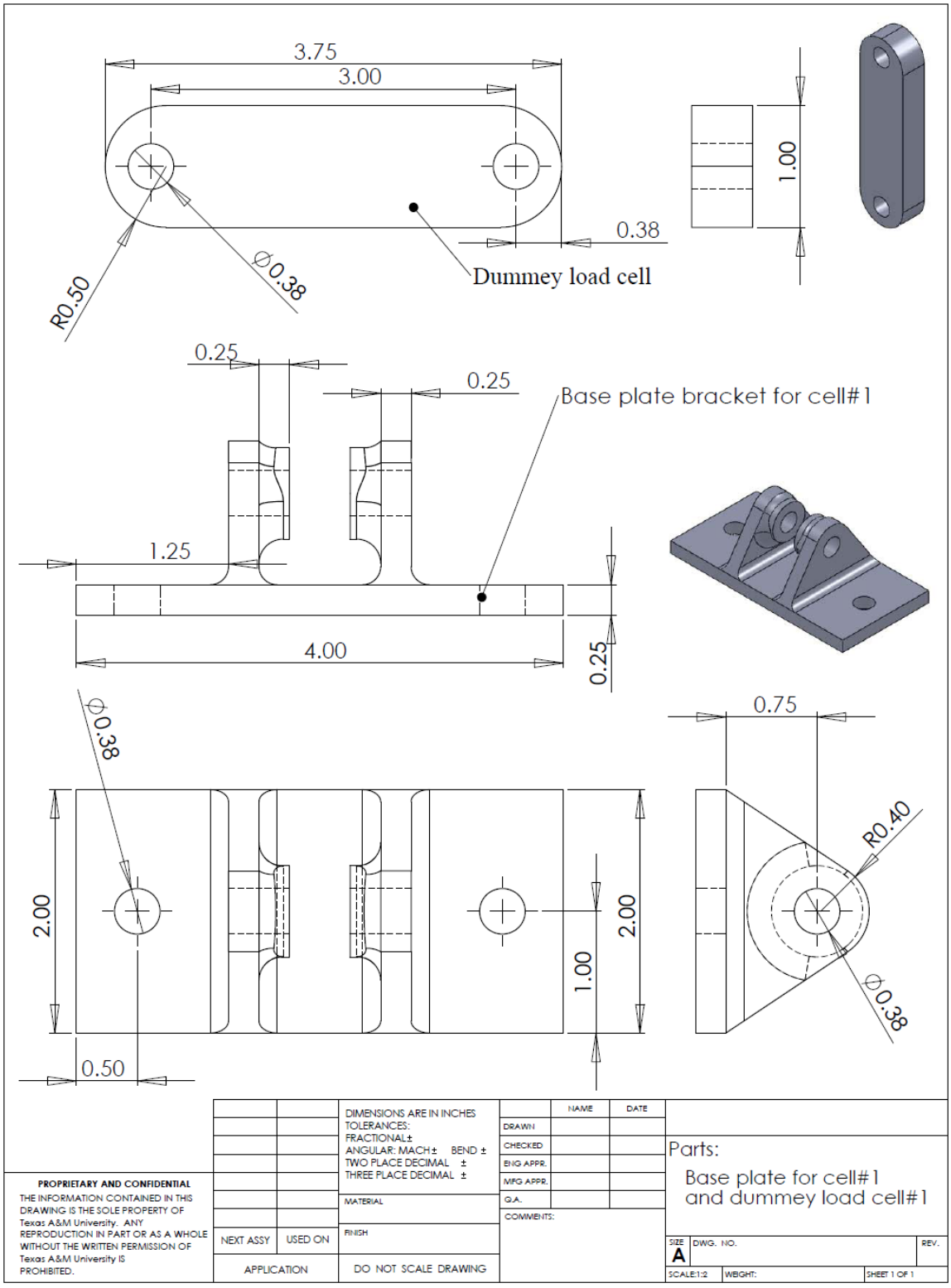

Figure A.6. Dimensioned cell 1 dummy cell and redesign base plate bracket (dimension are inches)

VITA

Dustin Ray Young received his Bachelor of Science in Ocean Engineering at Texas A&M University in College Station, Texas, in August 2007. He then decided to continue his higher education in 2007 and entered the Ocean Engineering Master's program at Texas A&M University and worked towards a Master of Science degree. His research interests consist of laboratory measurements of cutting forces on a dredge cutterhead and working with Dr. Robert Randall at the Reta and Bill Haynes Laboratory on several laboratory projects involving dredging and offshore dynamic modeling. Mr. Dustin R. Young received the "Best Student Paper" award for a paper submitted and presented at the WEDA XXIX and Texas A&M 40 conference in June 2009.

Address:
600 Discovery Dr
College Station, TX 77840
(979) 458-0188
c/o Dr. Robert Randall